AD-A189 829 IMPACT ANALYSIS OF THE CAMPACT SHIPPING CONTAINER(U) 1/1
SOUTHWEST RESEARCH INST SAN ANTONIO TX
D J POMERENING ET AL JUL 85 SWRI-06-8461-002
UNCLASSIFIED AMXTH-CD-TR-86056 F/G 13/4 NL

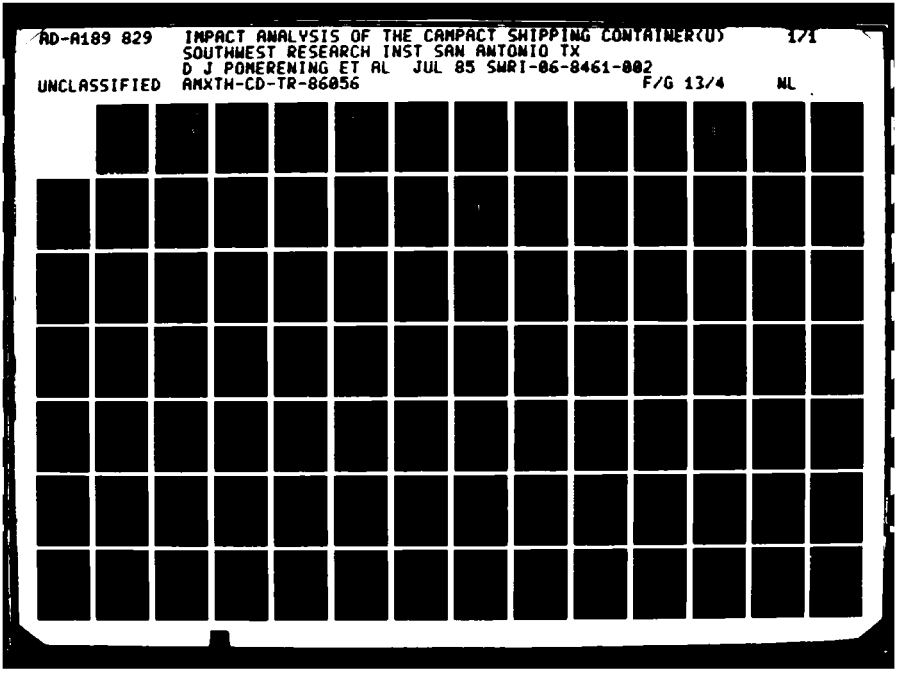

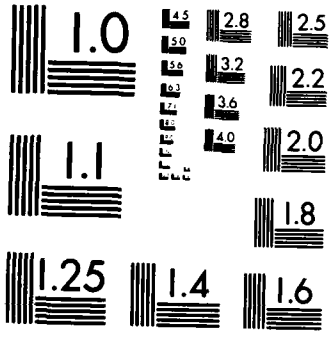

MICROCOPY RESOLUTION TEST CHART
NATIONAL BUREAU OF STANDARDS-1963-A

AMXTH-CD-TR-86056

(4)

DTIC FILE COPY

AD-A189 829

IMPACT ANALYSIS OF THE CAMPACT SHIPPING CONTAINER

by
D. J. Pomerening
P. A. Cox

FINAL REPORT
SwRI Project No. 06-8461-002

July 1985

DISTRIBUTION UNLIMITED / APPROVED FOR PUBLIC RELEASE

Prepared for

U.S. ARMY TOXIC AND HAZARDOUS MATERIALS AGENCY
ABERDEEN PROVING GROUND, MARYLAND 21010-5401

DISCLAIMER

The findings in this report are not to be construed as an official Department of the Army position unless so designated by other authorizing documents.

UNCLASSIFIED
SECURITY CLASSIFICATION OF THIS PAGE

REPORT DOCUMENTATION PAGE

1a REPORT SECURITY CLASSIFICATION Unclassified	1b. RESTRICTIVE MARKINGS None
2a SECURITY CLASSIFICATION AUTHORITY NA	3 DISTRIBUTION / AVAILABILITY OF REPORT Distribution Unlimited/Approved for Public Release
2b DECLASSIFICATION / DOWNGRADING SCHEDULE NA	
4 PERFORMING ORGANIZATION REPORT NUMBER(S) 06-8461-002	5. MONITORING ORGANIZATION REPORT NUMBER(S) AMXTH-CD-TR-86056
6a NAME OF PERFORMING ORGANIZATION Southwest Research Institute 6b OFFICE SYMBOL (If applicable)	7a. NAME OF MONITORING ORGANIZATION U.S. Army Toxic and Hazardous Materials Agency
6c. ADDRESS (City, State, and ZIP Code) P. O. Drawer 28510 6220 Culebra Road San Antonio, Texas 78284	7b. ADDRESS (City, State, and ZIP Code) Aberdeen Proving Ground, MD 21010-5401
8a. NAME OF FUNDING / SPONSORING ORGANIZATION H&R Technical Associates, Inc. 8b. OFFICE SYMBOL (If applicable)	9. PROCUREMENT INSTRUMENT IDENTIFICATION NUMBER
8c. ADDRESS (City, State, and ZIP Code) P. O. Box 215 Oak Ridge, Tennessee 37831	10. SOURCE OF FUNDING NUMBERS PROGRAM ELEMENT NO. / PROJECT NO. / TASK NO. / WORK UNIT ACCESSION NO.

11 TITLE (Include Security Classification)
Impact Analysis of the CAMPACT Shipping Container

12 PERSONAL AUTHOR(S)
Pomerening, D. J.; Cox, P. A.

13a. TYPE OF REPORT	13b. TIME COVERED	14. DATE OF REPORT (Year, Month, Day)	15. PAGE COUNT
Final	FROM _____ TO _____	85,07	88

16 SUPPLEMENTARY NOTATION

17 COSATI CODES			18. SUBJECT TERMS (Continue on reverse if necessary and identify by block number)
FIELD	GROUP	SUB-GROUP	M55 Transportation Accident, Impact Response, CAMPACT
15	02		

19 ABSTRACT (Continue on reverse if necessary and identify by block number)

Nonlinear impact analyses were performed on the CAMPACT shipping container. Longitudinal and lateral drops onto rigid surfaces were treated. Analyses were performed with the ADINA computer code, and included both geometric and material nonlinearities. Modeling of the CAMPACT emphasized the inner door and door attachments in an attempt to predict the onset of leakage at the inner door seal. The CAMPACT was loaded with pallets of M55 rockets and the floor roller assembly. The contents were treated as concentrated masses applied to the inner frame at appropriate locations for each impact direction.

Keywords: impact tests, [illegible] shipping containers

20 DISTRIBUTION / AVAILABILITY OF ABSTRACT	21. ABSTRACT SECURITY CLASSIFICATION
☐ UNCLASSIFIED/UNLIMITED ☒ SAME AS RPT ☐ DTIC USERS	Unclassified
22a NAME OF RESPONSIBLE INDIVIDUAL CPT Kevin J. Flamm	22b TELEPHONE (Include Area Code) (301) 671-2424 / 22c. OFFICE SYMBOL AMXTH-CD-L

DD FORM 1473, 84 MAR 83 APR edition may be used until exhausted
All other editions are obsolete

SECURITY CLASSIFICATION OF THIS PAGE
UNCLASSIFIED

SOUTHWEST RESEARCH INSTITUTE
Post Office Drawer 28510, 6220 Culebra Road
San Antonio, Texas 78284

IMPACT ANALYSIS OF THE CAMPACT SHIPPING CONTAINER

by
D. J. Pomerening
P. A. Cox

FINAL REPORT
SwRI Project No. 06-8461-002

for
H&R Technical Associates, Inc.
Oak Ridge, Tennessee

July 1985

Approved:

Alex B. Wenzel

Alex B. Wenzel, Director
Department of Energetic Systems

ACKNOWLEDGEMENTS

The authors greatly acknowledge the assistance provided to them by Mr. Everton McKenzie, who generated many of the finite element models used in the CAMPACT analyses; Ms. Deborah Stowitts, who edited the report; Mrs. Rosemary Rivas, who typed the draft report; and to Mrs. Sue White, who typed the final report.

TABLE OF CONTENTS

LIST OF TABLES

I. INTRODUCTION

A. Background

This work was performed for H&R Technical Associates in support of their evaluations of the CAMPACT shipping container (Figure 1) for the M55 rocket pallets (Figure 2). Only evaluations of the CAMPACT container are reported here; a companion structural analysis of the M55 pallet is reported under separate cover [1].

B. Objective

The objective of this analysis was to evaluate the CAMPACT container for impact loading from 30 ft. high free fall drops onto a rigid surface. The analysis utilized the finite element method and focused on the ability of the CAMPACT to maintain a seal between the inner door and the inner frame during and following the impact. Finite element models were created for the CAMPACT which were as realistic as practical, yet conservative. The results should be appropriate for the alternative analysis in which they will be used.

C. Scope of Work

Two drops were analyzed, a longitudinal drop and a lateral drop. For the longitudinal drop, impact was on the door end; for the lateral drop, impact was on the side of the container. It was assumed that all points on the impacting surface struck the rigid surface at the same time. Vertical, edge and corner drops were not addressed.

Two versions of the CAMPACT shipping container are under development, a truck version and a rail version. The truck version is in a more advanced design stage; thus, the analyses performed were for the truck version only. Even for this version detailed structural drawings could not be obtained. All dimensions, materials, structural components, and attachment details were obtained from Reference 2 and from conversations with design personnel [3].

Loading of the M55 pallets within the CAMPACT was provided by H&R Technical Associates. The truck version can transport a maximum of eight (8) pallets. This was the only loading configuration considered. Fewer pallets would result in higher pallet accelerations; however, eight pallets produce the worst case loading for the CAMPACT itself. The pallets and other internal

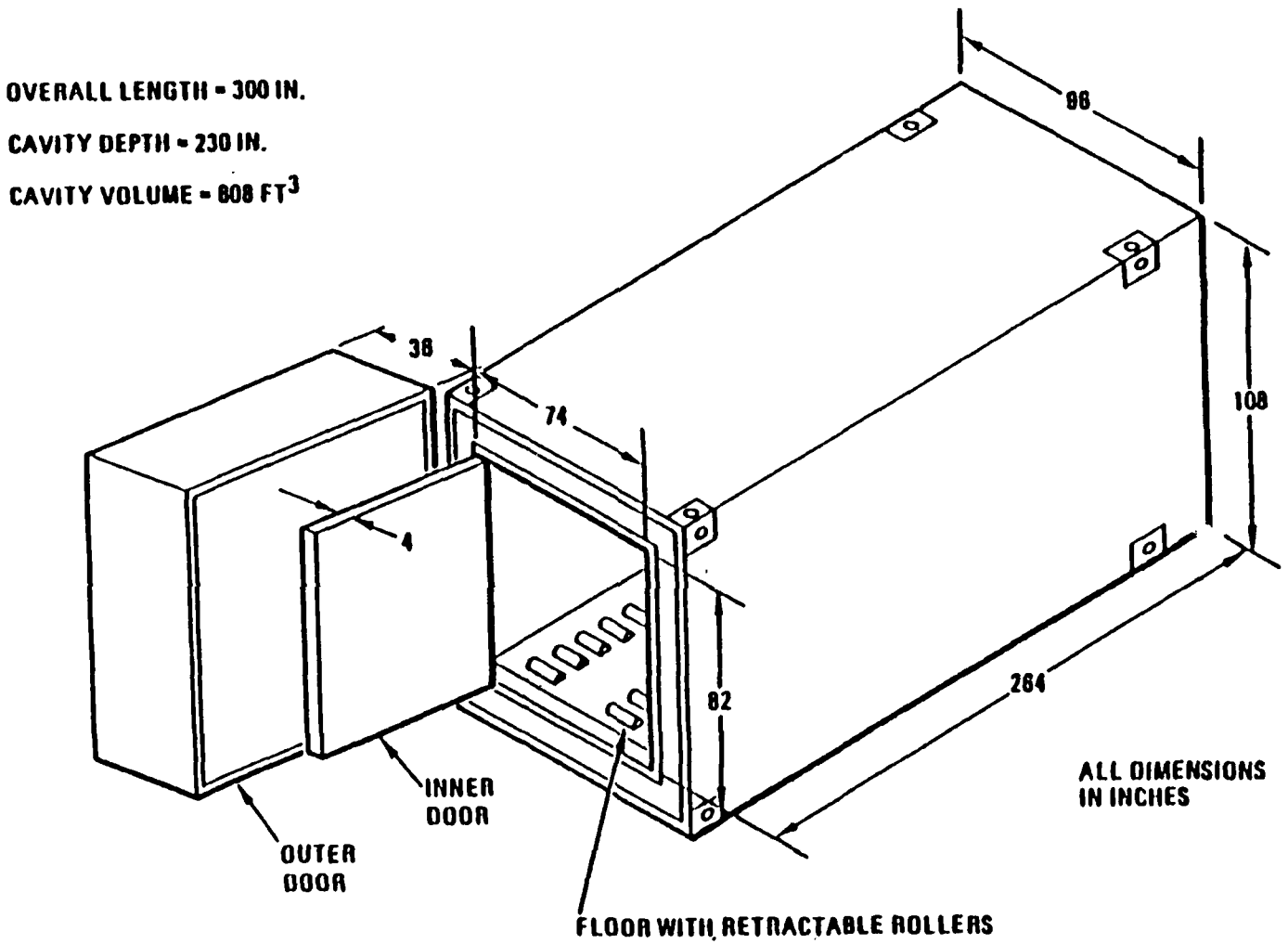

Figure 1. CAMPACT - Truck Version [Ref. 2]

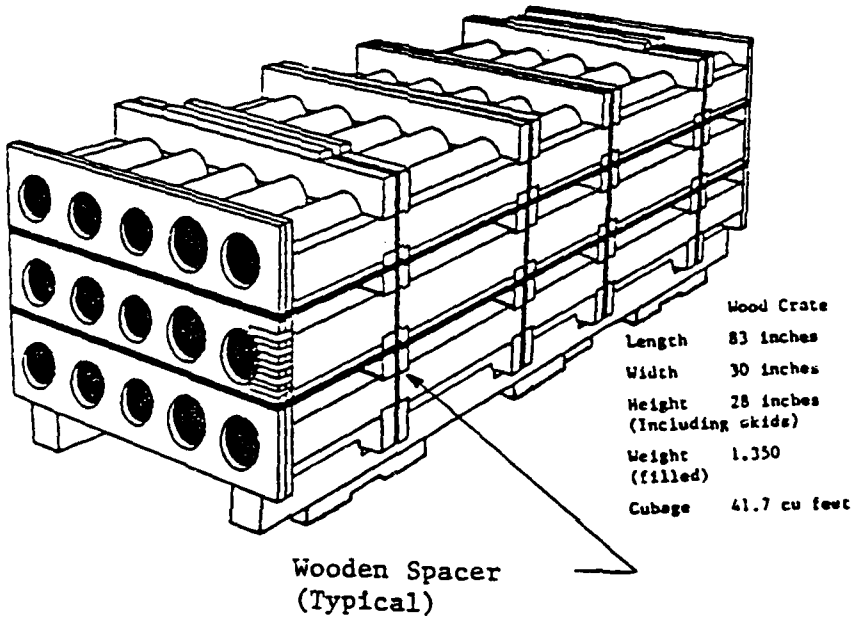

Figure 2. Pallet of M55 Missiles (in Launch Tubes) - [Ref. 2]

equipment, such as the floor roller assembly and blocking, were treated as rigid masses for the impact calculations. Details are provided in Section II.

D. Method of Approach

Impact of the CAMPACT on an unyielding surface can produce yielding and large deformations in the structural members. To accommodate these responses, models of the CAMPACT, which included both material and geometric nonlinearities, were formulated and solved using the ADINA computer program [4]. Two separate models were constructed, one for longitudinal impact and one for lateral or side impact. Both models included details of the inner door, inner frame adjacent to the door and connections between the inner door and the inner frame.

Because nonlinear analyses are costly to perform, steps were taken to reduce the size of the models as much as possible. For the longitudinal model, the CAMPACT was assumed to be symmetrical about both a vertical longitudinal plane and horizontal longitudinal plane, which is very nearly true. By modeling only one of these symmetrical pieces (¼th of the total structure), the size of the model was reduced substantially. The model was reduced further by using concentrated masses to represent the upper end of the CAMPACT, aft of the first bay of the inner frame, and by ignoring the outer frame and foam aft of the door. The size of the lateral model was reduced by a similar process. In this case a half model was developed, with symmetry about a vertical lateral plane at the midpoint of the inner frame. As with the longitudinal model, the outer frame was ignored. Details for both models are given in Section II.

In the truck version, eight (8) pallets are placed in the container: two abreast, two high and two deep. The long axes of the pallets are aligned with the long axis of the CAMPACT. This arrangement requires blocking to fill the empty spaces between the sides of container and the pallets. No space was assumed to exist between the pallets themselves which left 12 inches to be blocked between the pallets and the side walls and 62.5 inches to be blocked between the pallets and the container ends. This blocking was assumed to be equal on each side and each end, which centered the pallets on the floor of the CAMPACT. The pallets were assumed to rest on the floor, which required that 30.5 inches of blocking be placed above the pallets. In all analyses, it was assumed that the blocking was rigid and distributed the loading from the

pallets evenly to the inside surfaces of the CAMPACT. In addition, the pallets inside the CAMPACT were assumed to act as rigid masses during the impact, i.e., their motions, whether elastic or elastic-plastic, were not coupled to the CAMPACT response.

To describe the impact of the CAMPACT on the rigid surface, all parts of the model, except the boundary which struck the rigid surface, were given an initial velocity corresponding to a free fall drop of 30 ft. The striking boundary was fixed against motion. No other forces were applied and gravity was ignored during the impact. These initial conditions adequately describe the impact event.

Results obtained were in the form of deformed shapes, permanent plastic deformation of the members, and stresses in the elements. Interpretation of the results was complex because of the three-dimensional response of the CAMPACT. The analyses were also complicated by the geometry in the region of the inner door seal. Approximations made in the model development had to be considered during interpretation of the computed results.

II. CAMPACT ANALYSIS

A. Geometry

Overall geometry of the CAMPACT was shown in Figure 1, and Figure 3 gives an exploded view. The exploded view identifies the major components of the CAMPACT container. Further identification of CAMPACT components are given in Figures 4 and 5. In Figures 3 through 5 it is easy to see that the inner and outer frame assemblies are isolated from each other by a layer of structural foam. This foam is the major energy absorbing component of the system for the impact conditions being considered in these analyses.

Additional details of the CAMPACT are given in Figures 6 through 9. The truck version of the CAMPACT has an overall size of 301" x 96" x 108.5" (length x width x height) with an inside cavity of 230" x 74" x 86" (Figure 6). Figures 7, 8 and 9 show details of the door and the inner frame adjacent to the door. Special care was given to the modeling of this region of the structure because leakage of the seal was taken as the primary failure mode of the CAMPACT. Of course, any source of leakage would cause failure, but it was considered unlikely that distortions and strains would be sufficient to cause leakage in other parts of the structure. It was also assumed that the blocking offered no potential to damage the liner.

B. Material Properties

1. Requirements

Definition of the material properties for the CAMPACT system were based on the requirements of the computer programs used to generate and analyze the system. For the two models under consideration, two programs were utilized in the analysis sequence. GIFTS [5] was utilized to generate the model, while ADINA [4] was utilized to preform the nonlinear dynamic analysis. These two programs require a slightly different definition of the nonlinear material properties. The requirements for the two systems are:

GIFTS--For this program, the characteristics are defined in terms of the stress-strain pairs for the particular element/material combination under question.

ADINA--For this program, the characteristics required are dependent on the element type and the nonlinear model being used. For the majority of elements and materials, this required the definition of the elastic modulus,

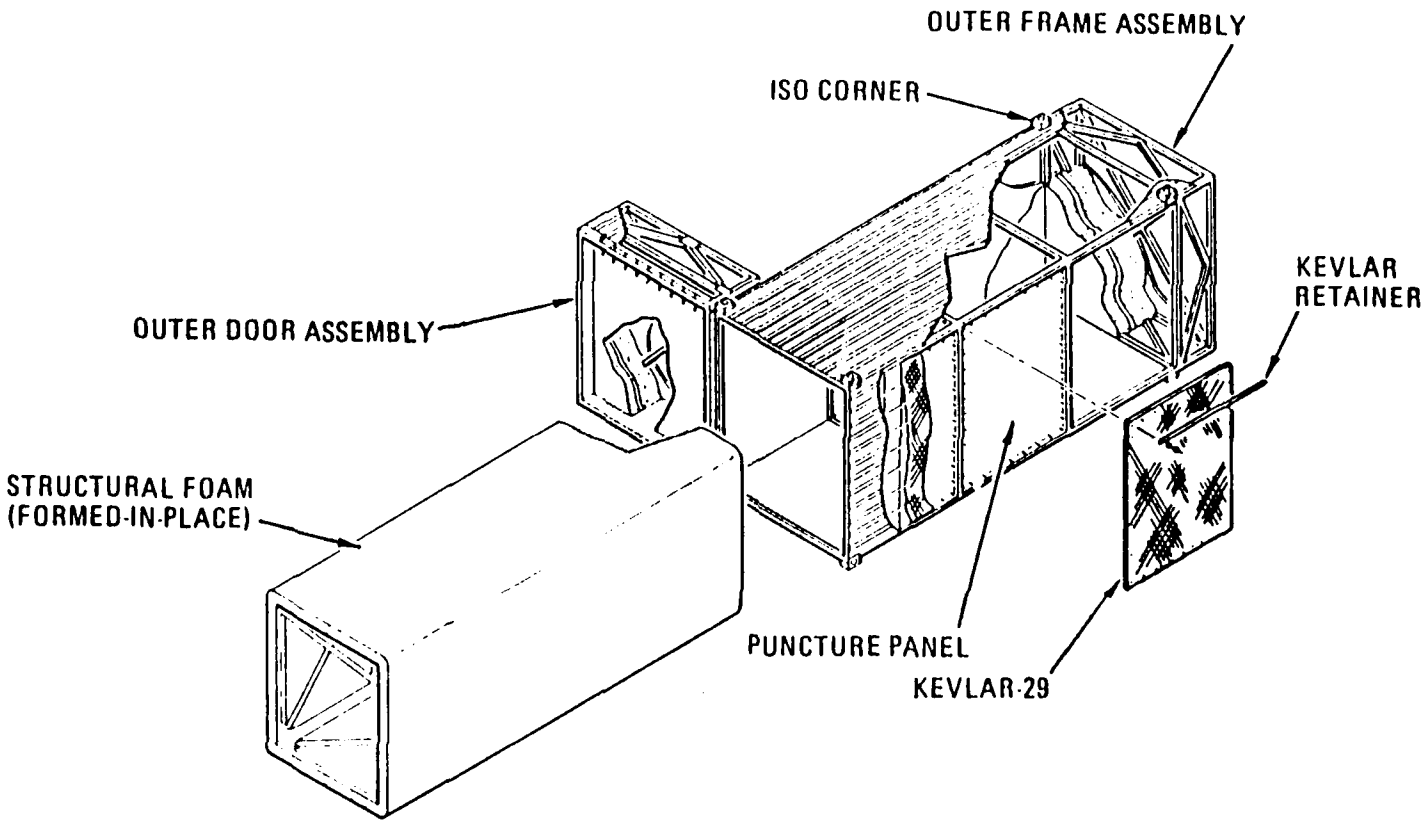

Figure 3. Outer protective structure of the shipping container. [Ref. 2]

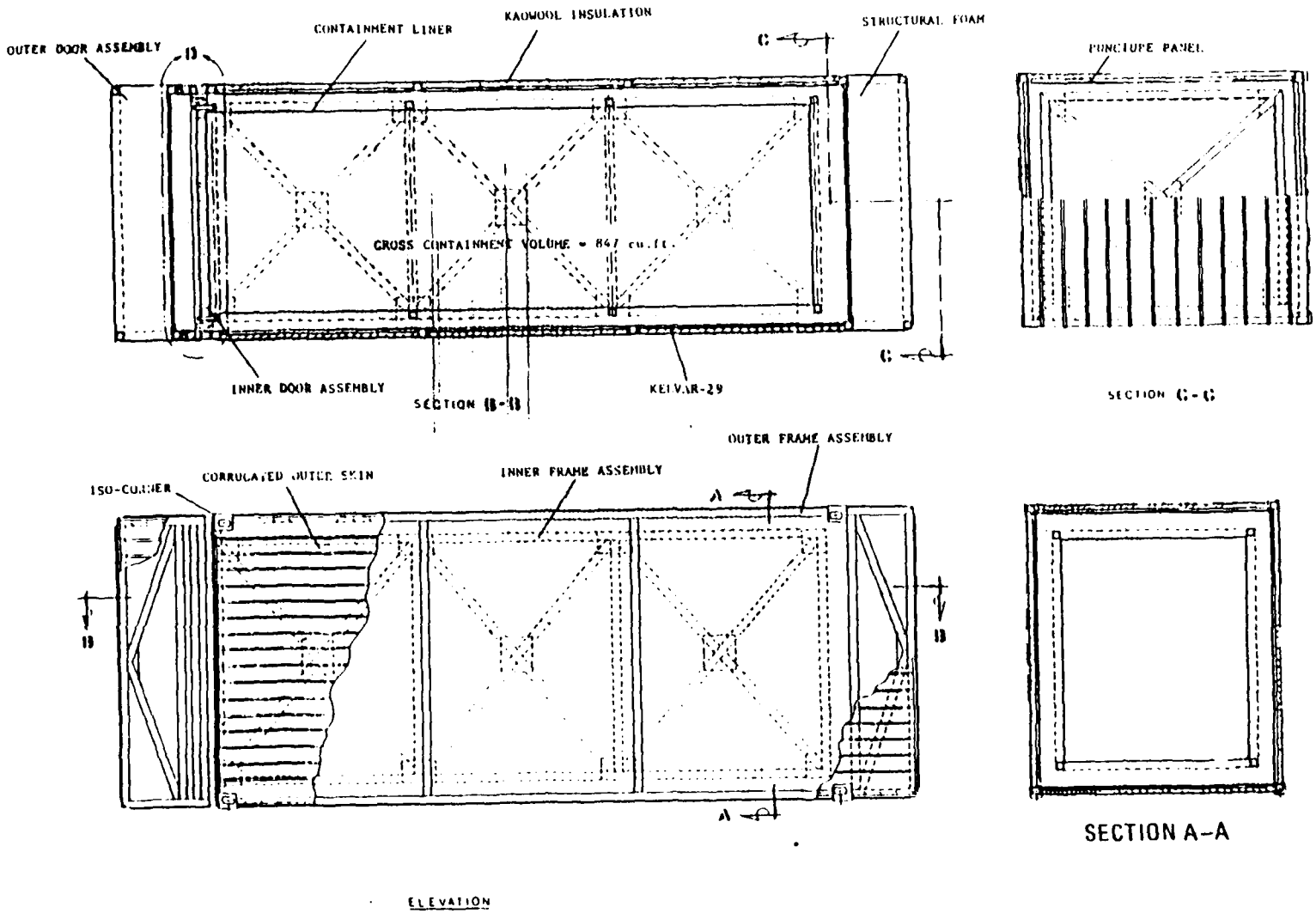

Figure 4. Component identification: overall [Ref. 2]

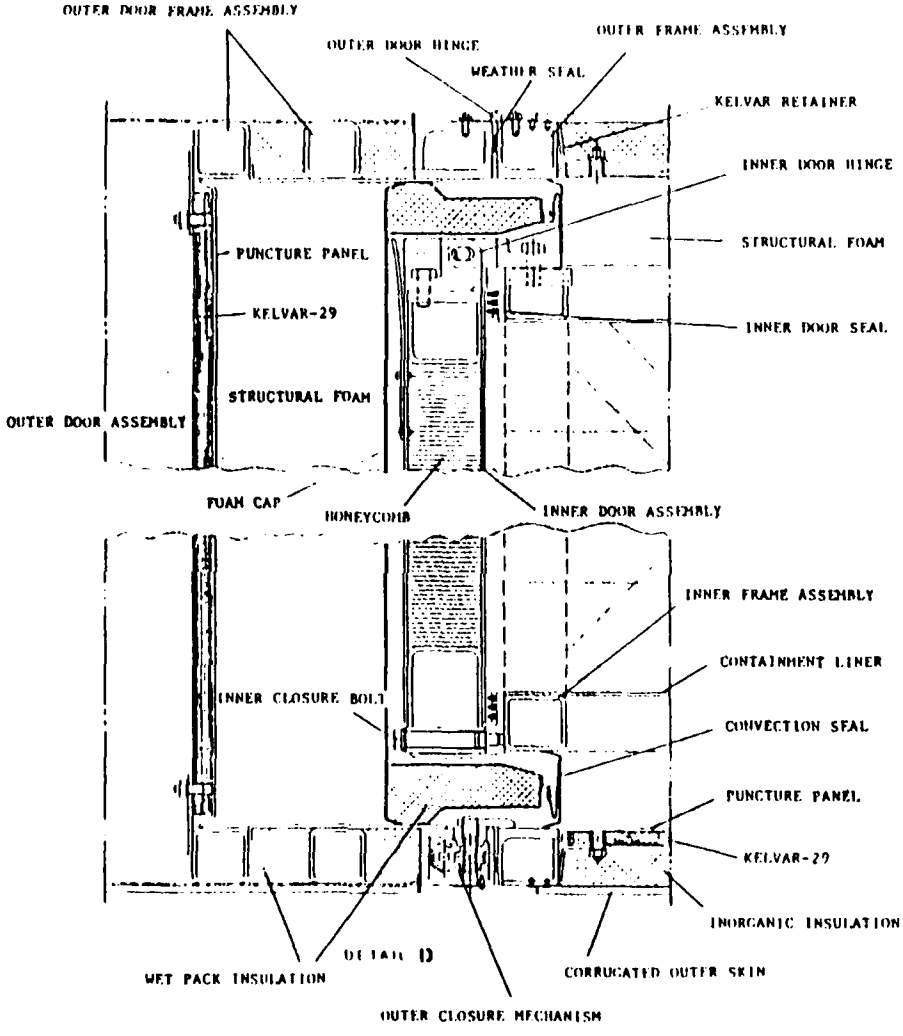

Figure 5. Component identification: closure end [Ref 2]

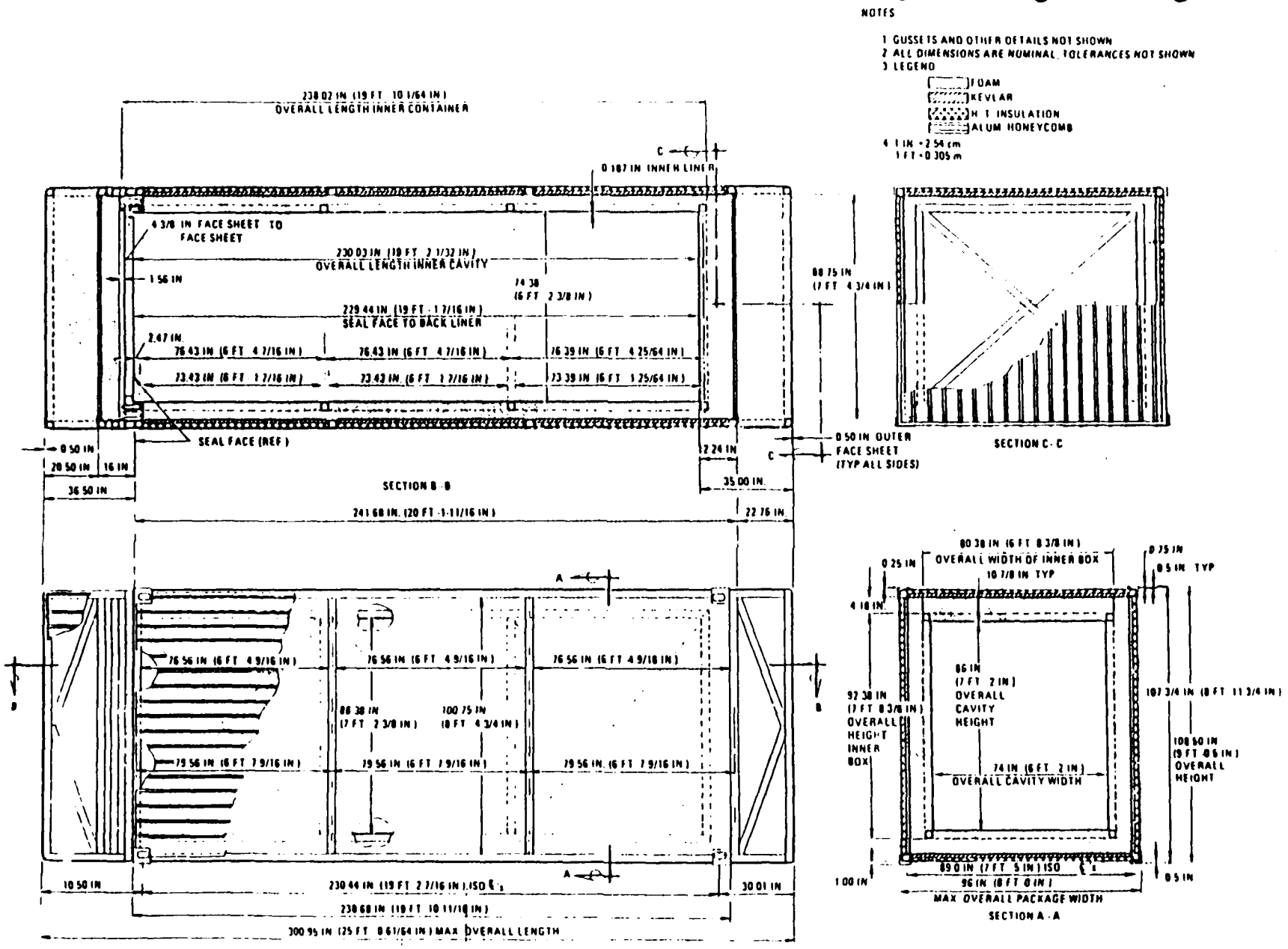

Figure 6. Configuration control layout [Ref. 2]

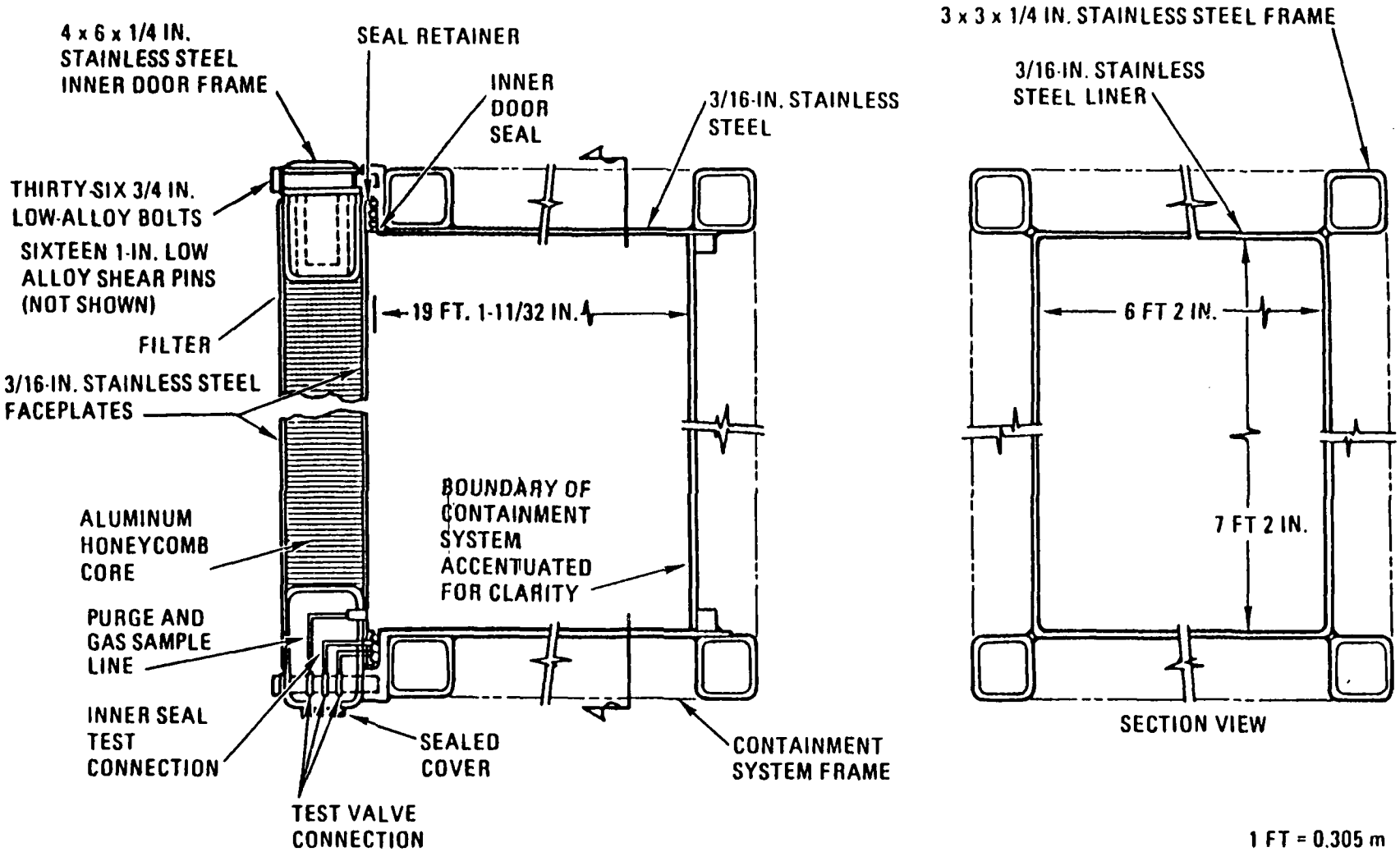

Figure 7. Containment system (for clarity, outer frame, door, and structural foam are omitted) [Ref. 2]

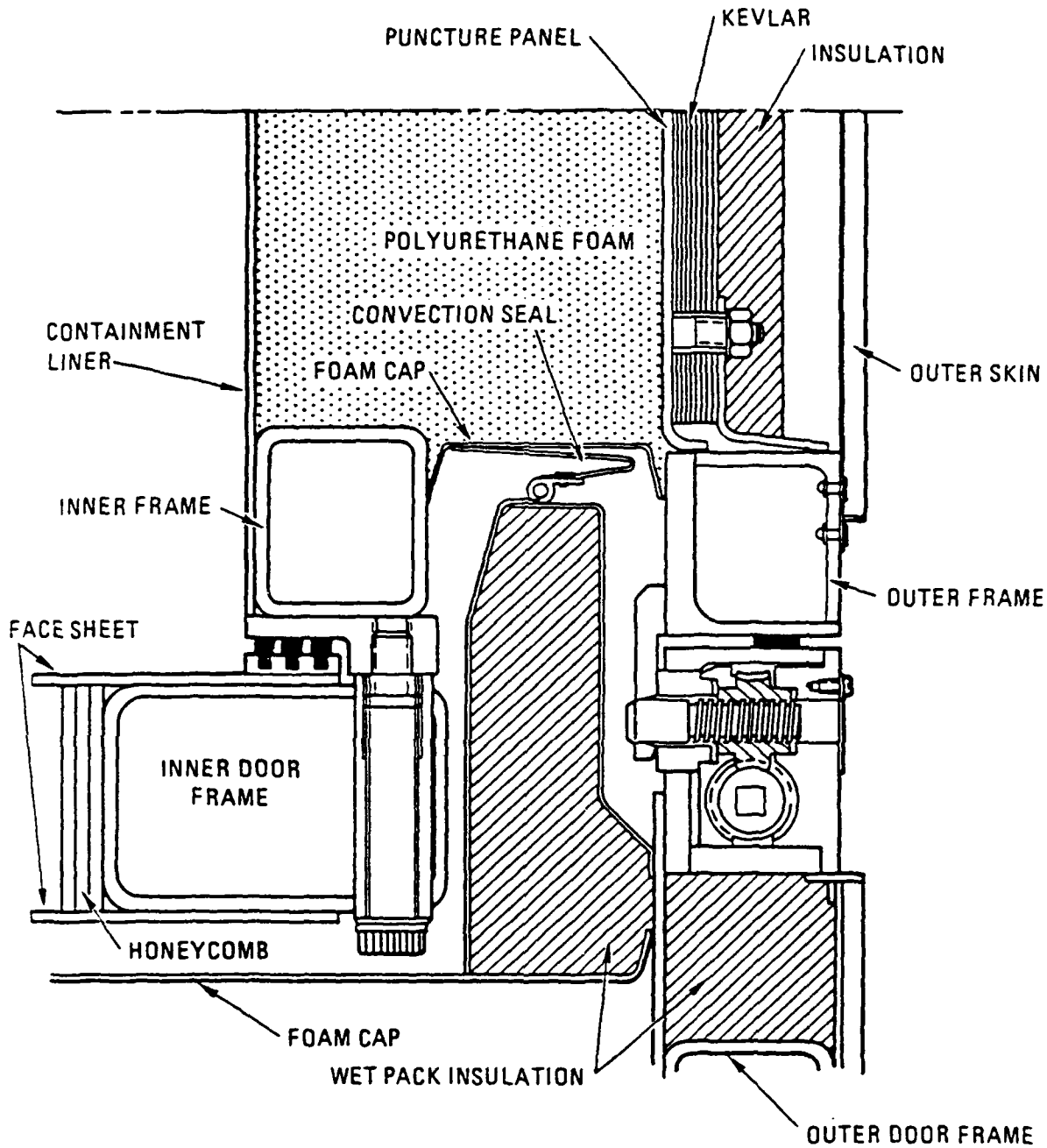

Figure 8. Detail of closure area [Ref. 2]

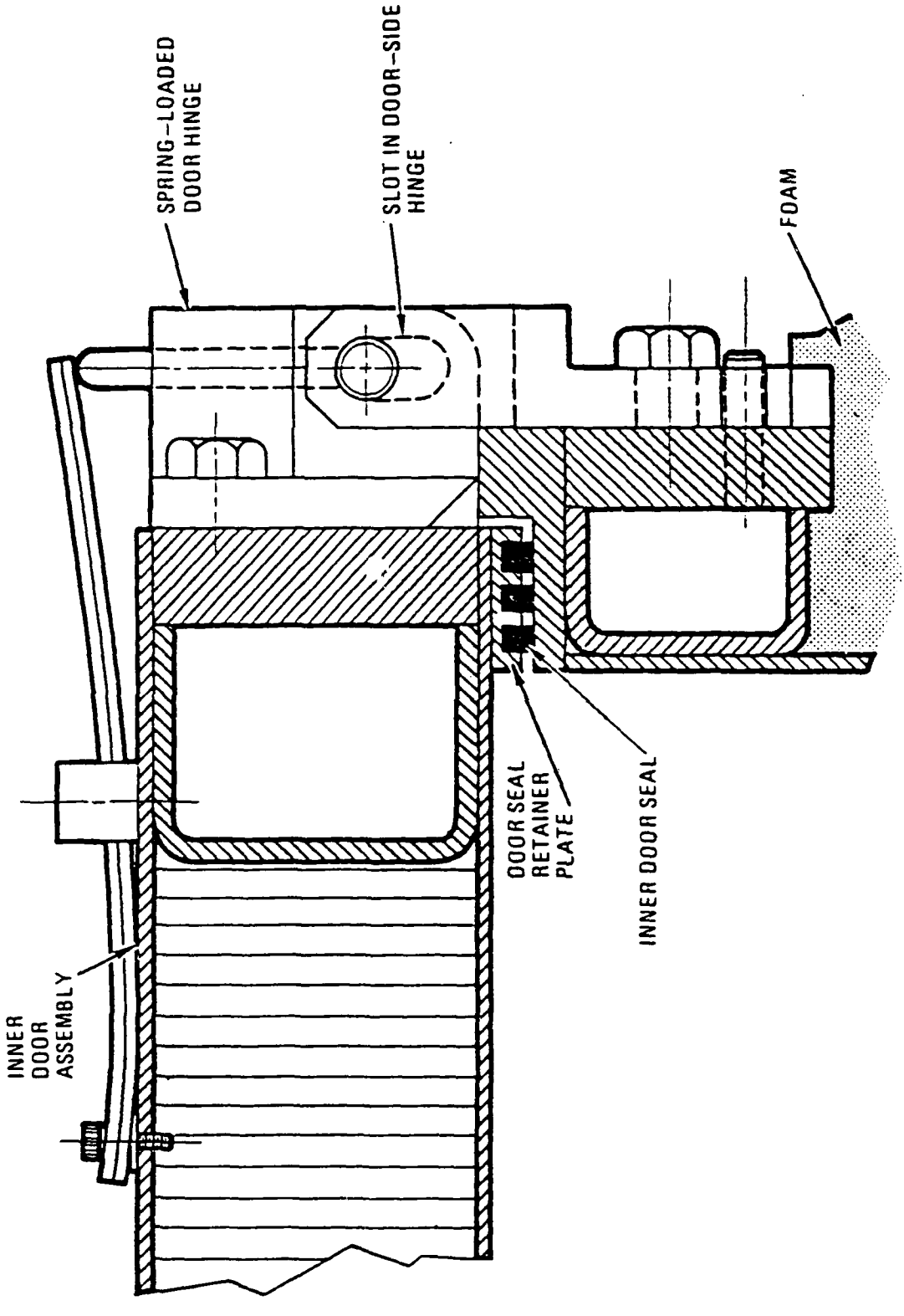

Figure 9. Detail of inner door seal and hinge [Ref. 2]

the yield stress, and the hardening modulus after yielding. The major exception was the foam, which was idealized as a tri-linear system. For this case, it was necessary to define the elastic modulus, the yield stress and the stress-strain pairs for the linear segments after yielding.

In all cases, these material characteristics were idealized as linear stress-strain relationships. All except the foam were considered to be bi-linear. Figure 10 gives a description of the majority of the materials used in the CAMPACT. For the models developed, definition of properties for the Type 304 Stainless Steel, the A320 Grade L7C steel bolts, and the polyurethane structural foam were required. Data on the material characteristics for the three were derived from References 2, 6, 7 and 8.

2. Properties

Table 1 gives material properties which were used for both the longitudinal and lateral models. For the analysis, it was sometimes necessary to adjust the values in Table 1 to take into account the geometry of the various elements under consideration. ADINA does not allow for hollow sections such as the 3 x 3 members of the inner frame. In ADINA, it was necessary to define the hollow sections as solid cross sections. To insure the proper bending stiffness or axial stiffnesses, it was necessary to modify both the geometry of the section and the material characteristics of the particular element. It was not possible to match all requirements, such as bending stiffness about both axes and the axial stiffness too. Depending on the type of element in question and its primary mode of response, the appropriate modifications were made. Specific modifications will be discussed in the appropriate sections of this report.

Another consideration is the fact that the values for the various material parameters were based on the static characteristics of the materials. For metals this approach is valid. The foam will display some change in response depending on the rate of loading [9]. Since the load rate was not known prior to the analysis it was not possible to define the actual material properties to account for strain rate effects.

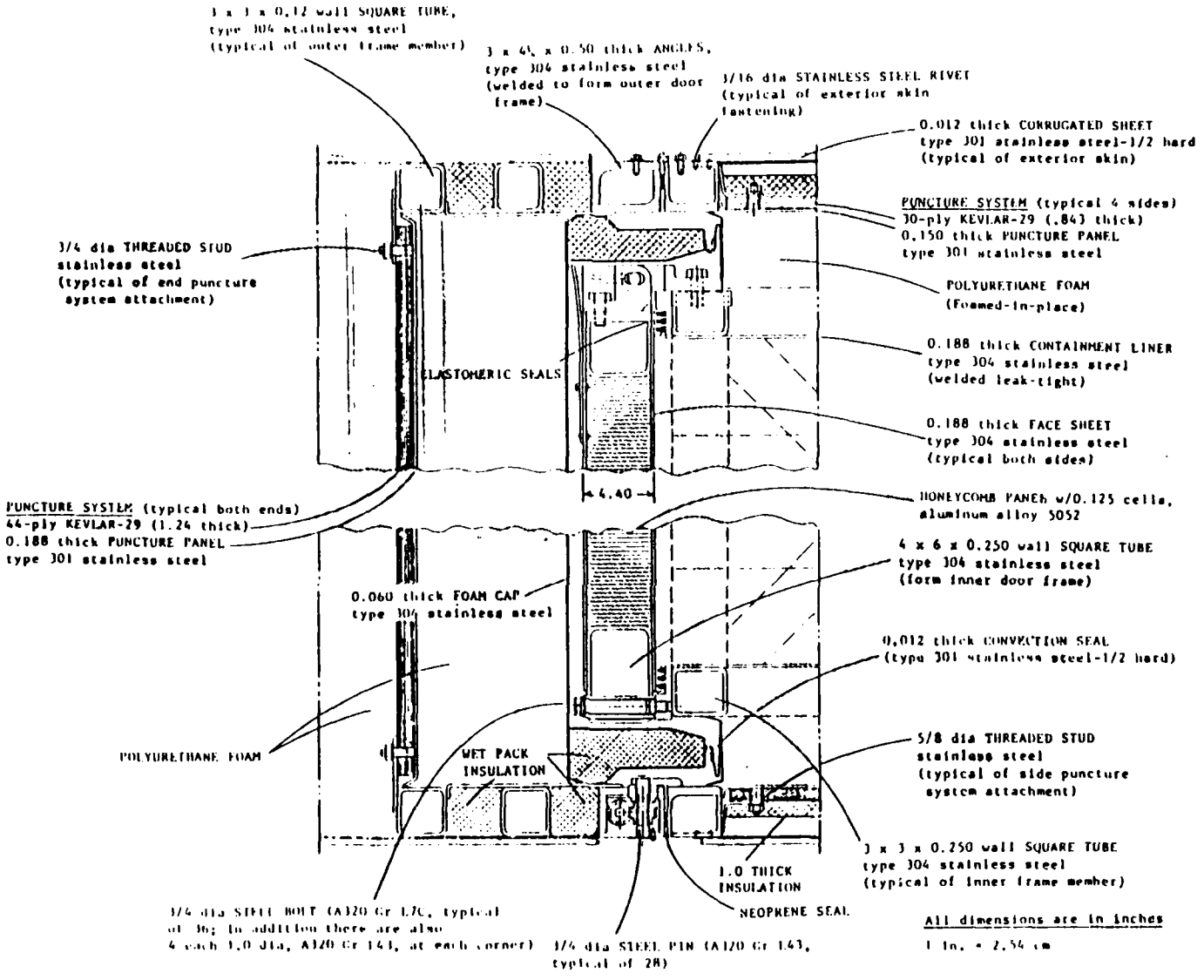

Figure 10. Material identification: closure end [Ref. 2]

Table 1. Summary of Nonlinear Material Properties

Type 304 Stainless Steel

Elastic Modulus	28.5×10^6 psi
Poission's Ratio	0.26
Yield Strength	30,000 psi
Hardening Modulus	113,000 psi
Density 0.290 lb/in^3	
Stress No. 1	30,000 psi
Strain No. 1	0.00105 in/in
Stress No. 2	75,000 psi
Strain No. 2	0.40 in/in

A320 Grade L7C Steel Bolts

Elastic Modulus	30×10^6 psi
Poisson's Ratio	0.30
Yield Strength	105,000 psi
Hardening Modulus	40,000 psi
Density 0.286 lb/in^3	
Stress No. 1	105,000 psi
Strain No. 1	0.0035 in/in
Stress No. 2	125,000 psi
Strain No. 2	0.5 in/in

Structural Foam

Elastic Modulus	3500 psi
Poisson's Ratio	0.30
Yield Strength	140.0 psi
Plastic Limit	0.52 in/in
Hardening Modulus	900 psi
Density 0.00347 lb/in^3	
Stress No. 1	140.0 psi
Strain No. 1	0.04 in/in
Stress No. 2	150.0 psi
Strain No. 2	0.52 in/in
Stress No. 3	970.0 psi
Strain No. 3	0.67 in/in

The material properties defined were appropriate for this design phase analysis. Properties were chosen to give comparative results for use in alternative analysis procedures.

C. Preliminary Analyses

1. Mass

The first task was to determine the mass/weight characteristics of the truck version of the CAMPACT. From the limited drawings of the system, estimates of the weights of the various components of the system were made. Table 2 gives a summary of the major components and their corresponding weight. The total weight of the system was estimated to be 40,153 lb. These calculations neglect the weights of such components as the hinges, vents, bolts, etc. Their weight was assumed to be insignificant.

Table 2. Estimated Weight CAMPACT Components--Truck Version

ELEMENTS	DESCRIPTION	WEIGHT (lb)
Outer Skin	Type 301 SS	501
Outer Frame	Type 304 SS 3 x 3 x 0.125 Square Tubing	3016
Puncture Panel	Kevlar-29 and Type 301 SS	9738
Structural Foam	Polyurethane	4315
Inner Frame	Type 204 SS 3 x 3 x 0.25 Square Tubing	4345
Inner Door	Type 304 SS 4 x 6 x 0.25 Square Tubing Aluminum Honeycomb Panel with Type 304 SS Faces	1403
Inner Liner	Type 304 SS	4335
Roller Floor	1200	
Pallets	Eight @ 1350 lbs each	10800
Blocking	Wood 500	
TOTAL	40153	

2. Foam Crushing - Static

As a part of the analysis procedure, some static runs were made to verify the stiffness of the models elements, the mass of the system and to give an indication of system response. For these cases, an acceleration of 1g was applied to the models, and a preliminary analysis was preformed to estimate the deflection of the system. For the longitudinal model, the total deflection was estimated to be 0.0227 inches. This calculation was made using the formula:

$$\delta = Pl/AE$$

where P = the load (lb)
L = the length of the foam elements (in)
A = the area of the foam elements (in^2)
E = the Elastic Modulus (psi)

For the lateral model two static cases were considered. Since the model could respond in both the lateral (X) and vertical (Z) directions (due to the mass loading of the system), static analyses were preformed along both the axes. For the lateral load, the deflection was calculated to be 0.0014 inches while the vertical load resulted in a deflection of 0.0013 inches. In both cases, the load was assumed to be uniformly distributed over the foam.

3. Foam Crushing - Dynamic

As part of the preliminary analysis, an estimate of the dynamic response of the system was made. Relating the potential energy associated with the 30 ft. drop height, h_o, and the kinetic energy at impact, the impact velocity, V, can be calculated from:

$$\tfrac{1}{2}(MV^2) = Mgh_o$$

giving

$$V = (2gh_o)^{\frac{1}{2}}$$

where M is the mass of the system and g is the acceleration of gravity (386 in/sec^2). For the 30 ft. drop height, the velocity was calculated to be 527 in/sec.

To determine the dynamics of the CAMPACT on impact, it was necessary to determine the deflection, duration and acceleration of the response. The displacement was calculated by equating the kinetic energy at impact to the energy absorbed by the crushing of the foam. For this analysis, it was assumed that the foam behaved like a rigid, perfectly plastic material, and the deflection is calculated by using

$$\delta = Mgh_o/(\sigma_y A - Mg)$$

where σ_y is the yield stress of the foam and A is the area of foam in compression.

From a free body diagram, the acceleration of the system was calculated using

$$a(g's) = \sigma_y A/Mg - 1.0$$

It was then necessary to determine the duration of the pulse. As for the calculation of the deflection, a constant deceleration, based upon crushing of the foam was assumed. The resulting pulse duration is given by:

$$t = (2h_o/a^2 g)^{\frac{1}{2}}$$

Table 3 summarizes the results obtained from this preliminary analysis. One important fact learned was that it is not likely that the foam will lock up during a 30 ft. drop.

4. Buckling

A consideration in the analysis of the system was the potential for buckling of the members of the inner frame during the impact. Estimates of both the buckling loads and the yield loads of these elements were made including the potential for a load offset. From this analysis, it was determined that the buckling loads of the system were significantly higher than the yield loads. Since this was the case, buckling of the members was not considered in the finite element analyses. Also, the buckling loads will be higher than those calculated due to the added restraint of the containment liner and the foam on the frame members. Appendix A gives buckling loads for some members as part of the calculation to determine the crushing strength of

the CAMPACT. These calculations also show that buckling loads for the members exceed their yield strength, without consideration of lateral support which is provided by the liners and foam. Some moments will clearly be created at the ends of some compression members during the impact event but we believe that these will be adequately reacted by the liner and foam.

Table 3. Preliminary Dynamic Foam Crushing Results *

Longitudinal Impact

Foam Area = 92.38 x 80.38 = 7425 in^2
Weight = 22583 lb
Mass = 22583/386 = 58.505 $lb\text{-}sec^2/in$
δ = (22583 x 360)/(140 x 7425 - 22583) = 7.99 in
Percent Crush = 7.99/36.0 = 22%
Peak Acceleration = 140 x 7425/22583 - 1.0 = 45 g's
Duration = $(2 \times 360)/(45^2 \times 386)^{\frac{1}{2}}$ = 0.0304 sec

Lateral impact

Foam Area = 92.38 x 236.3 = 21829 in^2
δ = 2.68 in
Percent Crush = 2.68/7.31 = 37%
Peak Acceleration = 134 g's
Duration = 0.0102 sec

Vertical Impact

Foam Area = 80.38 x 236.3 = 18993 in^2
δ = 3.08 in
Percent Crush = 3.08/7.56 = 41%
Peak Acceleration = 117 g's
Duration = 0.0117 sec

*Note that the values given in Table 3 assume that energy is absorbed only by the foam. Additional energy absorption by other components in the CAMPACT will shorten the duration of the impact event.

5. Static Crushing Strength

Conservative estimates of the static crushing strength of the CAMPACT were made for the assumption that the structure was loaded by two parallel rigid plattens. It is clear from the analyses, included as Appendix A, that the outer frame will collapse first and that the final crush strength is determined by the inner frame and surrounding foam. The crush forces, computed for longitudinal and vertical loads, are:

longitudinal------852,000 lb
vertical--------2,310,000 lb

D. Longitudinal Impact

1. Model Development

a. Finite Element Grid

As noted in Section I, symmetry conditions were imposed to reduce the size of the finite element models developed for analysis with the ADINA computer program. For longitudinal impact, vertical and horizontal planes of symmetry were taken along the longitudinal axis of the structure. To reduce the model further, only the front part (the door end) of the structure was modeled explicitly. The rear end was represented by the addition of lumped masses to the front part of the structure. Plastic deformations were not expected in the rear of the structure, and the local dynamic motions of the neglected part would have little effect on the deformations near the door. Other simplifications and justification for their use are:

* Neglect of the outer frame--The assumption here is that motions of the inner frame occur independently from the outer frame for longitudinal impact. We believe that is a good assumption for simultaneous impact between the striking surface of the CAMPACT and the rigid surface. Any tendency of the CAMPACT to rotate from the vertical is already eliminated by the boundary conditions placed on the planes of symmetry. Further, the contact surface between the structural foam and the outer frame is smooth. The bond strength at this contact surface is unknown and slippage could occur. If slippage does not occur, then this assumption is equivalent to postulating that the outer

frame and foam translate forward during impact at the same rate as the inner frame. Of course, loads from the outer frame are transferred directly into the outer door frame assembly during longitudinal impact.

* Neglect of the foam on the sides and top of the inner frame--For longitudinal impact, the only function of the foam on the sides and top of the inner frame would be to transfer load from the inner frame to the outer frame if differential motions occurred between the two components. For the reasons cited above, the outer frame was neglected, and so the foam was neglected also. Neither its mass or its stiffness was included.

* Neglect of the containment liner stiffness and strength--Stiffness of the liner could be quite high in shear, if it does not buckle, but quite low in compression. This phenomenon is not easily represented in the finite element model. Because the primary response during longitudinal impact is expected to be compression, its contribution to the stiffness and strength of the inner frame was neglected. Its mass was included in the model.

* Neglect of the puncture panel in the outer door assembly--The puncture panel should absorb little energy during the longitudinal impact and should not interfere with crushing of the foam by longitudinal translation of the inner frame. It may cause the layer of foam between the panel and the door to crush first, but it should not prevent crushing of the foam below the panel.

*Neglect of pallet response within the CAMPACT--The assumption of rigid body motion of the pallets during impact is a reasonable assumption for the longitudinal analysis. This assumption should produce high (conservative) loads on the inner door. Also, to have included the response of the pallets in the analysis, and still have modeled the door region in detail,

would have increased the finite element model to a size which would have exceeded our current computer resources at SwRI (with the existing heavy utilization of the computer facilities, it would make run times unbearable). Further, it did not make sense to include the pallet response and ignore the stiffness of the blocking, for which we had no information. Thus, the pallets and blocking were included in the model as concentrated masses, distributed over the inner door.

An outline of the model developed for longitudinal impact of the CAMPACT is shown in Figure 11. It represents approximately one-quarter of the exterior door (the foam) and one-twelfth of the inner frame. The top and right sides of the model are longitudinal planes of symmetry. Only the front bay of the inner frame of the CAMPACT is described by finite elements. Lumped masses were added to the back of the front bay to represent the top two bays. Figure 12 shows more detail of the frame. The elements have been reduced (shortened) for clarity, the beams have a width dimension, and trusses are represented as lines. Ten beams were used to describe the inner frame adjacent to the door.

The door is shown in Figure 13. Beams were used to describe the door frame and triangular shell elements represented the honeycomb door. Bolts were inserted between the beams of the inner frame and door to join the two components together. This is shown in Figure 14.

To complete the geometry of the model, three-dimensional solid foam elements were added to the front of the door. The block of foam elements is shown in Figure 15. There are three elements in the longitudinal (crush) direction and six elements in the two transverse directions, for a total of 108 foam elements. The width and height of the foam block are greater than the door. This is seen more easily in the outline of Figure 11, which shows the location of the door relative to the foam. Constraint equations were used to couple the door to the foam in the longitudinal (y) direction.

Table 4 summarizes the elements used in the ADINA model. All elements were specified as nonlinear with both material and geometric nonlinearities permitted. After eliminating all boundary and dependent degrees of freedom (dof), the model had 702 equations. After optimization, the mean half bandwidth was 125.

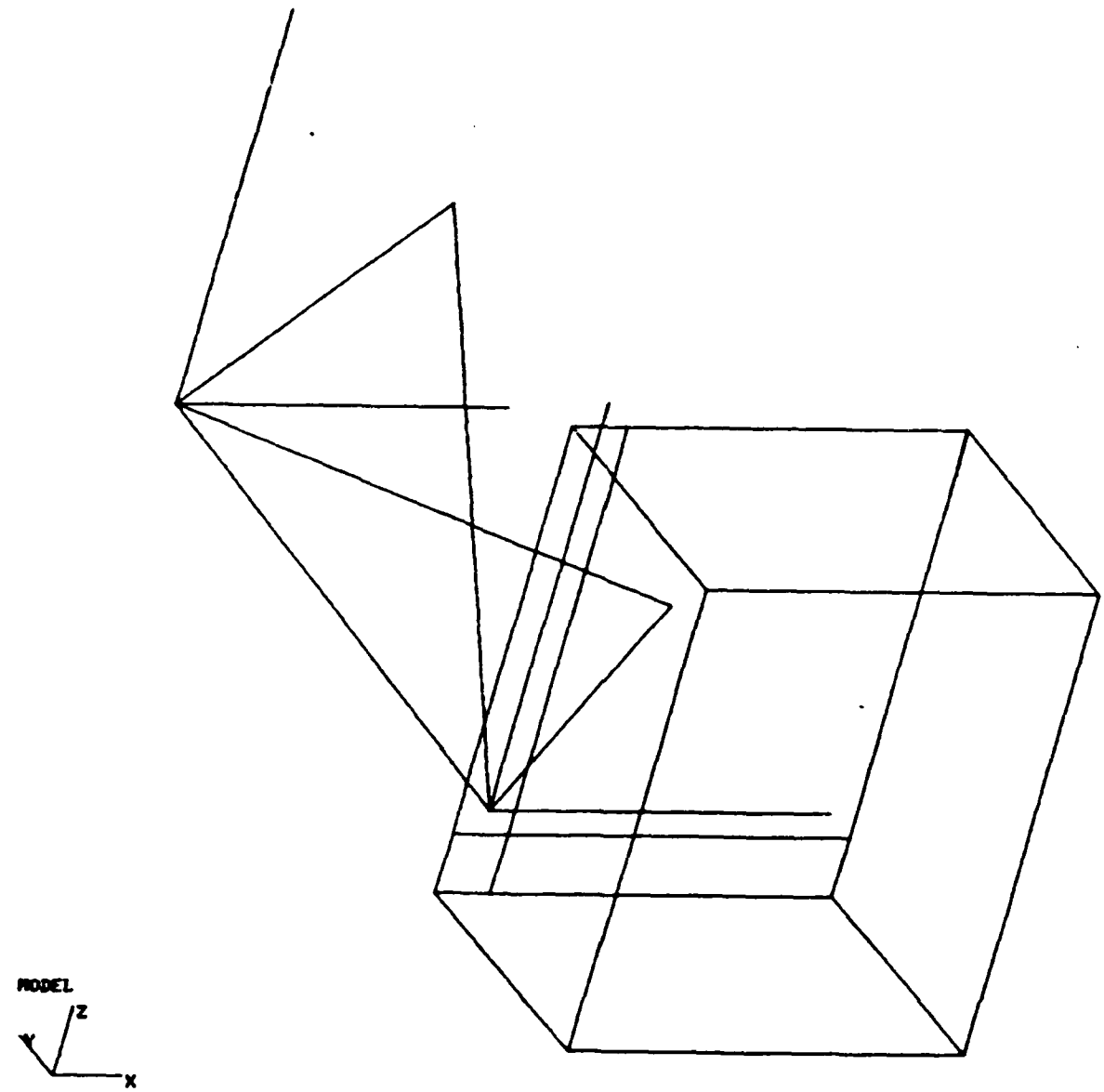

Figure 11. Outline of the Longitudinal Model

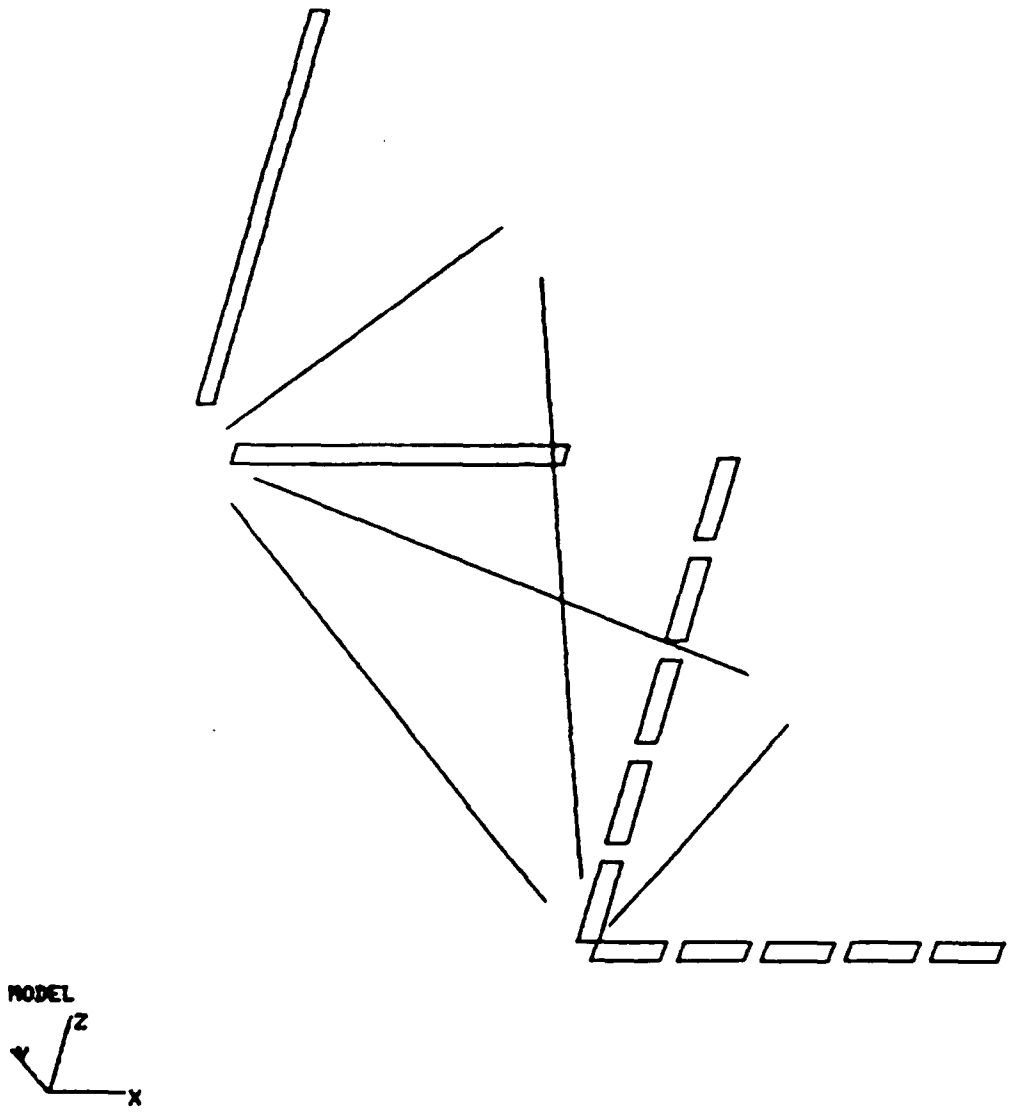

Figure 12. Inner Frame - Longitudinal Model

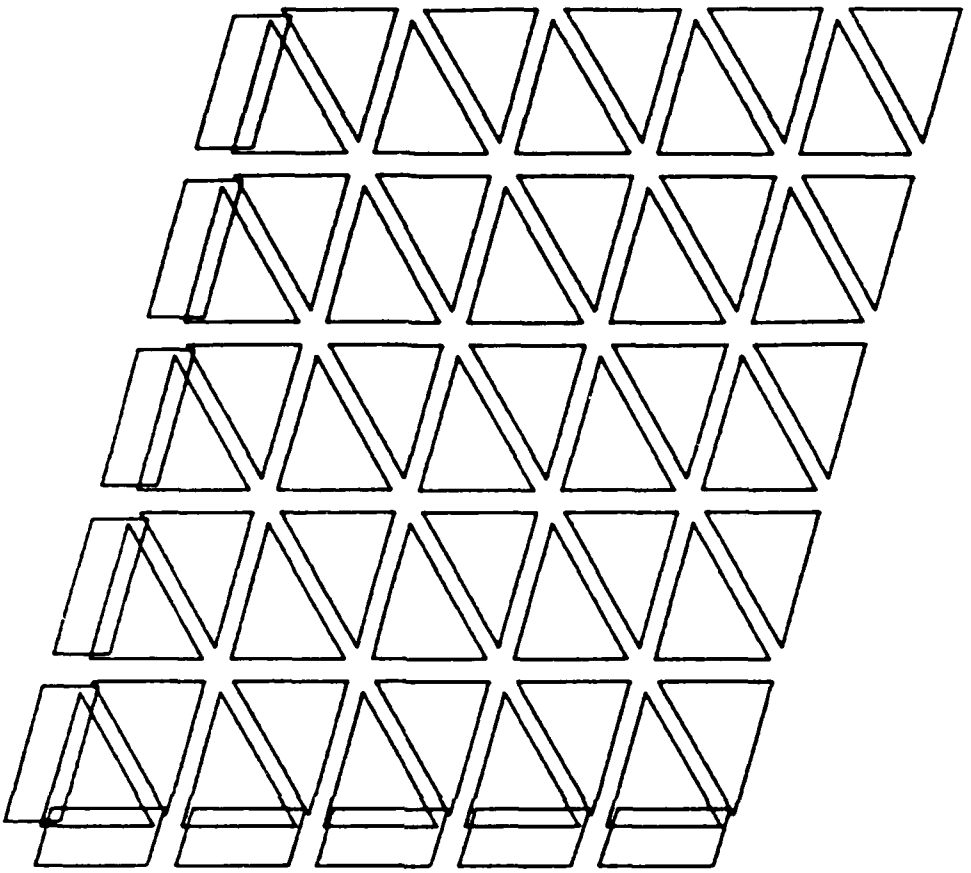

Figure 13. Door - Longitudinal Model

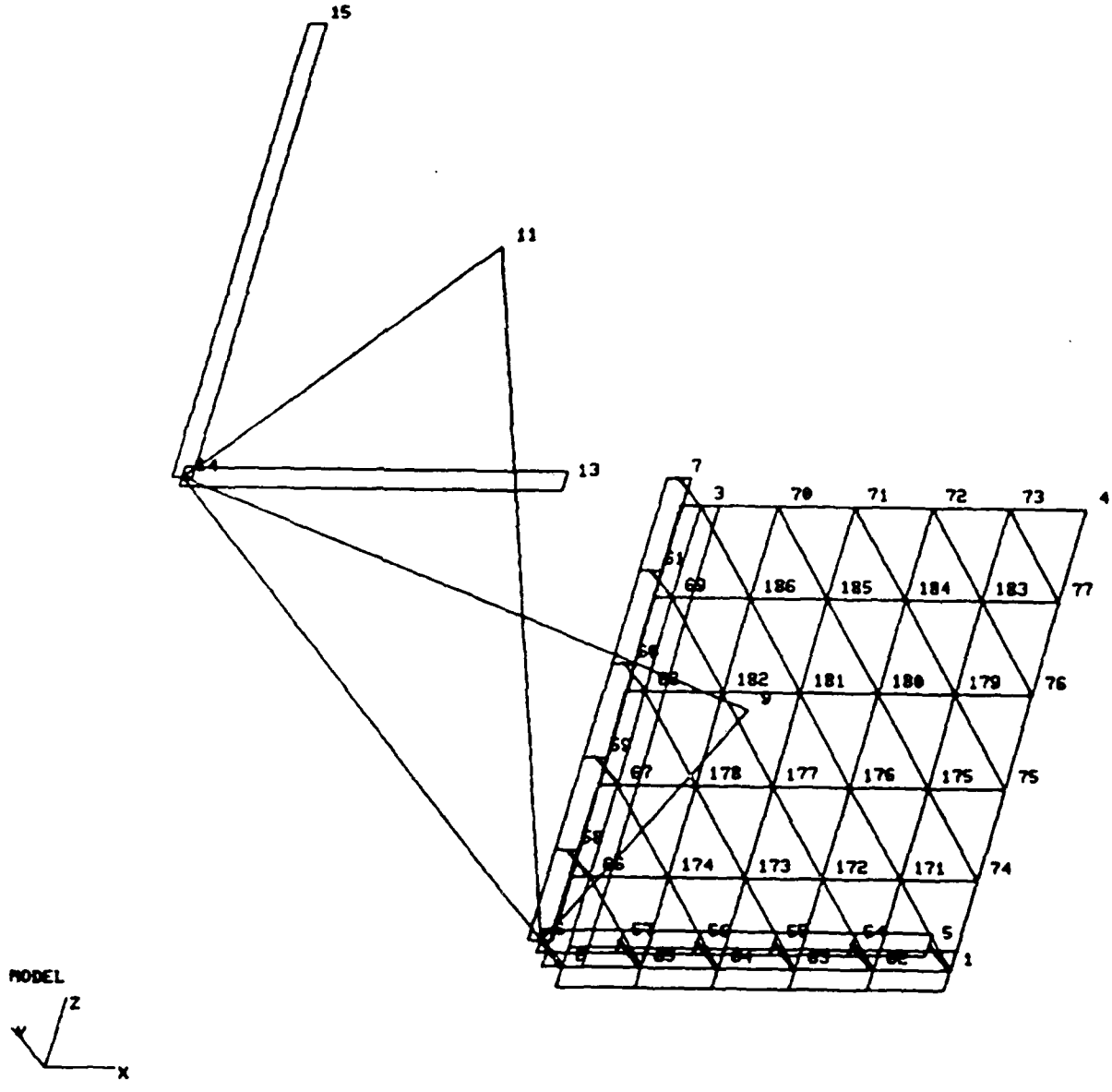

Figure 14. Inner Frame, Door and Bolts - Longitudinal Model

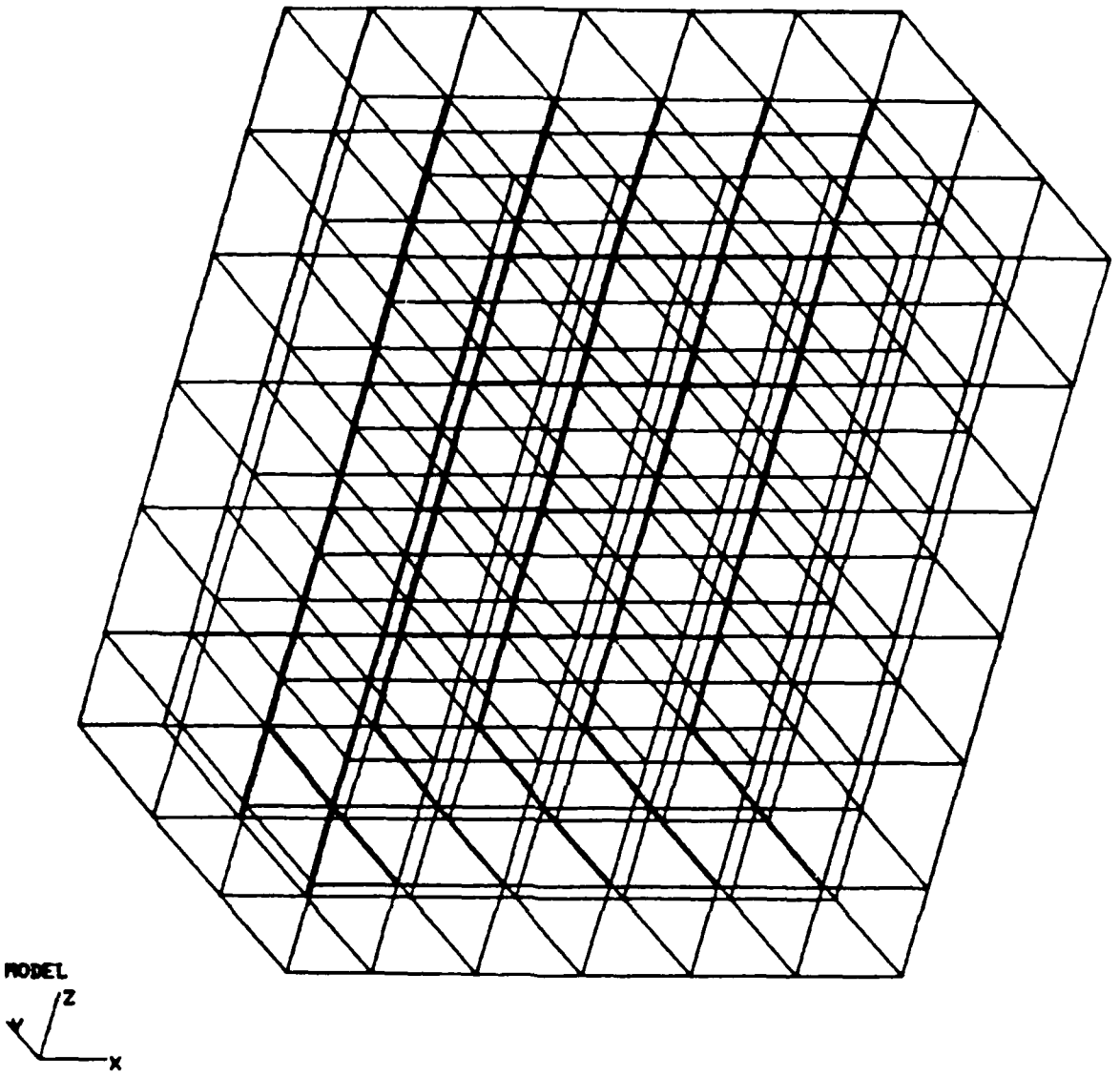

Figure 15. Foam - Longitudinal Model

Table 4. Elements and Nodes for the Longitudinal Model

Frame

3-D trusses	5
3-D rectangular beams (off-set)	12

Door

3-D rectangular beams (off-set)	10
3-D triangular shell elements	50

Bolts

Corner: 3-D circular beam	1
Symmetry planes: 3-D rect. beams	2
Other: 3-D circular beams	8

Foam

3-D 8-noded solid elements	108

Nodes

Total	384
Independent	248

b. Concentrated Masses

ADINA computes the masses of the elements in the grid and, for this problem, concentrated the masses at the nodal points. In addition to the element masses, concentrated masses were added to represent the internal equipment (pallets, blocking and floor roller assembly) and missing parts of the structure. The mass of the containment liner was added in a rational manner to the nodes of the inner frame (see Figure 12). These masses were quite small. The mass of the two upper bays of the inner frame were added to the upper corner node of the inner frame.

All internal masses were added to the door. One half of the mass of the floor roller assembly (600 lb) was added uniformly to the bottom row of nodes on the door (see Figure 13). Placing all of the roller mass on the door is somewhat conservative because the roller is wedged laterally against the sides of the inner frame; however, slipping will most certainly occur and this will represent the worst-case loading condition for the door. Mass of the pallets and blocking was distributed evenly to the remaining nodes of the door. This mass was estimated to be 11,300 lb, 10,800 lb for the eight pallets and 500

lb for the blocking. One-fourth of this weight was concentrated (in mass units) on the door. In all, 8844 lb of mass was added to the model at 50 nodal locations.

2. Impact and Boundary Conditions

As discussed previously, an idealized impact condition was assumed, whereby the end of the CAMPACT struck uniformly against the rigid surface. To achieve this condition, a uniform velocity of 527 inches per sec was applied to all nodes of the model. This velocity corresponds to a drop height of 30 ft. Figure 16 shows the velocity vectors applied to the model. Velocities at the impacting surface are also shown in the figure, but these were eliminated by constraining the nodal degrees of freedom (dof) in the y-direction on the striking surface.

The translational dof of the striking surface are shown graphically in Figure 17. Small lines at the nodal locations indicate the dof directions in which motion was permitted. Note that no motion is allowed in the y-direction on the impacting surface. The only other boundary conditions applied to the model were those of symmetry applied to the top surface (horizontal mid-plane) and right side (vertical mid-plane) of the CAMPACT. On the top surface z-displacements, x-rotations and y-rotations were restrained; on the right side x-displacements, y-rotations and z-rotations were restrained.

3. Solution Results

The model was solved using the ADINA computer code. A direct integration of the equations of motion was performed by a Newmark integration procedure. Equilibration iterations were performed at each integration time step of 0.0001 sec, and the stiffness matrix was reformulated at every third (and sometimes every) time step. The integration was carried out to a time of 0.025 sec. All of the steel components in the model, except for one bolt, had returned to a totally elastic state at 0.022 sec. At 0.024 sec, all steel components were elastic, and at 0.025 sec, only two foam elements were still showing plasticity, one at one integration point and the other at two integration points.

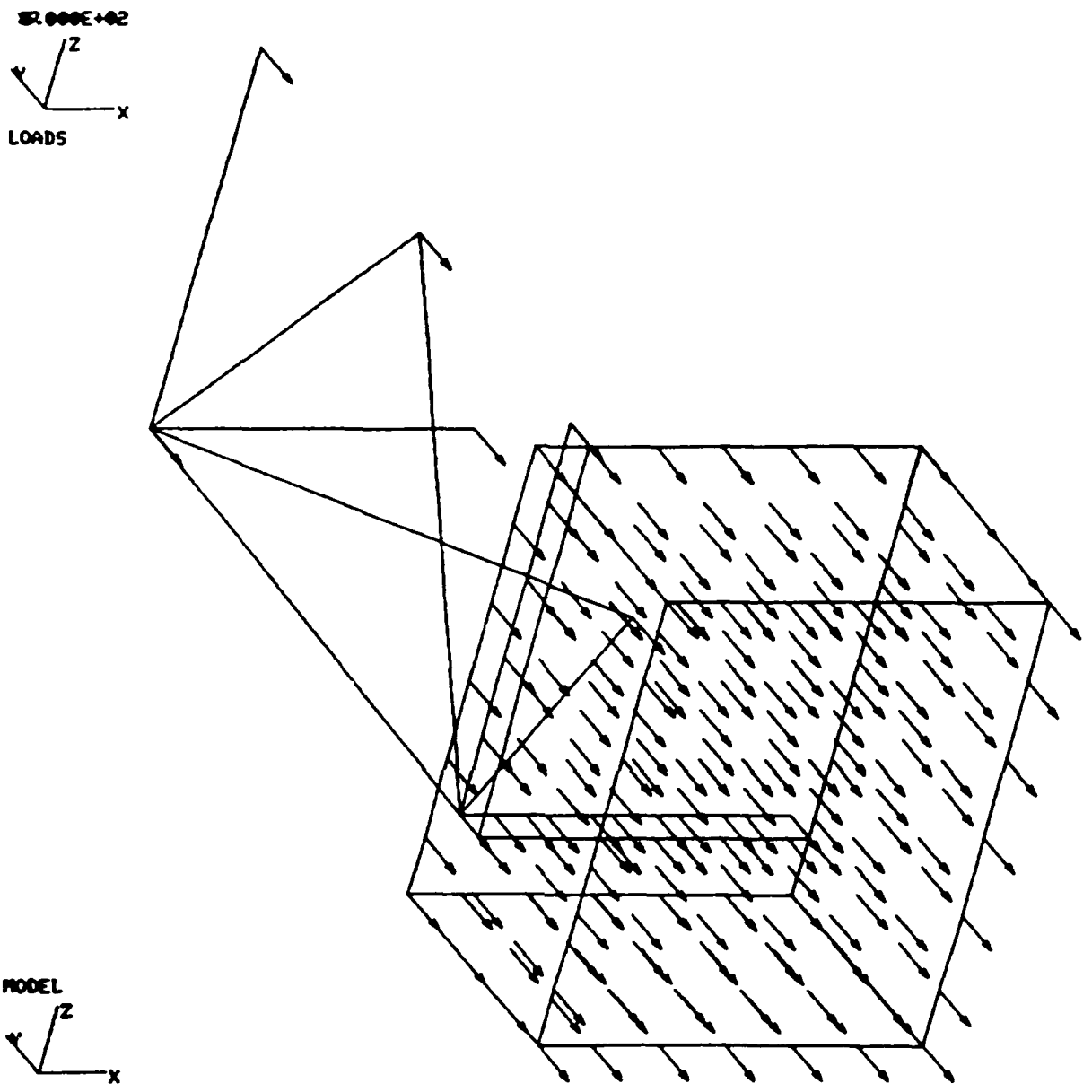

Figure 16. Velocity Vectors - Longitudinal Model

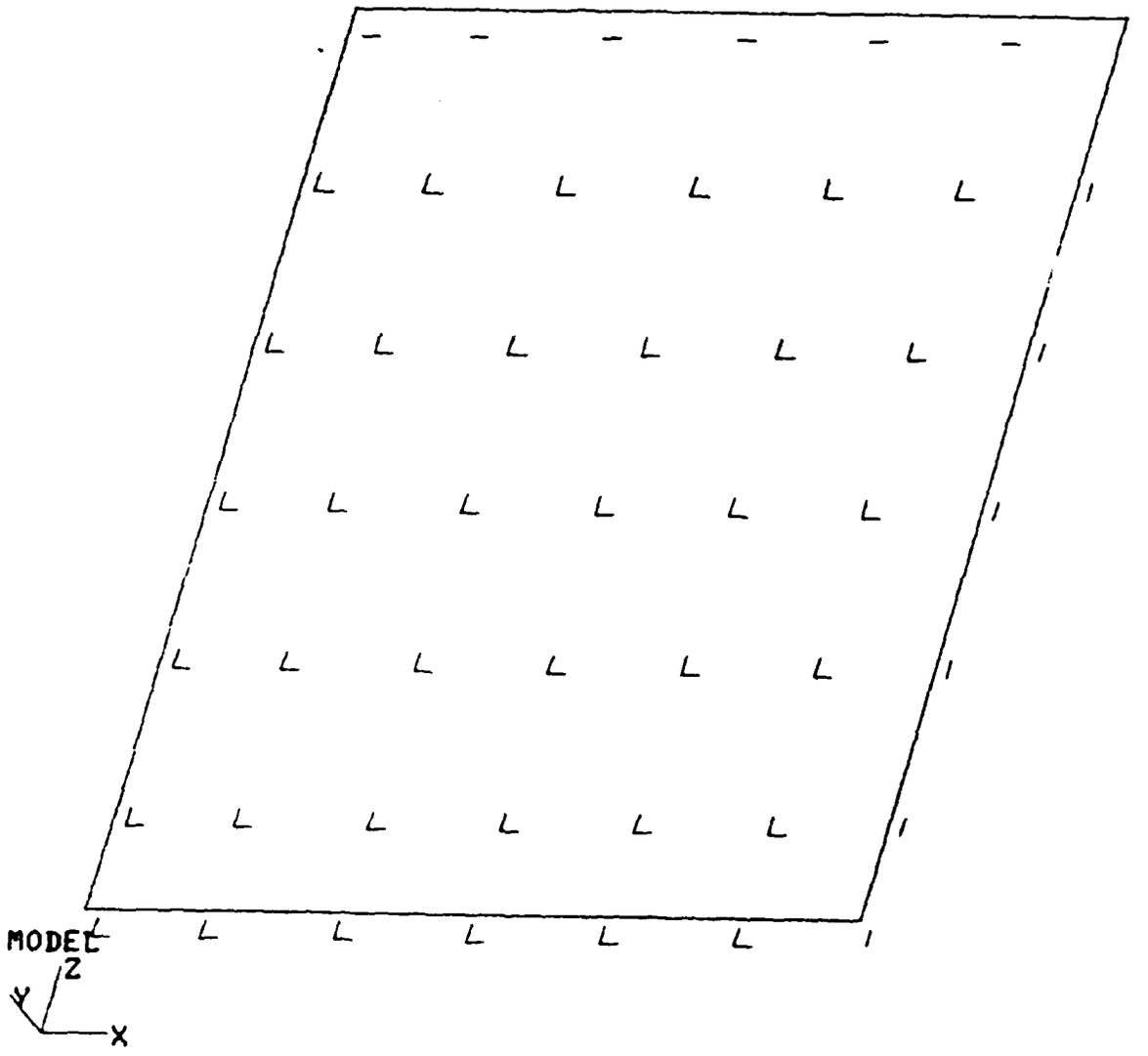

Figure 17. Translational Degrees-of-Freedom at the Impact Surface of the Foam - Longitudinal Model

Four points on the door are plotted out to 0.022 sec in Figure 18*. At this time, nodal points 118 and 247 (on the horizontal centerline) have reached their peak displacements. Nodal points 10 and 166 (on the bottom of the door) reach their peaks at 0.023 sec. Rebound of all points on the door and frame is occurring after 0.023 sec. Some distortion of the door is apparent, and some local yielding of the door frame occurred at the horizontal centerline. This result and others are discussed on a component by component basis in following paragraphs.

Inner frame--Yielding in the inner frame occurred in the longitudinal truss member of Figure 12 and in the beams adjacent to the door. The axial residual compressive strain in the truss member reached 0.08%, which indicates that it just yielded. As shown in the preliminary analyses of Section II.C.3, buckling of the frame should not occur for small plastic straining.

Distortion of the inner frame around the door occurred, just as it did for the door. This was indicated by Figure 18 discussed previously. Distortions in the frame were exaggerated in the model by compressive yielding of the bolts which joined the door and the frame. This yielding was a consequence of the finite element model and will not occur in the CAMPACT. In the model, the bolts were allowed to compress; whereas, in the CAMPACT, the inner frame and door frame are in direct contact and bolt compression is prevented. In spite of the exaggerated distortion permitted by the model, the residual plastic strain in the frame at the door reached only 0.26%, which is small. It should be no more than that which occurred in the door.

Door--Distortions in the door, indicated by Figure 18, caused minor yielding of the door frame to occur at the horizontal centerline. Residual plastic strain in the door reached only 0.02% at this location, which is insignificant. The load on the door which produced these distortions was caused by the corner loads from the frame and the loads at the bottom of the door from the roller assembly. No yielding occurred in the honeycomb door panel.

Bolts--As noted above, axial compression of the bolts occurred which would not occur in the CAMPACT. Because this behavior was not prevented in the model, compression strains in the corner bolt reached 6.9%. Of this

*Figure 18 was drafted in final form before the final calculations from 0.022 sec to 0.025 sec were made.

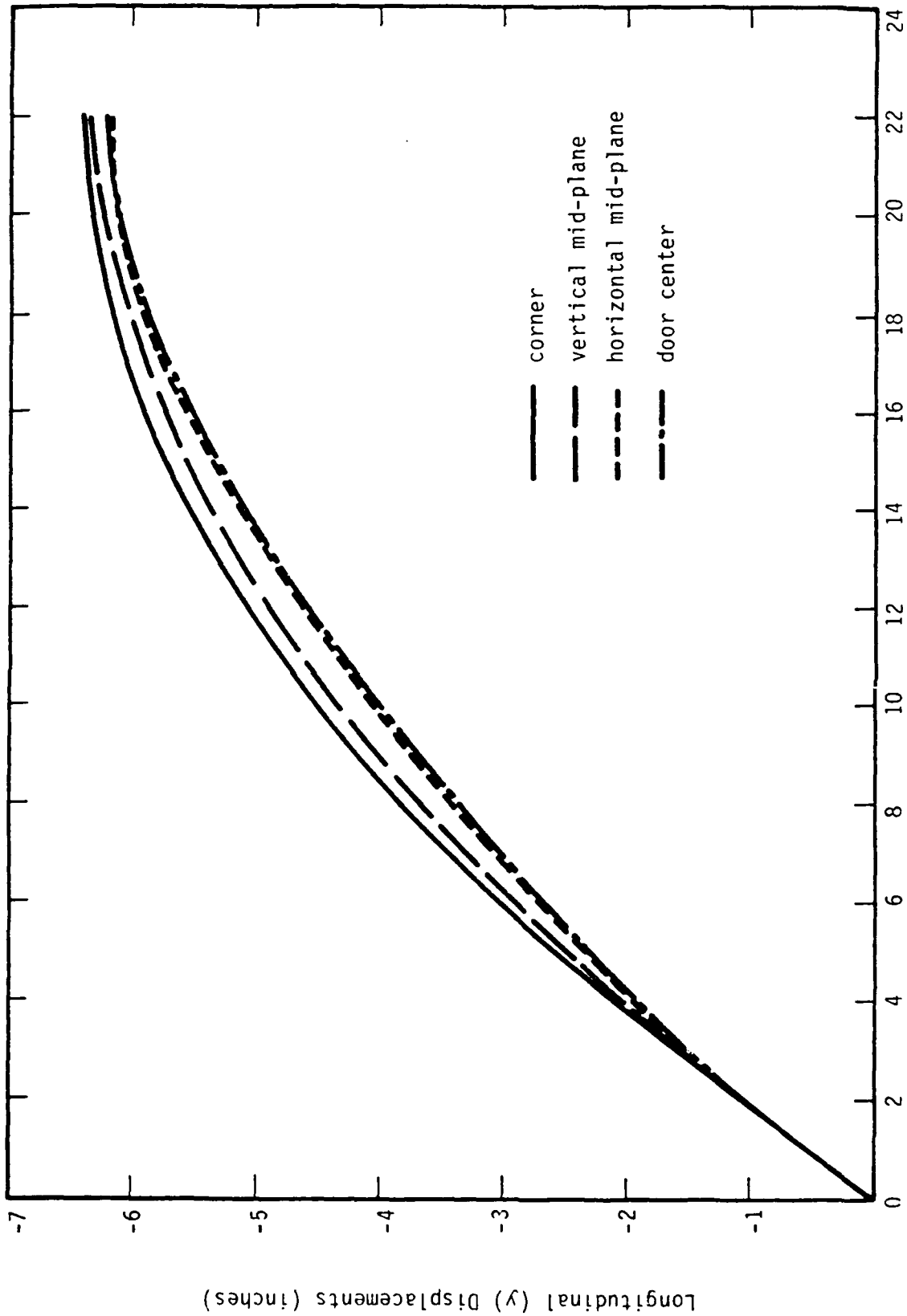

Figure 18. Displacements of the door after impact in the y-direction

strain, 5.4% was produced by axial compression and 1.53% by bending. These strains were caused by simplified modeling of this region of the CAMPACT and we estimate that no plastic straining of the bolts would have occurred in the CAMPACT during longitudinal impact. No tension occurred in any of the bolts, and smaller strains were produced in bolts away from the corner. The next highest strains occurred in the bolts adjacent to the corner and they reached 2.7%. Bolts on the centerlines of the CAMPACT did not yield, nor did those adjacent to them.

Foam--Full plasticity occurred in all foam elements. Maximum residual plastic strains reached 23.4%. They occurred in elements immediately below the corner of the door. Nominal strains in the foam were in the range of 17-19%. The foam yields at 4% strain, and lockup occurs at about 50% strain, so the foam can absorb considerably more energy than it absorbed during this simulated 30 ft. drop.

Door Seal--No separation of the door frame and inner frame will occur during longitudinal impact. All bolts are placed in compression by the impact which will serve to increase the compression between the two members; however, relative rotation of the door and frame can and did occur which affects the compression in the seal. The amount of relative rotation in this analysis reached a maximum value of 0.0194 radians. From the bolt location to the center of the seal is about 2 inches, so the maximum separation at the seal caused by this rotation would be about 0.0388 inches. This separation is 16.2% of the initial seal compression [2]; thus, no seal leakage should occur as a result of longitudinal impact produced by a 30 ft. drop.

4. Estimate of Impact Crush Strength

Using the results of the ADINA calculations, an equivalent crush force was determined for the CAMPACT. It can be used to evaluate impact of the CAMPACT, but only under very similar conditions. The calculations, reported in Appendix B, equate the kinetic energy at impact to the deformation energy of the CAMPACT. Using the maximum deformation computed in the CAMPACT by the ADINA analyses, the equivalent crush force was found to be 1.27×10^6 lb. This value is just slightly higher than the crushing strength of the foam in the end of the CAMPACT, which is 1.25×10^6 lb. Thus, most of the energy absorbed by the CAMPACT during longitudinal impact was absorbed by the foam.

E. Lateral Impact

1. Model Development

a. Finite Element Grid

As noted in Section I symmetry conditions were imposed to reduce the size of the finite element models developed for analysis with the ADINA computer code. For the lateral impact model, a vertical plane of symmetry normal to the longitudinal axis was taken at the midpoint of the inner frame. Figure 19 shows a line drawing of the model used for the lateral impact. The impact surface is on the left side of the figure while the door is forward. For this figure the viewpoint is forward, to the left and above the CAMPACT. This viewpoint will be utilized throughout this section. Note that the CAMPACT is oriented as it would be in service. The various elements of the model can be seen in Figure 20. This drawing is complex and the various elements are shown separately in Figures 21 to 24.

The front half of the inner frame was modeled as shown in Figure 21. All frame members except those at the door were represented by nonlinear 3-D truss elements. It was felt that their primary load carrying capabilities would be axial. In most cases, bending would be prevented by the proximity of the foam elements. This approximation allowed for a reduction in model degrees of freedom. Various dof associated with the nodes of the inner frame were coupled using multiple-point constraints. These constraints were applied in regions where the stiffness was small and would tend to produce numerical instabilities during the dynamic nonlinear analysis. Different constraints were utilized for the static and dynamic solution. The result of the dynamic constraints is that the frame surface will act as a unit with limited local deformation. As with the longitudinal model, the region near the door was described in the most detail. The frame members in this region were represented by 3-D beam elements.

Figure 22 shows the door used in this model. The honeycomb panel was represented by triangular plate bending elements. The plate elements were assumed to remain elastic during the analysis. Calculations showed that the bending stiffness of the honeycomb was dominated by the thickness and strength of the face plates themselves. The core provided little resistance to bending except to separate the face plates. The 4 in. by 6 in. edge beam of the door was modeled using beam elements. The size and material properties of these elements were adjusted to match the bending about

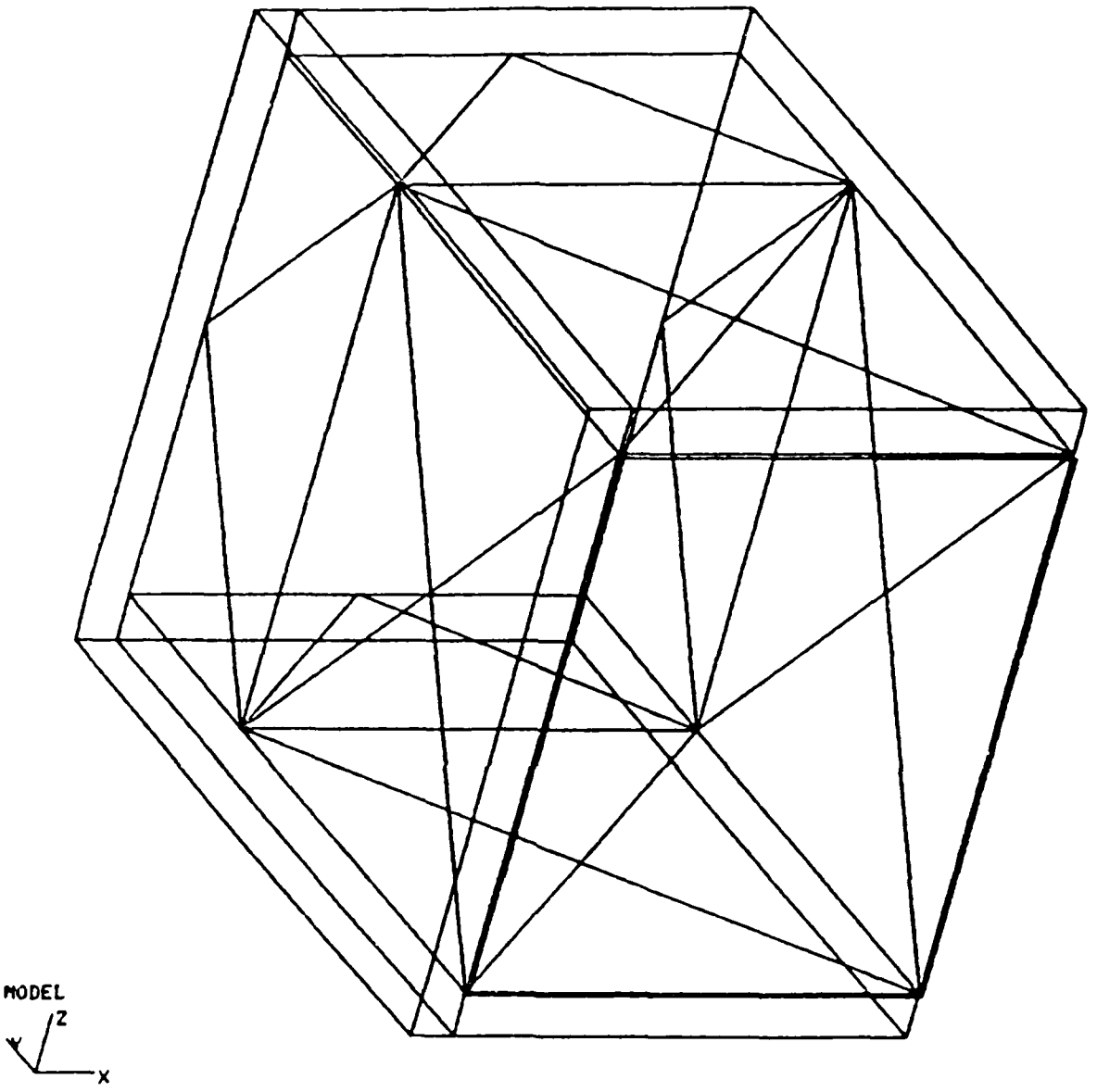

Figure 19. Outline of the Inner Frame and Foam - Lateral Model

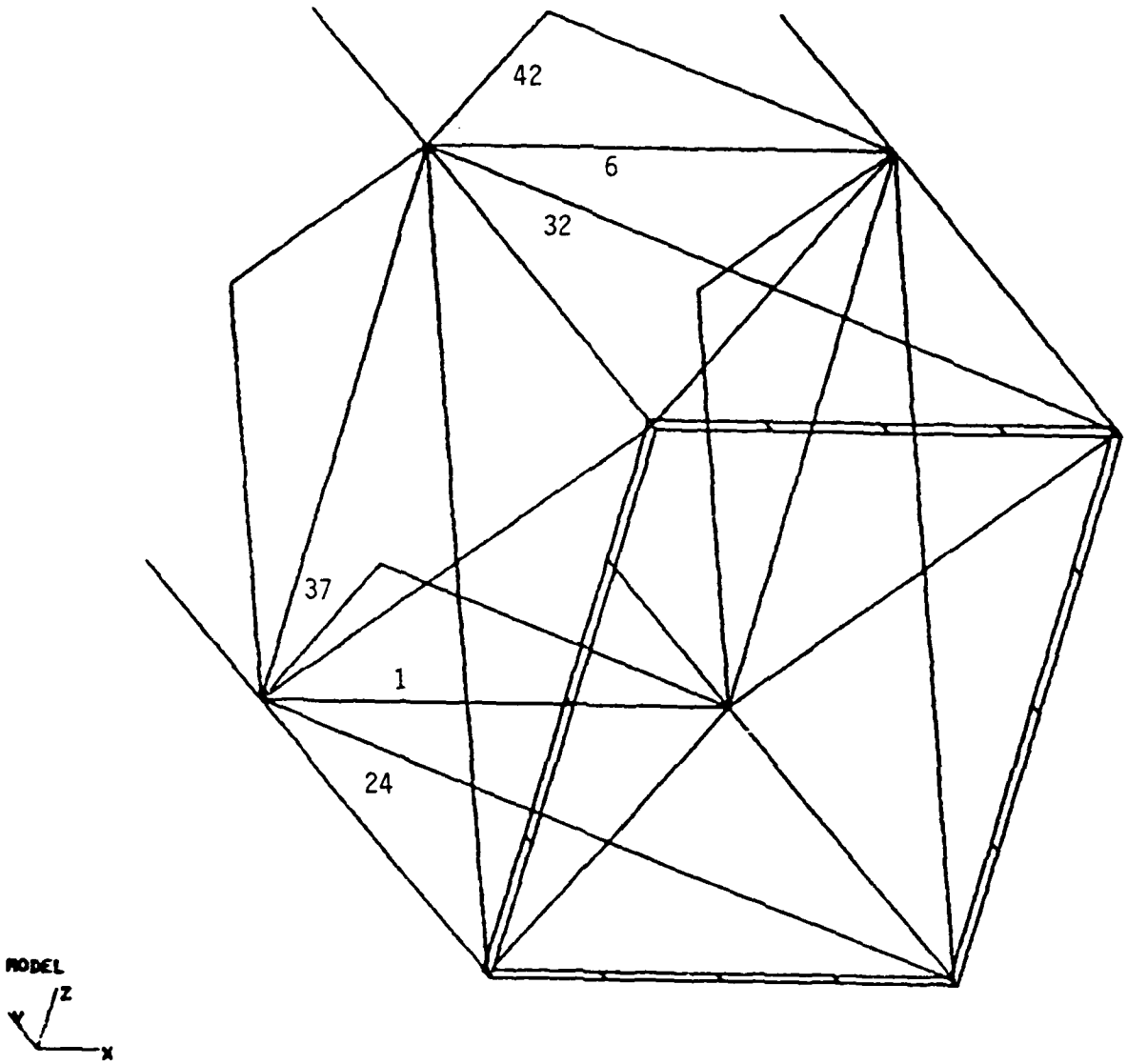

Figure 21. Trusses and Beams of the Inner Frame - Lateral Model

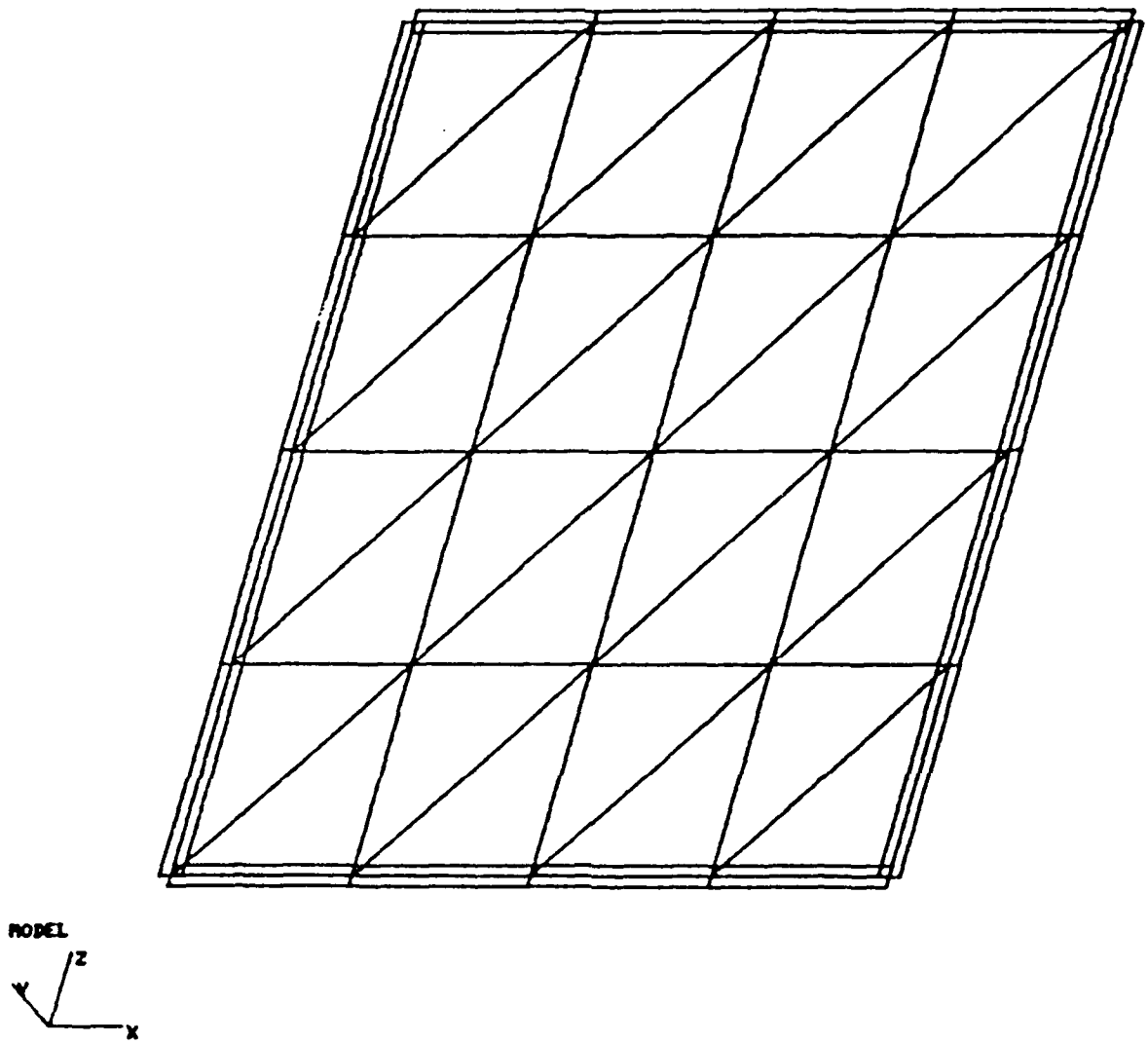

Figure 22. Door - Lateral Model

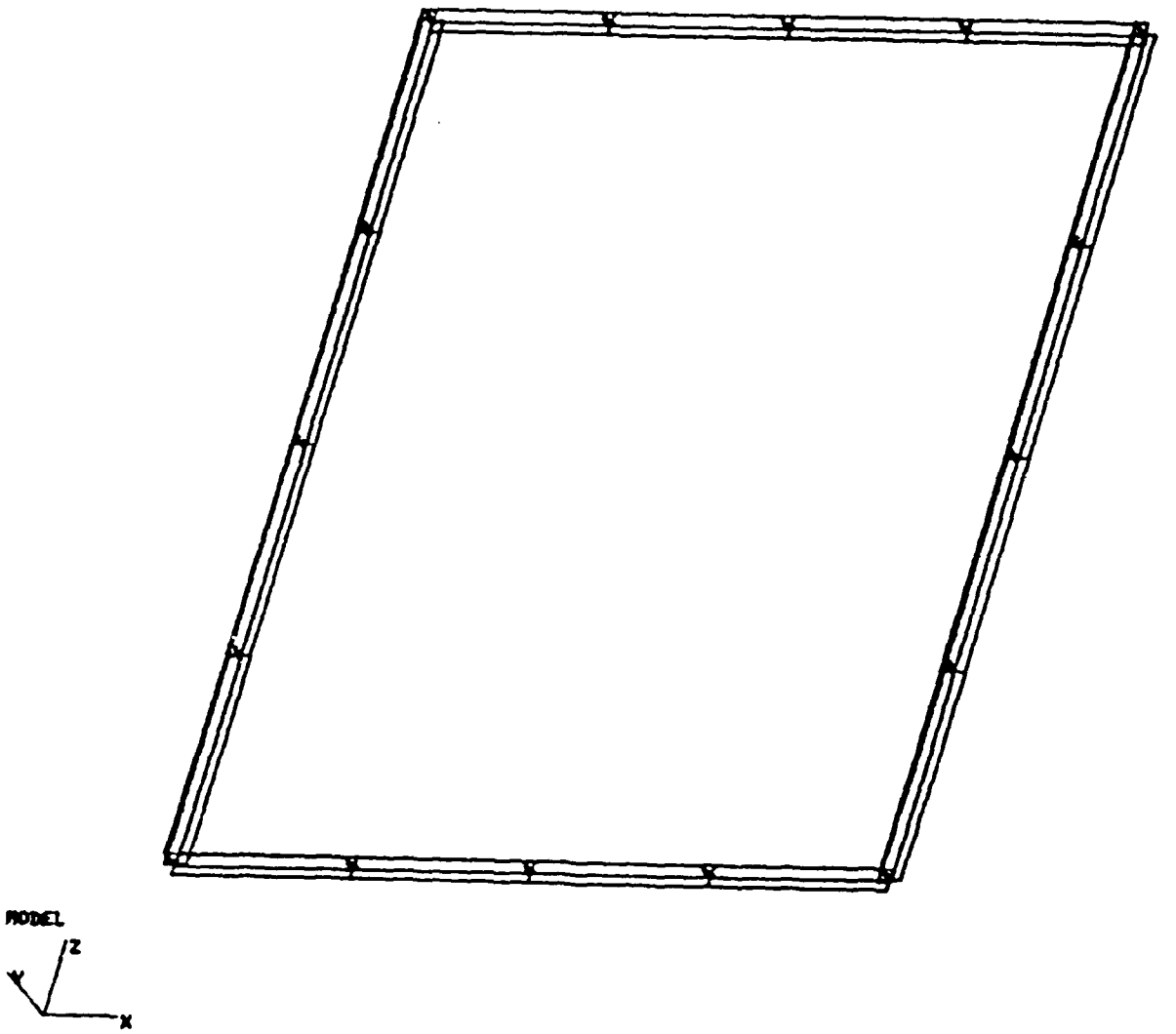

Figure 23. Inner Frame, Door Frame and Interconnecting Bolts - Lateral Model

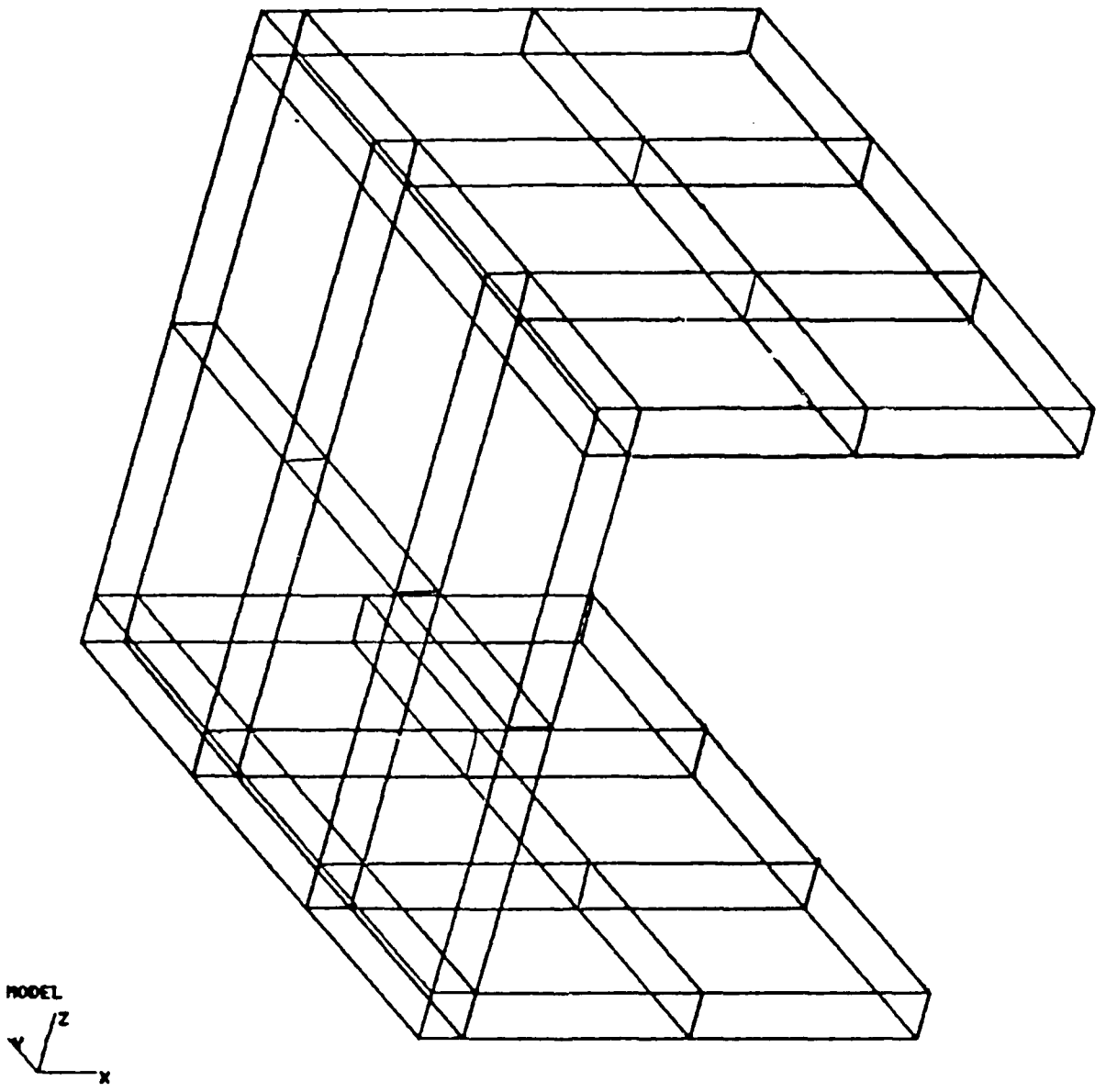

Figure 24. Foam Elements - Lateral Model

the two axes of the member. The resulting member had an axial stiffness greater than the CAMPACT.

Attachment of the door to the inner frame was again made using beam elements. For this model, the four corner bolts were modeled as in the CAMPACT itself. Only three beams were utilized to model the nine bolts actually present on each side of the door in the CAMPACT. Since for this model the primary action of the bolts would be in shear, the resulting beams were proportioned to have the correct area, not the correct bending stiffness. In the CAMPACT, the centerlines of the door and inner frame members are seven inches apart. For the longitudinal model, this distance was maintained in the model. For the lateral impact model, the distance was reduced to one inch. It was felt that this would more accurately represent the actual conditions. Some details of the door-to-inner-frame connection can be seen in Figure 23.

The foam elements utilized in this model are seen in Figure 24. Only the foam on the side where the impact occurred and on the top and bottom was modeled. The foam on the opposite side from the impact was ignored because the material has little resistance to tension. The top and bottom foam was modeled because of the expected three-dimensional response of the system. The foam forward of the door was also ignored since it will not significantly contribute to the energy absorption characteristics of the lateral model. In this model, only one element was used through the thickness of the foam in the direction of impact. To limit numerical instabilities, a token mass of 0.01 lb-sec^2/in was added to all foam nodes on the upper and lower surfaces.

In addition to the approximations described above, the following assumptions were made concerning the model.

* Neglect of the outer frame--The basic assumption here is that the energy at impact associated with the outer frame, puncture panels and the outer skin will be absorbed by local deformation of the outer frame. In addition, motions of the inner frame occur independently from the outer frame for lateral impact. We believe that is a good assumption for simultaneous impact between the striking surface of the CAMPACT and the rigid surface. Further, the contact surface between the structural

foam and the outer frame at the puncture panel is smooth. The bond strength at this contact surface is unknown and slippage could occur. If slippage does not occur, then this assumption is equivalent to postulating that the outer frame and foam translate laterally during impact at the same rate as the inner frame.

* Neglect of the containment liner stiffness and strength--Stiffness of the liner could be quite high in shear if it does not buckle but quite low in compression. This phenomenon is not easily represented in the finite element model. Because the primary response during lateral impact is expected to be compression, its contribution to the stiffness and strength of the inner frame was neglected. Its mass was included in the model.

* Neglect of the puncture panel system--The puncture panel should absorb little energy during the lateral impact. It is assumed that the kinetic energy associated with this mass will be absorbed by the outer frame.

* Neglect of pallet response within the CAMPACT--The assumption of rigid body motion of the pallets during impact is a reasonable assumption for the lateral analysis. This assumption should produce high (conservative) loads on the side wall. Further, it did not make sense to include the pallet response and ignore the stiffness of the blocking, for which we had no information. Thus, the pallets and blocking were included in the model as concentrated masses, distributed as required.

Table 5 summarizes the elements used in the ADINA model. All elements except the door plate elements were specified as nonlinear with both material and geometric nonlinearities permitted. After eliminating all unnecessary degrees of freedom, the model had 347 equations. After optimization, the mean half bandwidth was 63.

Table 5. Elements and Nodes for the Lateral Model

Frame	
3-D truss elements	44
3-D beam elements	16
Door	
3-D beam elements	16
Triangular plate elements	32
Bolts	
Corner: 3-D circular beam elements	4
Sides: 3-D circular beam elements	12
Foam	
3-D 8-noded solid elements	24
Nodes	
Active	109

b. Concentrated Masses

ADINA computes the mass matrix of the model from the lumped masses of the elements and concentrated masses at the nodal points. The concentrated masses were added to represent the internal components (pallets, blocking and floor roller assembly) and elements ignored in the stiffness formulation. For this model, the locations of the added masses in the three principal axes were different. This reflects our estimation of how they would be distributed during the lateral impact. The mass of the containment liner was added to the nodes on the inner frame in proportion to the tributary area of each node. This mass was associated with all three axes. One half the mass of the roller floor (600 lb) was added uniformly to the bottom row of nodes on the door in the longitudinal direction, along the intersection of the side wall and floor for the lateral direction and distributed over the floor for the vertical direction.

Mass of the pallets and blocking was distributed over the side for lateral response, over the door for longitudinal response, and over the floor for vertical response. For the vertical direction, the load was distributed uniformly over the floor. For the longitudinal and lateral directions, the load was distributed linearly from the floor (1.75 times the average) to the top (0.25 times the average) on the side and door, respectively.

An apparent error occurred during the automatic generation of the concentrated masses which resulted in less mass and lower than desired gravitational forces in the static analyses of the lateral model. The error was found and corrected before the impact calculations were performed. For the static analyses, the amount of added concentrated mass for the three axes relative to the required mass was: X-axis 61%, Y-axis 94% and Z-axis 78%.

2. Impact and Boundary Conditions

As discussed previously, an idealized impact condition was assumed, whereby the side of the CAMPACT struck uniformly against a rigid surface. To achieve this condition a uniform velocity of 527 in/sec was applied to all nodes of the model. This velocity corresponds to a drop height of 30 ft. Figure 25 shows the velocity vectors applied to the model. Velocities at the impacting surface are also shown in the figure, but these were eliminated by constraining the nodal dof in the x-direction on the striking surface.

The translational dof of the model are shown graphically in Figure 26. Small lines at the nodal locations indicate the dof direction in which motion was permitted. Note that no motion is allowed in the x-direction on the impacting surface. The only other boundary conditions applied to the model were those of symmetry applied at the centerline of the CAMPACT. On this surface, the y-displacement, x-rotation and z-rotation were restrained at each node.

In addition to restraints, some of the the nodes were coupled to other nodes along specific axes. These were primarily on the side opposite the impact where the trusses were not capable of carrying a load in the x-direction. For these nodes, the x-response was coupled to the appropriate x-responses at nodes that did have a component of stiffness in the x-direction. Additional nodal restraints were added to the dynamic model as described previously.

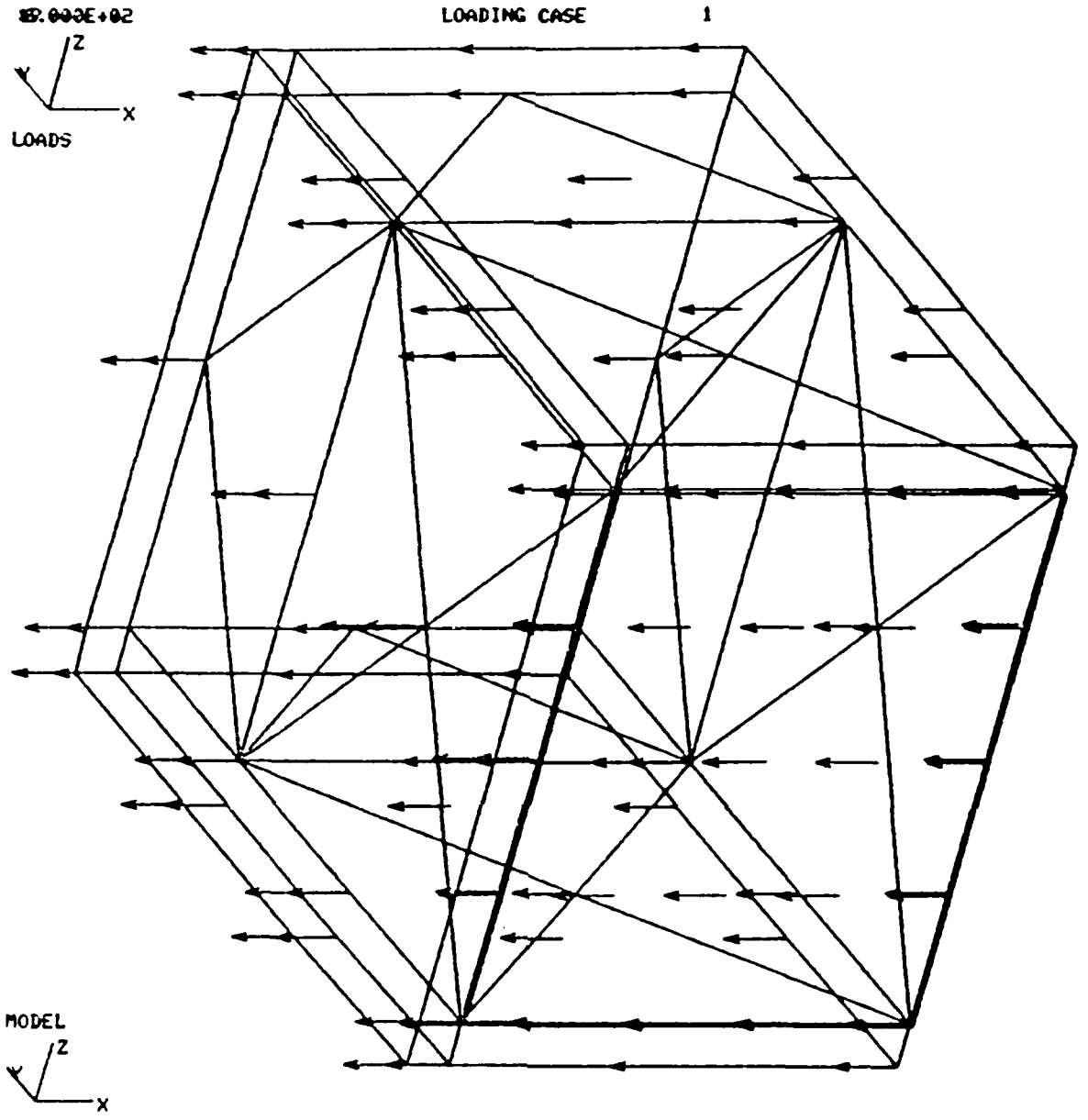

Figure 25. Velocity Vectors - Lateral Model

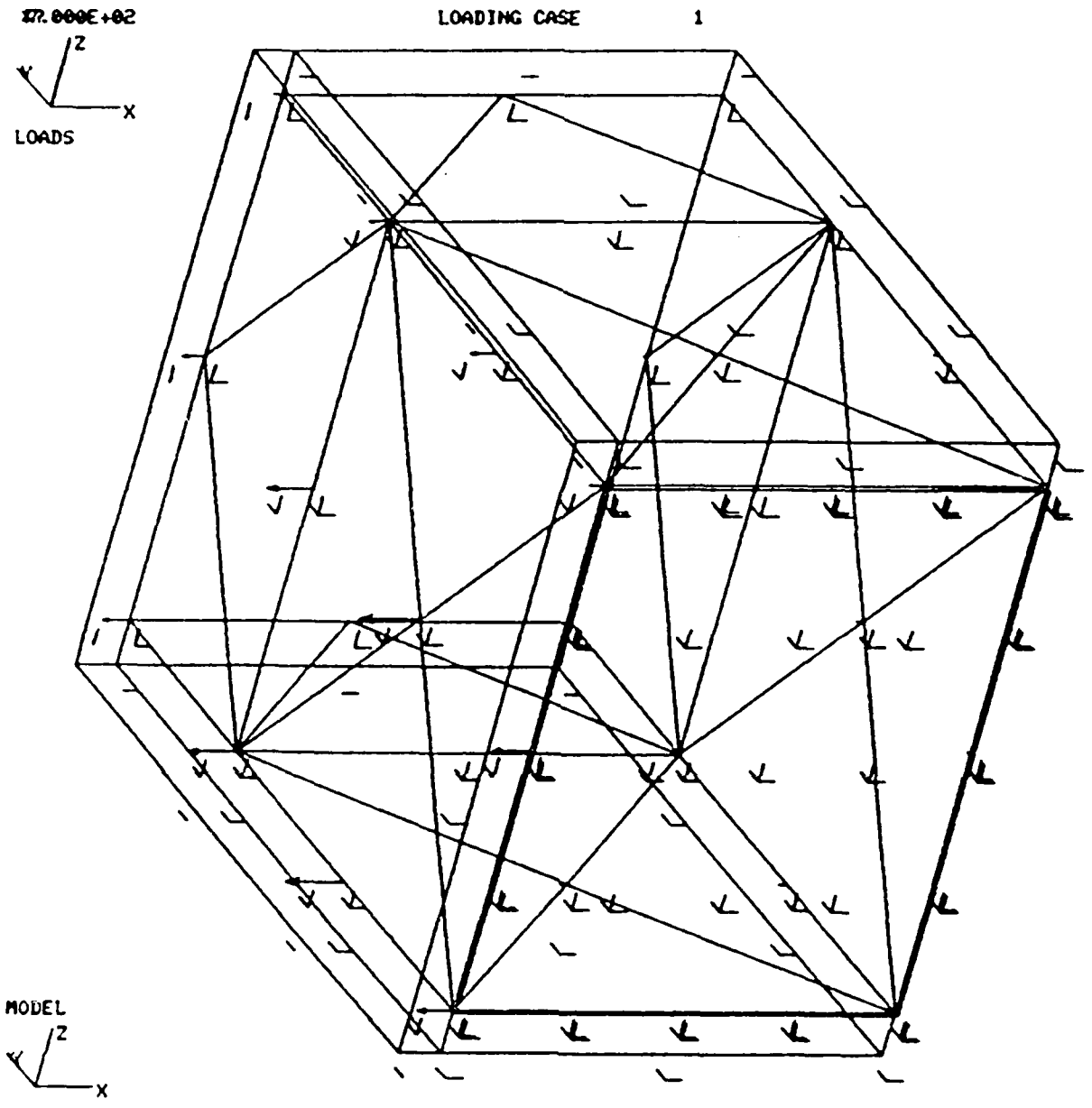

Figure 26. Translational Degrees-of-Freedom - Lateral Model

3. Solution Results

a. Static Results

Two different static load cases were applied to the model. They corresponded to a 1g acceleration in the lateral (x) direction and a separate 1g acceleration in the vertical (z) direction. The loads applied to the nodes for the first load case, lateral acceleration, are shown in Figure 27. These represent the concentrated masses to which the lumped masses of the elements were added. The resulting deflected shape is shown in Figure 28. Note that the deflections are multiplied by a factor of 5000 in relationship to the geometry of the model to make them visible. For the nodes on the inner frame closest to the impact surface, the average defection was 0.00059 inches with a maximum of 0.00146 inches. Making a correction associated with the concentrated masses, the preliminary analysis deflection for this direction is 0.00085 inches (0.61 x 0.0014), which compares favorably. There is significant local variation of the displacements which can be seen from Figure 28. These are plots of the deflected shape as seen from in front and above the model. On the back surface of the inner frame, opposite the impact surface, the displacement is more uniform with an average of 0.00121 inches and a maximum of 0.00155 inches. This indicates that there will be a variation in deflection between the impact and the opposite sides of the inner frame. One observation from Figure 28 is that there is more deflection at the bottom than at the top. This is representative of the distribution of the pallet loads and how they were applied.

A similar analysis for the vertical static load was also performed. The load (Figure 29) and displacements (Figure 30) are as expected. In this case, the loads are more uniform and so the results show less localized deformations. The average displacement was 0.0087 with a maximum at the center of the panel of 0.0179 inches. In section II.C.2, the preliminary calculation for the static deflection in the vertical direction gave a prediction of 0.0013 inches. Accounting for the reduced mass used in the static ADINA calculations (78% of the actual mass as explained in Section II.E.1.6), the corresponding prelimninary static deflection in the vertical direction would be

$$\delta_{st} = 0.78 \times .0013 \text{ inches} = 0.0010 \text{ inches}$$

which compares favorably.

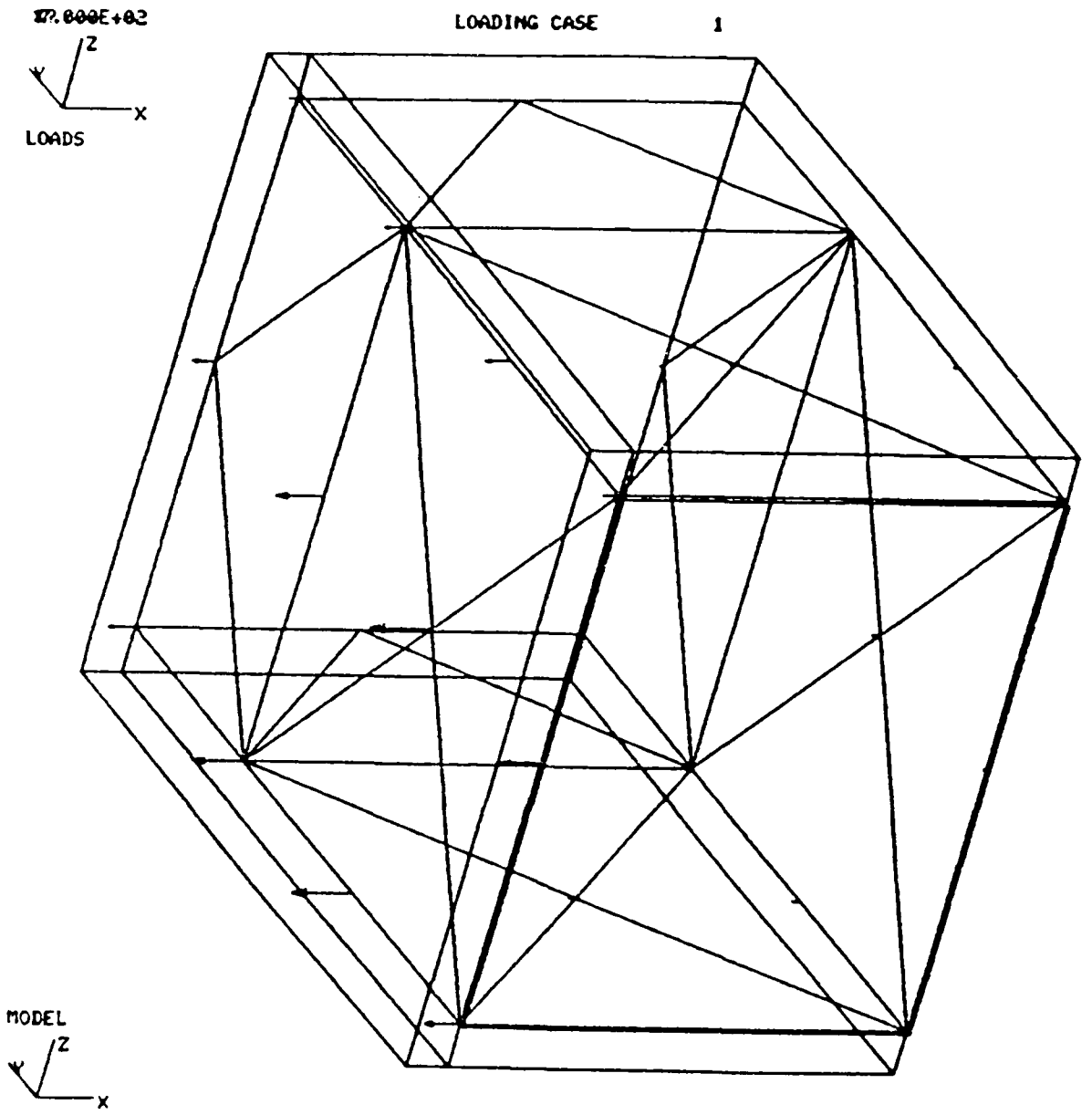

Figure 27. Static Load Case 1 - Lateral Model

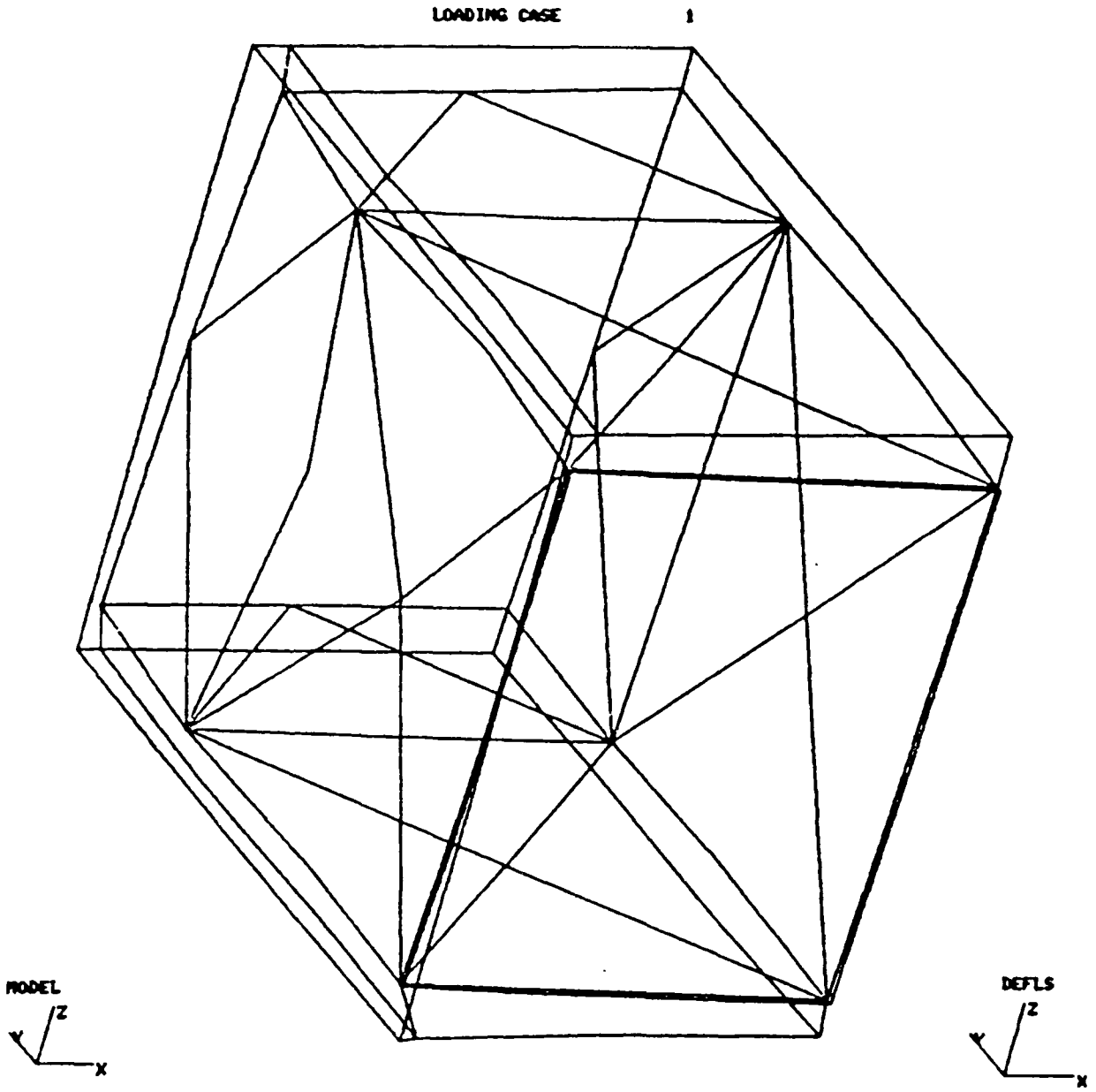

a. isometric view

Figure 28. Deflected Shape - Static Load Case 1 - Lateral Model

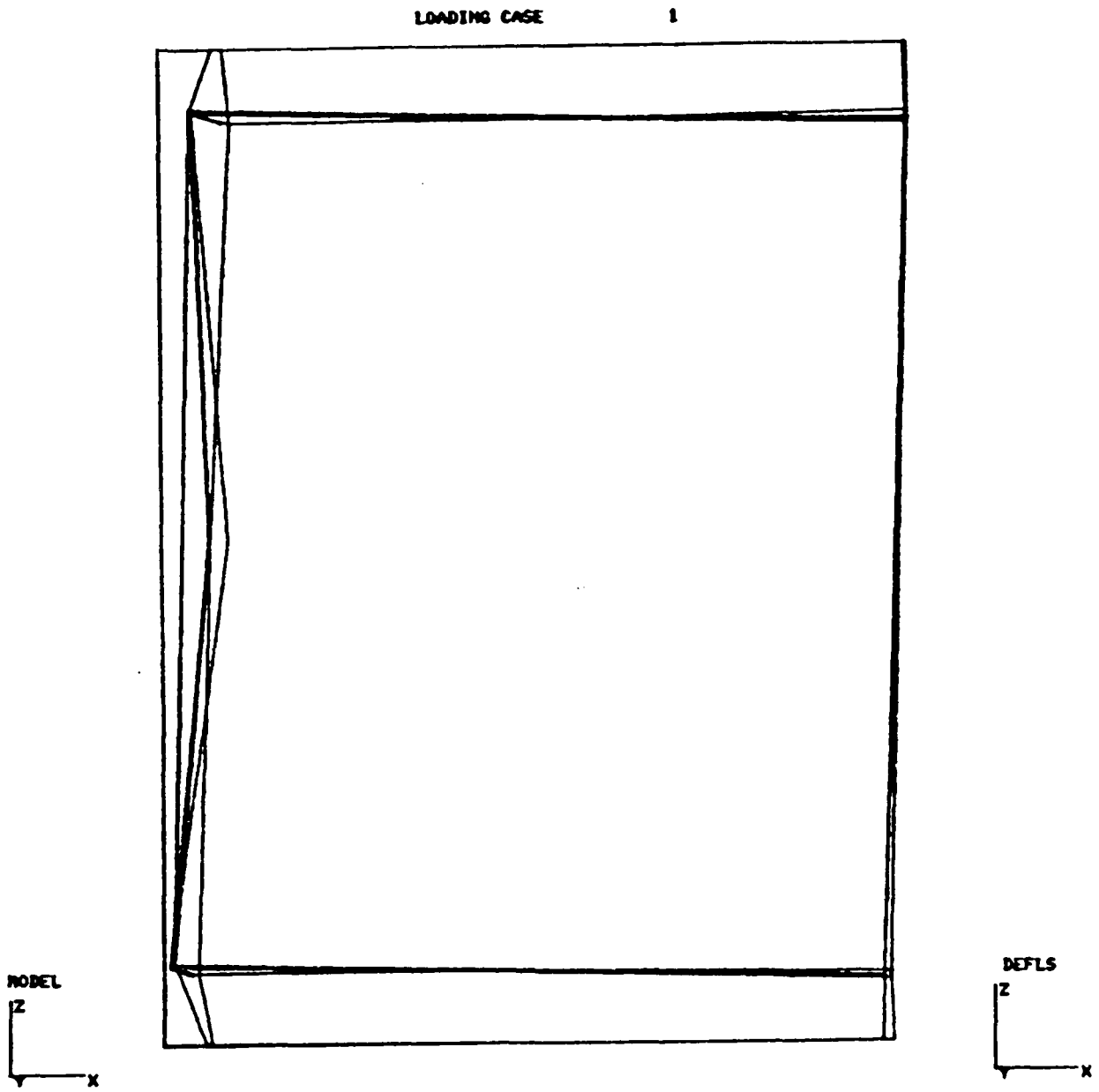

b. front view

Figure 28. (Cont'd.) Deflected Shape - Static Load Case 1 - Lateral Model

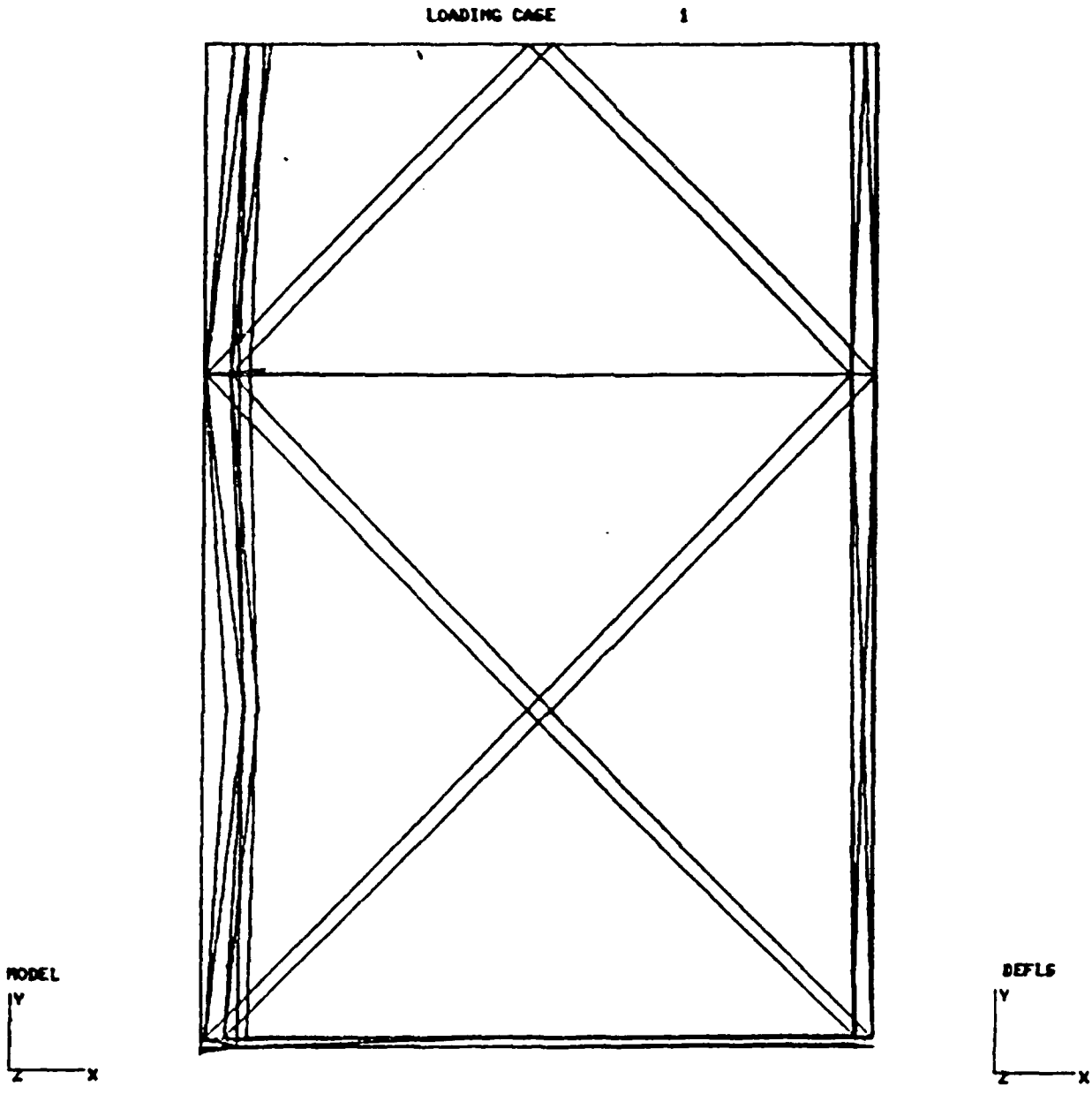

c. top view

Figure 20. (Concluded) Deflected Shape - Static Load Case 1 - Lateral Model

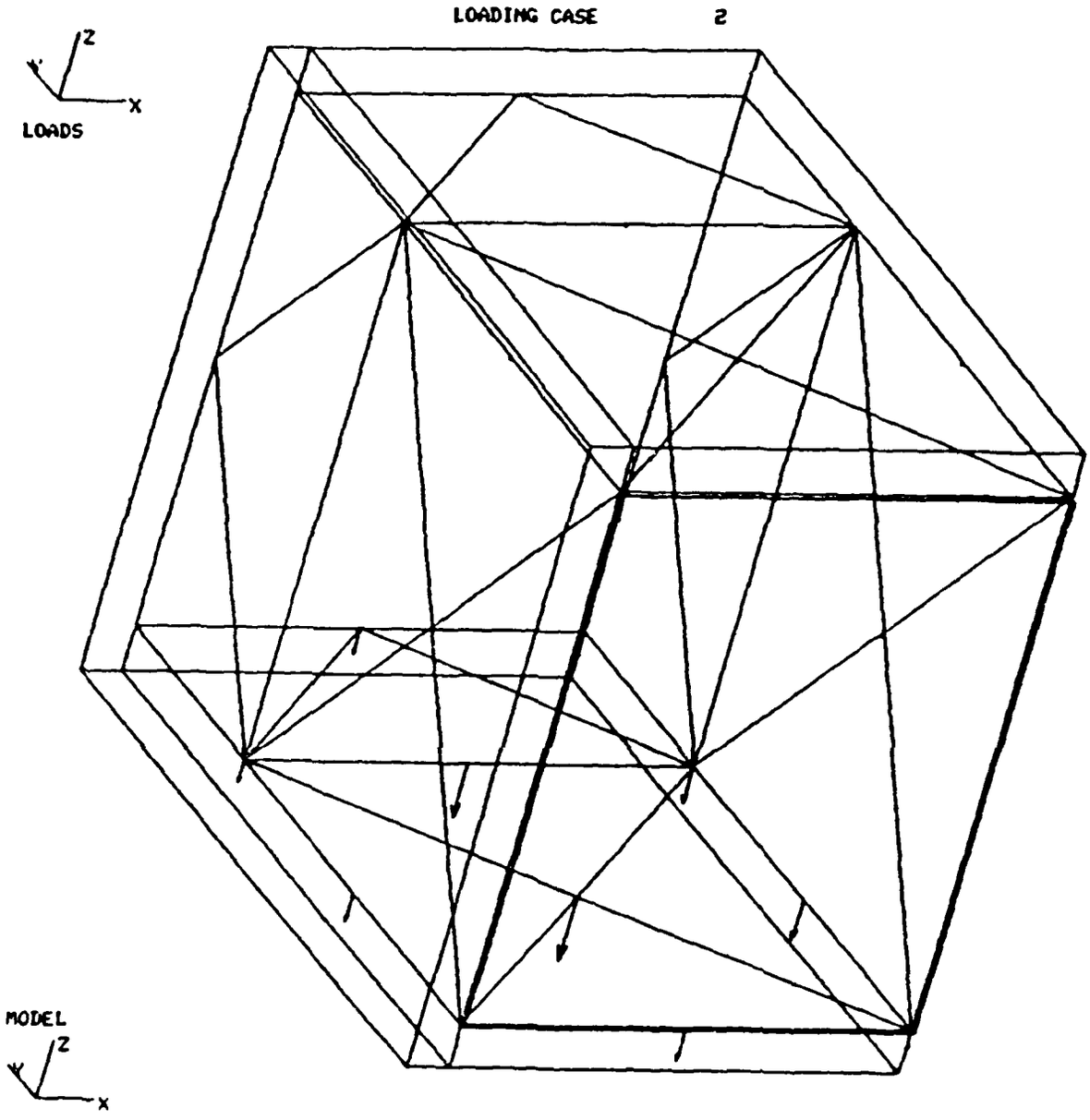

Figure 29. Static Load Case 2 - Lateral Model

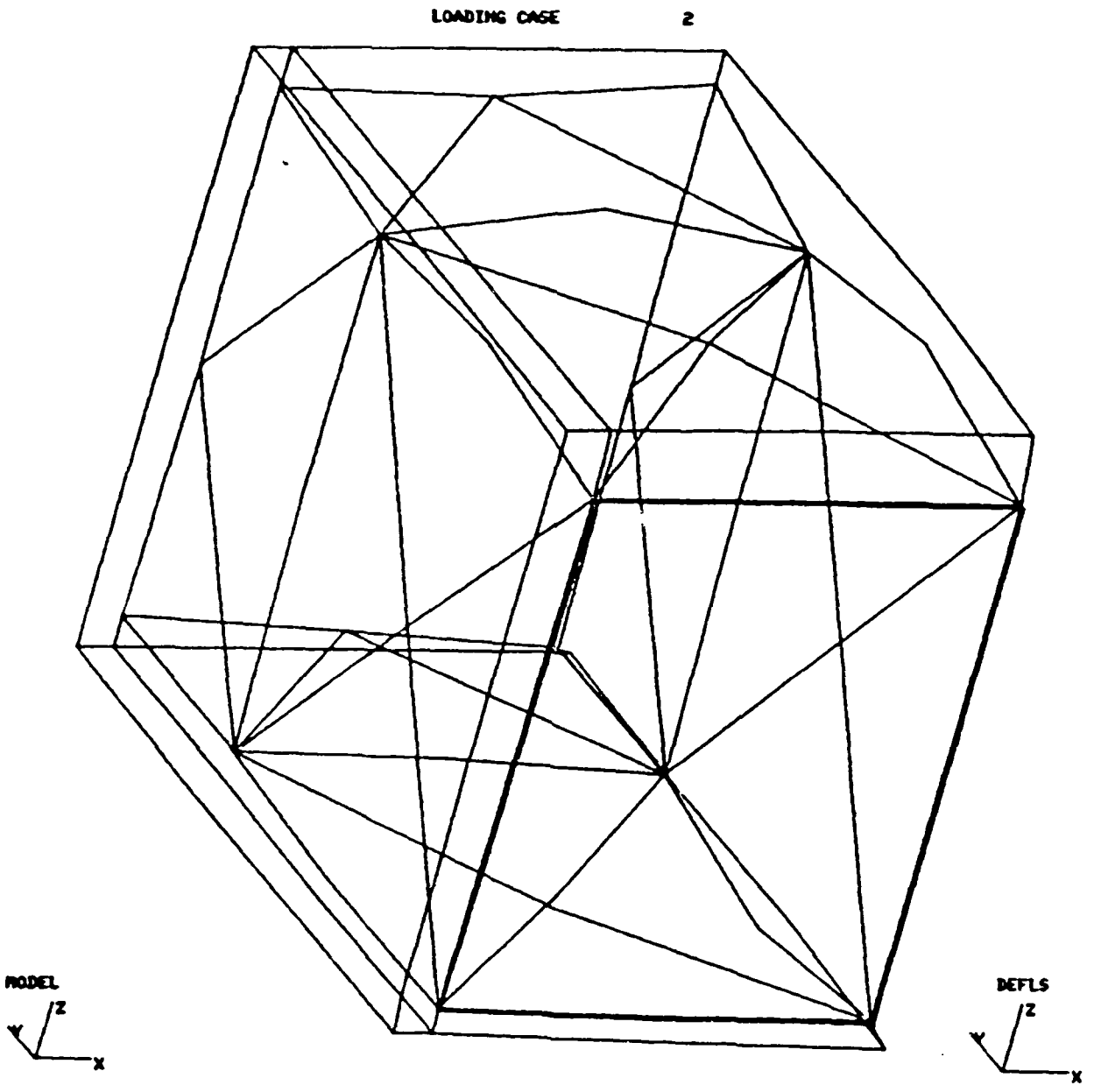

a. isometric view

Figure 30. Deformed Shape - Static Load Case 2 - Lateral Model

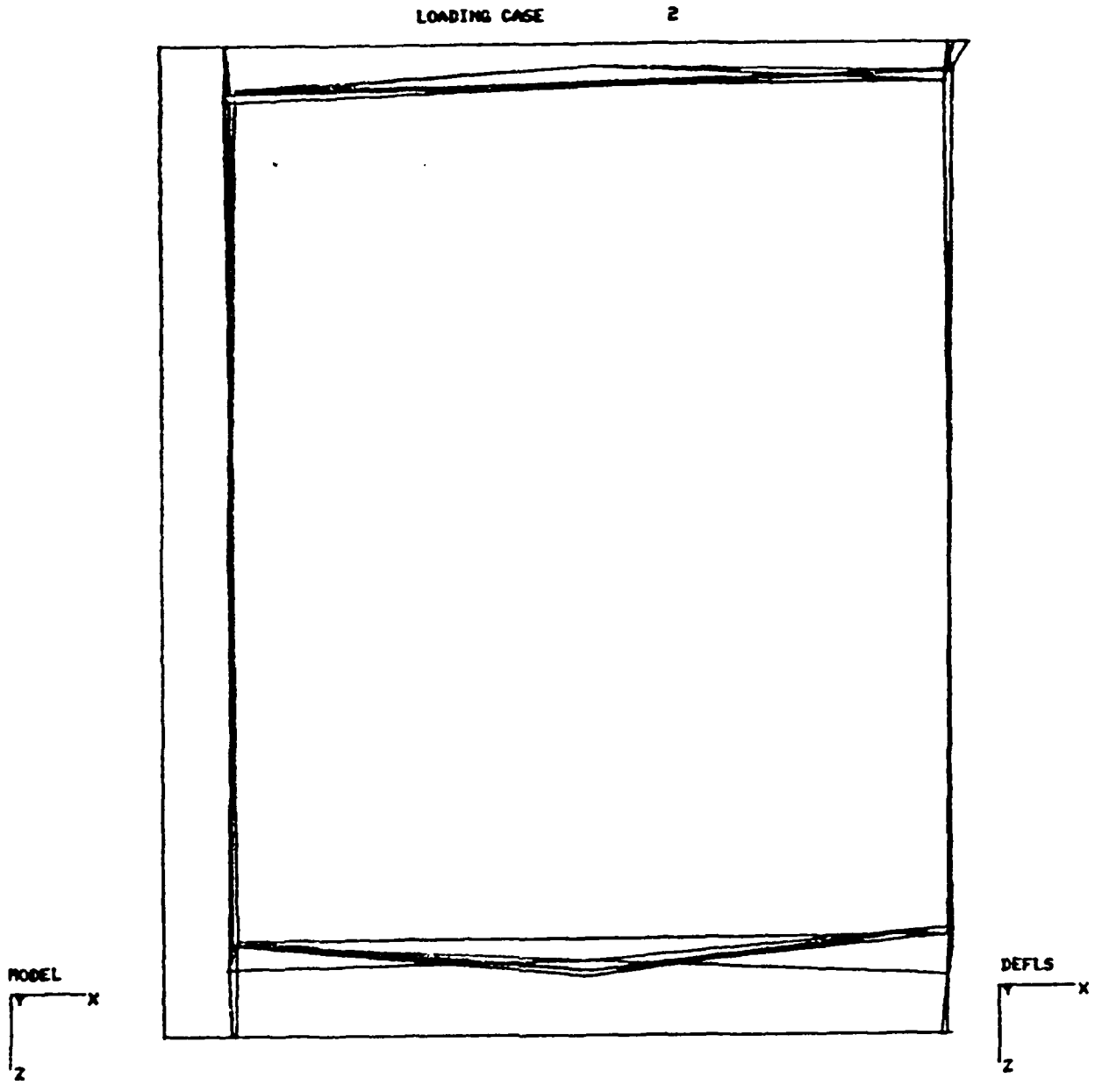

b. front view

Figure 30. (Cont'd.) Deformed Shape - Static Load Case 2 - Lateral Model

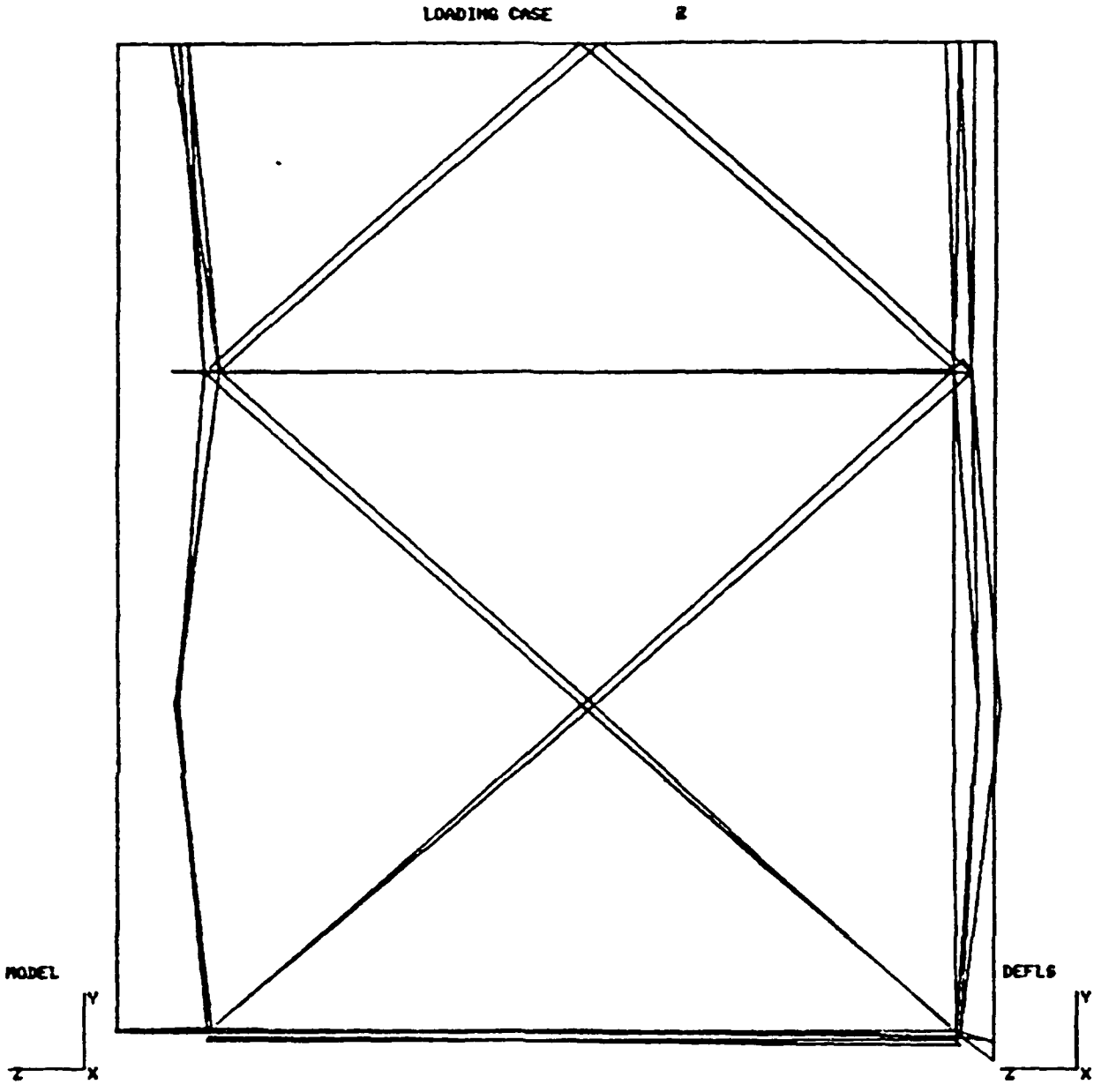

Figure 30. (Concluded) Deformed Shape - Static Load Case 2 - Lateral Model

b. Dynamic Results

The model was solved using the ADINA computer code. A direct integration of the equations of motion was preformed using a Newmark integration procedure. Equilibration iterations were preformed at each time step of 0.00002 seconds and the stiffness matrix was reformulated at every second time step. The integration was carried out to a time of 0.0065 seconds at which time all nodes had reached their maximum negative deflection.

Deflections--The deflections of the model due to the lateral impact are extremely complex. This is due to the complex geometry of the model and the distribution of the masses from the pallets, blocking and roller. Figures 31, 32, and 33 are plots of the displacement of twelve points on the structure as a function of time. These three plots correspond to the four nodes at the corners of the first major cross member of the inner frame, the inner frame at the door, and the door itself. Of the three groups, the door demonstrates the least amount of relative deflection. This is to be expected because of the stiffness at the frame and panel elements. The relative displacement at the first major cross member resulted in significant stress in three members, Figures 34 and 35. As can be seen, the points all move at a slightly different rate and end up at different locations at the conclusion of the analysis.

An important parameter when considering the response of foam to dynamic loads is the percent of crush. This is the amount of deflection in relationship to the original depth of the foam. Figure 36 gives the maximum plastic strain in the six large foam elements on the impact face. This strain is calculated based on a Von Mises stress which is always positive. Because of this, the plot was stopped when the elements went into tension, effectively unloading the elements. To this plastic strain, the elastic strain, 4%, must be added to get the total strain of the element. For this model, the maximum total strain on the side face of the foam for the times considered was 19% which corresponds to the percent of crush. This is significantly below the value of 52% which is given as the lockup value for this type of foam [6]. A similar result is obtained by taking the maximum deflection at the door, 1.47 and dividing by the initial length, 7.31 inches, giving a 20% crush. In the preliminary analysis a 37% foam crush was calculated. This calculation was

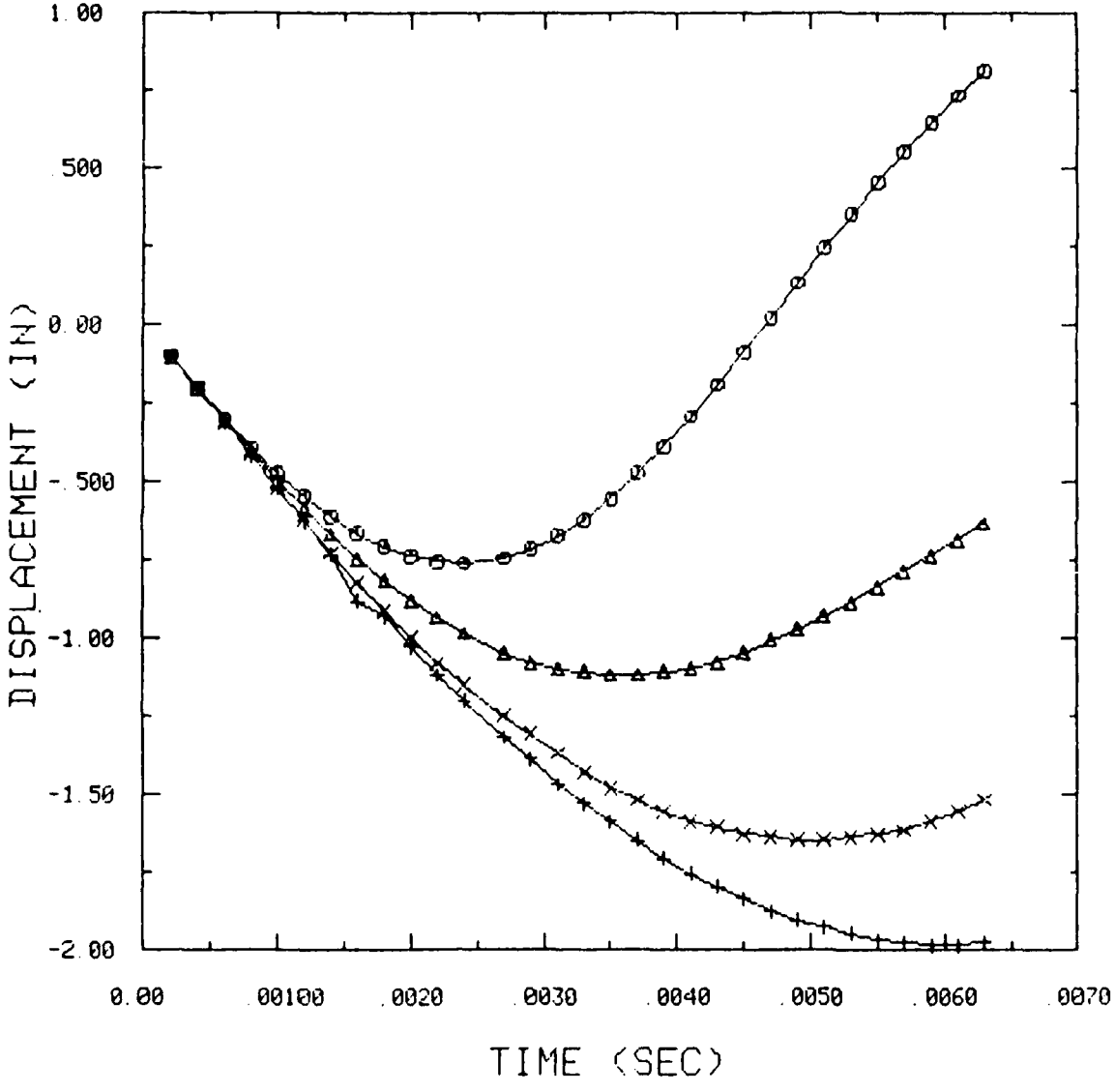

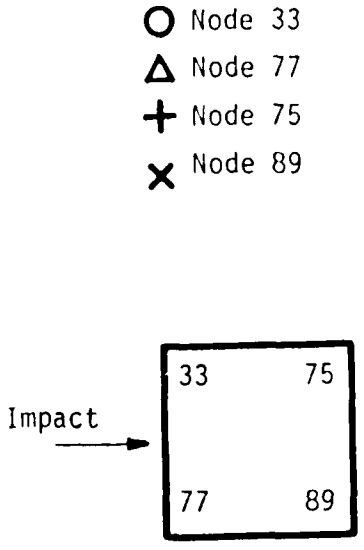

Figure 31. Deflection of 1st Major Cross Member

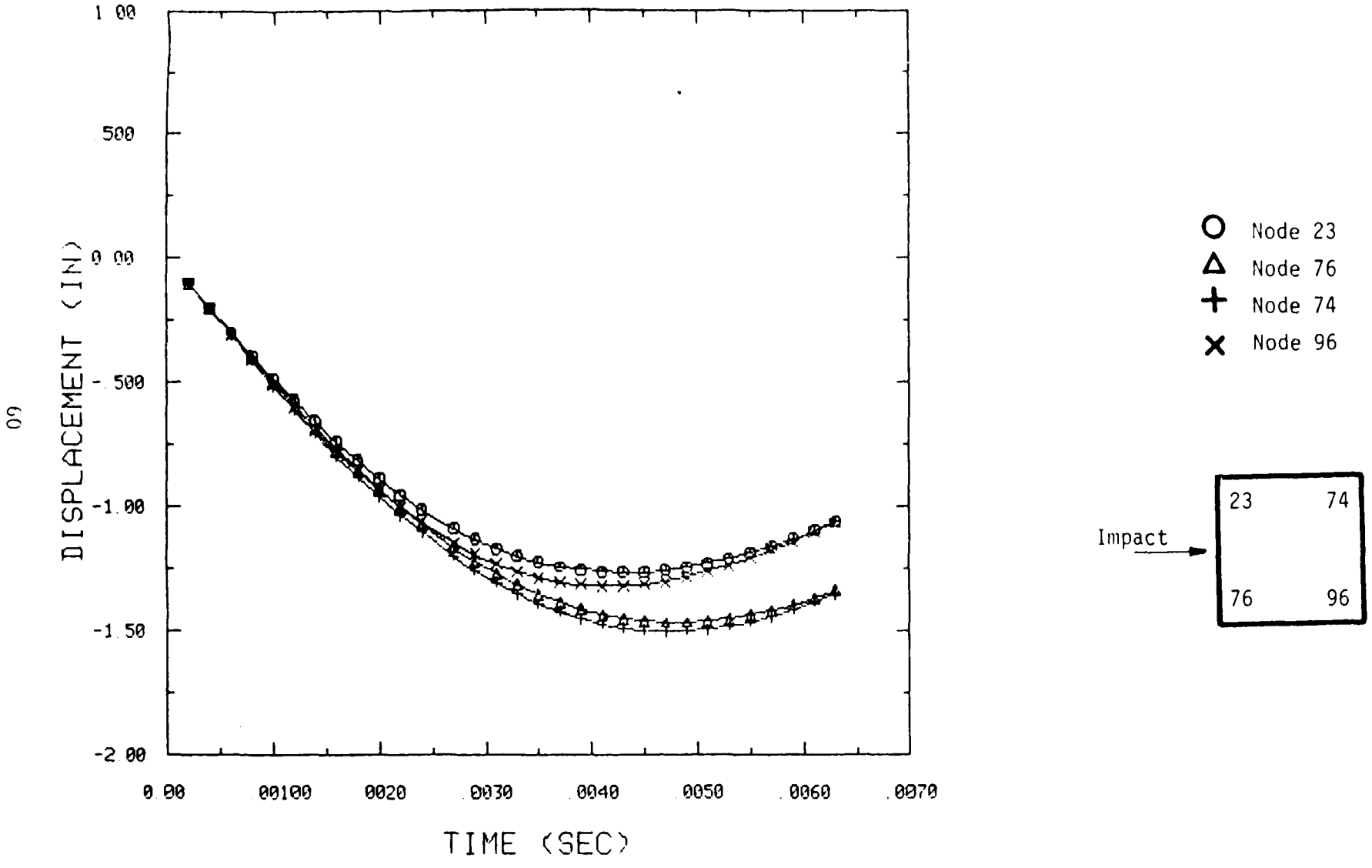

Figure 32. Deflection of Inner Frame at Door

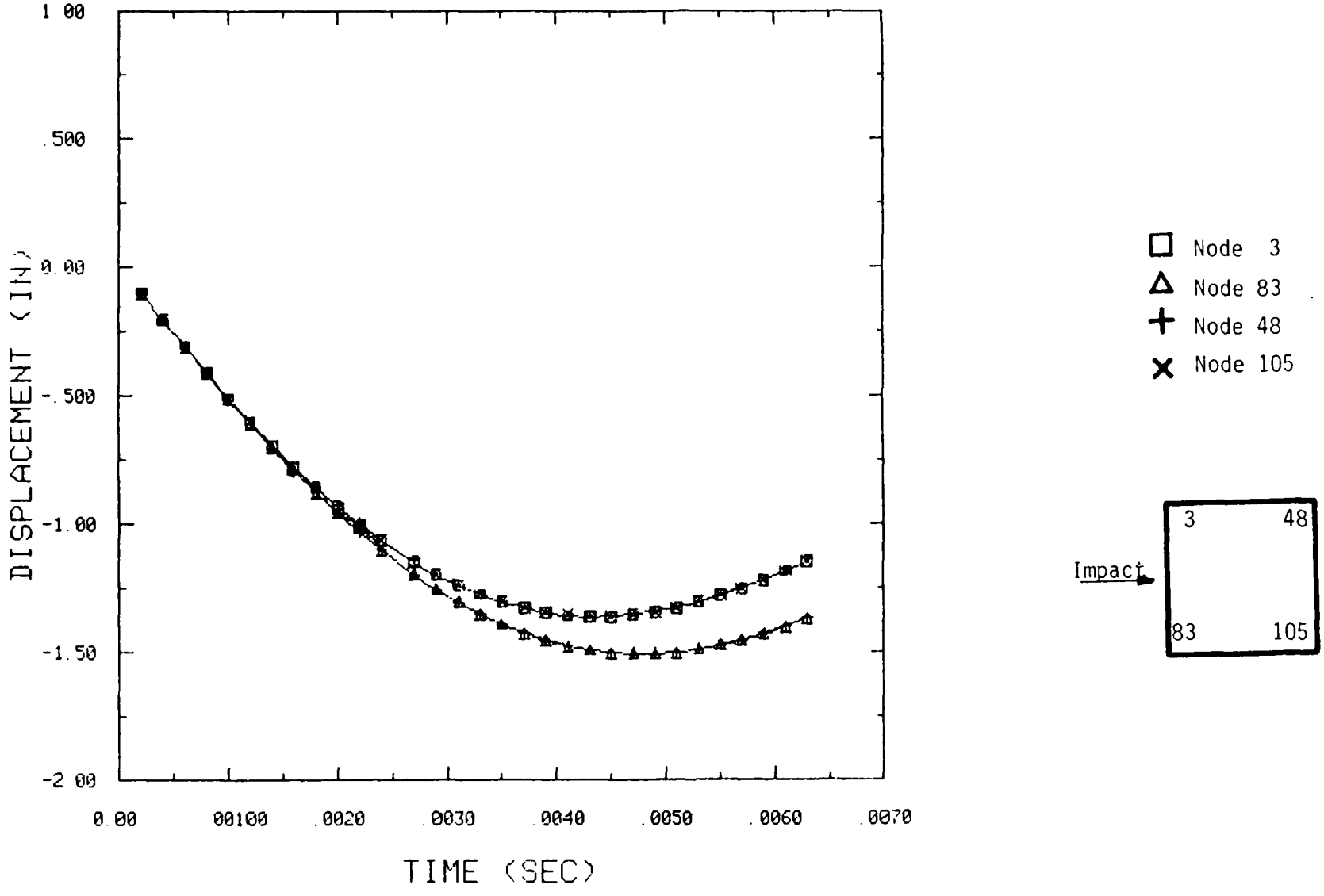

Figure 33. Deflection at Door

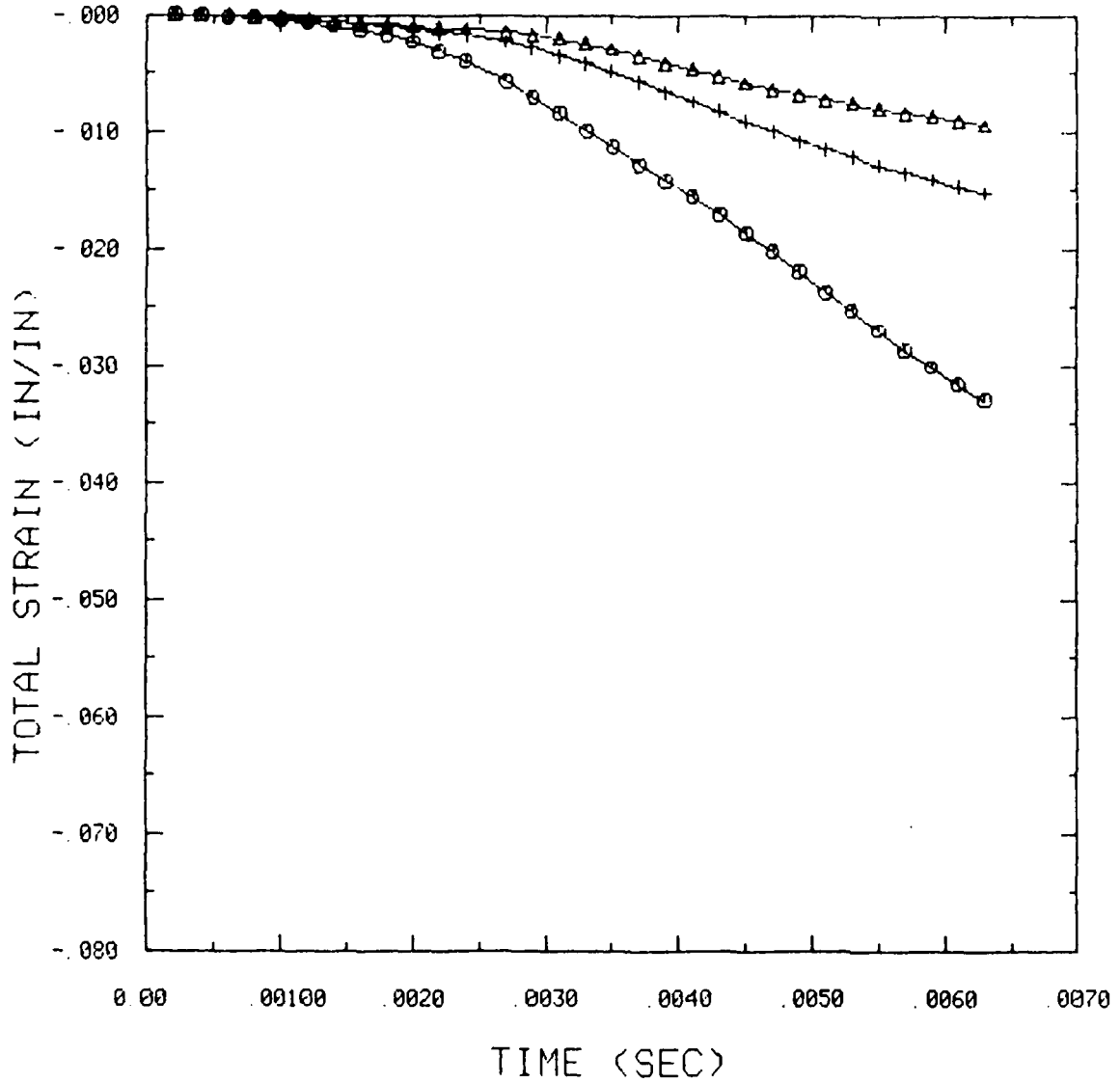

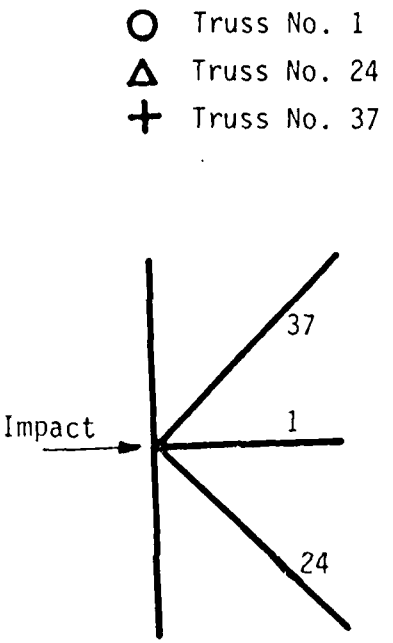

Figure 34. Strain in Truss Element on Bottom of Inner Frame at First Major Cross Member

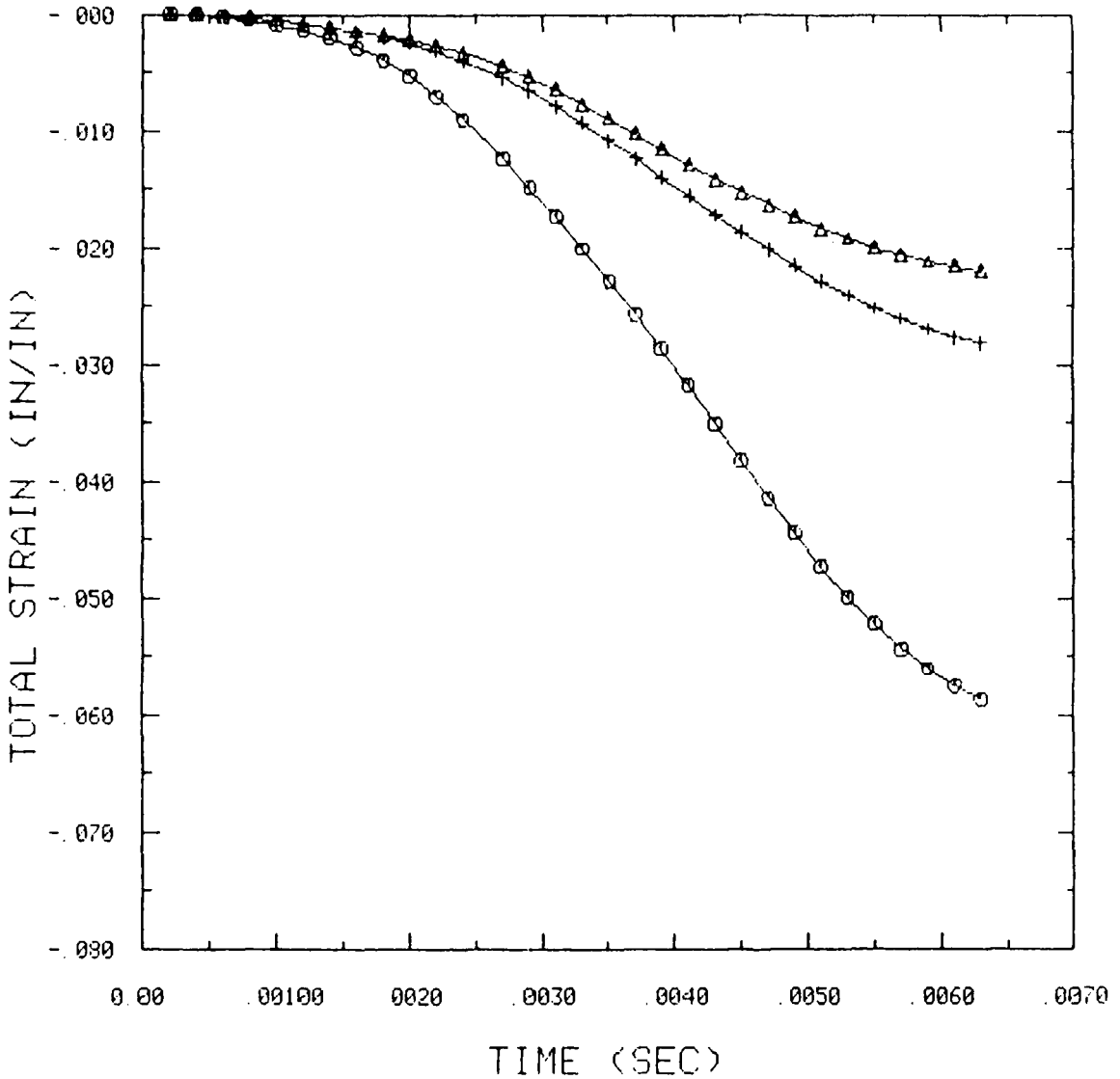

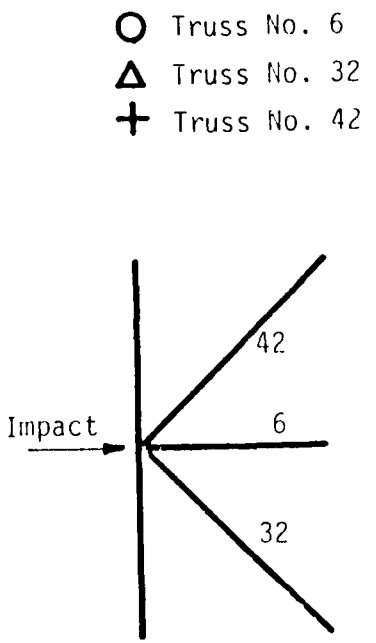

Figure 35. Strain in Truss Element Top of Inner Frame at First Major Cross Member

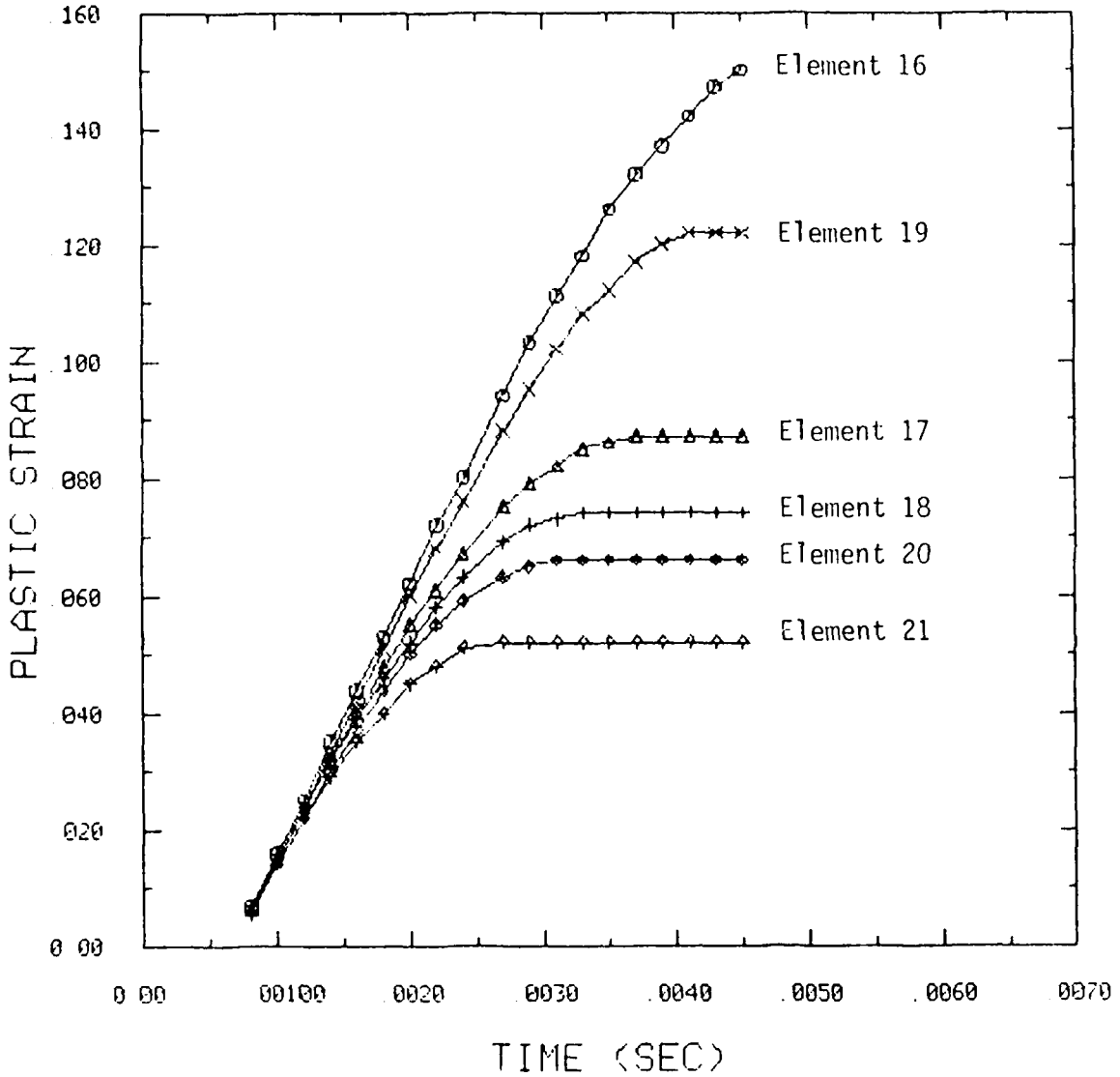

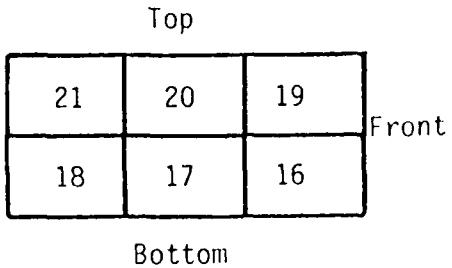

Figure 36. Plastic Strain in the Foam Elements on the Impact Face

based on a rigid inner frame. For this model, there was significant yielding and corresponding energy absorption in the inner frame. The result was less foam crush than predicted by the preliminary analysis. See also the comments in Section II.E.4, Estimate of Impact Crush Strength.

Inner Frame--There was yielding of the inner frame truss members early on in the event, at the time of 0.0012 seconds. The majority of yielding was associated with compression in the members. Figures 34 and 35 give the strains associated with three truss elements on the top and bottom portions of the inner frame at the major cross member near the impact surface. Elements 1 and 6 are the lateral members and the remaining four are the diagonal members. Note that due to relative displacement differences these strains have not leveled off. The maximum strain at the end of the event was located in truss 6, 5.9% of which 5.7% was residual plastic strain. This value is significantly below the 40% ultimate strain level defined for these stainless steel trusses (Table 1). There was some yielding of the inner frame at the door along the edge closest to the impact surface. The maximum plastic strain was 0.2%. It is felt that the majority of this yielding is due to the conservative approximation made in the modeling in this region. The first approximation was the fact that the nine bolts on each edge were modeled using only three beam elements. In addition, the foam elements were attached to these beam elements only at the corners and the midpoints. These two approximations resulted in excessive load transfer between the door and the inner frame at the corners and the midpoints. A more detailed model with all bolts included and a finer mesh for more uniform load transfer between the foam and the truss elements, would most certainly have produced much less yielding of the inner frame. A "30 ft" lateral impact test of the CAMPACT should produce no significant yielding of the inner frame at the door.

Door--The frame members around the door did not yield at any time during the analysis; however, some problems were encountered in the modeling of the honeycomb portion of the door. In the analysis, the elements were assumed to remain elastic. A check of the membrane forces in some of the elements indicated that local yielding would have occurred. Assuming that the membrane forces are resisted only by the two stainless faces, 0.1875 inches thick each, the allowable force per unit length, without yielding, was calculated to be 1.125×10^4 lb/in. Local forces up to three times this value were calculated during the analysis. These conservative levels are in part

due to the approximations described previously which gave excessive loads at the midpoints.

To estimate the overall membrane forces consider the deformation pattern of the four nodes given in Figure 33. There is little relative motion between the two nodes on the top and bottom surfaces at the door. Any relative deflection of these points would tend to produce compression in the face plates. The primary distortion which can potentially produce yielding of the door will be the relative motion between the top and bottom surfaces. For this condition the stress is given by

$$\sigma_{xy} = \frac{Eu}{(1+\nu)2b}$$

where u is the relative displacement (0.1942 inches) and b is the height of the door (89.38 inches). For this case the stress was calculated to be 25,200 psi. The yield stress for stainless is 30,000 psi; therefore, there will most likely be no overall yielding of honeycomb door. There may be some localized stresses in excess of 30,000 psi but they will not be as high as those indicated in the analysis.

Bolts--There was significant yielding of the bolts attaching the door to the inner frame during the event. The first to yield were the corner bolts which were represented at their true size in the model. Due to the approximations made, their area could have been increased slightly with a corresponding decrease in the area of the inner bolts. The maximum residual stresses in the four corner bolts according to the analysis were 17%, 9%, 26% and 35%. The highest value corresponds to the upper corner closest to the impact surface. This can be seen by comparing Figures 32 and 33 which show the displacements of these points as a function of time. The maximum relative displacement at this point is 0.101 inches occurring for t = 0.0047 seconds. The majority of the stress in the bolt is caused by the moments resulting from the relative lateral displacement of the bolt ends. Clearly, the high strains in the corner bolts were caused by the conservative modeling of this region, i.e., a free bolt length of 1 inch and a model which transferred most of the loads through the corner bolts and the bolts at the centerline.

The stresses and strains in the other bolts calculated by this analysis are also conservative. Calculated residual plastic strains, up to 170% at the centerline bolts, are not realistic. For all the bolts, the

failure strain is given as 50%. As for the corner bolts, the reasons for these conservative results are the approximations made in the modeling. The nine bolts on each side were represented by only three elements whose diameter was defined by matching the appropriate shear area rather than the bending stiffness. If the bending stiffness were matched, the diameter of the bolts would be larger resulting in lower stress and strains. Also, the attachment of the inner frame at the door to the foam, only at the midpoints and ends, loaded the midpoint bolts excessively. As an estimation of the expected stress and strain on these bolts, the assumption will be made that the stress and strain in the corner bolts are correct. (In reality they will probably be lower than calculated as described above.) If we then assume that the displacements of, or loads at, the other bolts can be calculated by interpolation between the corner bolts, corresponding stresses and strains in the side bolts can be estimated.

We will assume that bolt strains are directly proportional to the relative lateral displacements of the bolt ends, i.e., end rotations will be ignored. This lateral sway condition, shown in Figure 37, produces bolt bending strains which are directly proportional to Δ, the relative displacement of the ends, or

$$\varepsilon_{max} = \frac{3d\Delta}{L^2}$$

Where d is the bolt diameter.

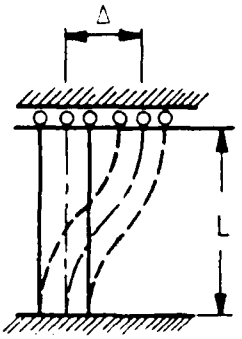

Figure 37. Bolt in lateral sway

The relative displacement in the impact direction between the inner frame and door at the corners can be estimated from Figures 32 and 33. At the four corners the maximum relative values are approximately:

Top left ($UX_3 - Ux_{23}$) : 0.0875 in.
Bottom left ($UX_{83} - UX_{76}$) : 0.1625 in.
Top right ($UX_{48} - UX_{74}$) : 0.0875 in.
Bottom right ($UX_{105} - UX_{76}$) : 0.125 in.

At the bottom left corner bolt the maximum strain is thus

$$\varepsilon_{max} = \frac{3d\Delta}{i^2} = \frac{3(1.0 \text{ in.})(.1625 \text{ in.})}{(1 \text{ in})^2}$$

$$= 0.4875$$

This value is higher than the strain of 35% predicted by ADINA and suggests that end rotations occurred that reduced the strain. At the side bolt adjacent to the bottom left corner bolt, a linear interpolation of relative displacements gives:

$$\Delta = .0875 + \frac{0.1625-0.0875}{89.38} \times 80.44 = 0.155 \text{ in.}$$

The corresponding strain for the bolt is

$$\varepsilon_{max} = \frac{3(0.75 \text{ in.})(.155 \text{ in})}{(1.0)^2} = 0.349 < \varepsilon_{ult} = 0.50$$

This is the most highly loaded side bolt, and this conservative analysis suggests that the bolt will not exceed the ultimate strain for the material. A more realistic, but still conservative, estimate of the stress is obtained if we reduce this value by the ratio of the ADINA calculated strain for the corner bolt to that estimated by this procedure. The reduced value is

$$\varepsilon_{max} = 0.349 \times \frac{0.35}{0.4875} = 0.25$$

On the basis of these calculations the maximum expected bolt strain would be that of the most highly loaded corner bolt or 35%. This strain level is quite high for a bolt, even though it is less than the ultimate strain of 50% for the bolt material. Thus, we believe that the design is marginal, even though it has survived side impact from a 30 ft. drop [2]. A modest redesign of the mating surfaces between the door and the inner frame could relieve the shear load on the bolts which led to the high strains observed.

Foam--All the foam elements on the side face of the CAMPACT yielded during the impact event. The maximum deflection was shown previously to be 1.47 inches with a corresponding percent crush of 20%. The region of foam at the floor of the CAMPACT was subjected to the most crushing as would be expected from the mass distribution. Some of the elements on the top and bottom surfaces yielded due to localized deformations.

Door Seal--If there is significant yielding of the bolts, precompression in the seal may be affected; however, at the corner nodes, the longitudinal differential deflection between the door frame and the inner frame all tend to increase the compression in the seal. The maximum relative displacement is 0.0036 inches. The maximum relative rotation is 0.00083 radians which, assuming a 2 inch distance from the center of rotation to the seal, would produce a relative displacement of 0.0017 inches. From Reference 2 the initial compression of the seal is 0.24 inches. Therefore, the seal will not be broken at the corner due to the calculated deflection. We expect this to be true along the sides of the door as well.

4. Estimate of Impact Crush Strength

An eqivalent crushing force for lateral impact of the CAMPACT was estimated as shown in Appendix B. Because substantial deformation occurred in the inner frame as well as in the foam for lateral impact, calculations were made to bound the crush force. The upper bound considers deformation in the foam only and the lower bound considers total back face to front face crush of the CAMPACT. The calculated bounds are:

$$2.43 \times 10^6 \text{lb} \leq F_{cru} \leq 6.3 \times 10_6 \text{ lb}$$

F. Summary of Results

1. Longitudinal Impact

The ADINA calculations performed in this study have shown that the CAMPACT can survive a 30 ft. longitudinal drop without failure. Here, failure is defined as breaching the inner containment boundary, either through rupture of the containment liner or loss of door seal. Neither of these events is likely to occur for the conditions analyzed. Based on a conservative model of the door-to-frame connection, maximum separation on the seal was only 16.2% of initial seal compression, resulting in no loss of contact.

For a higher drop height, forces in the inner frame and door will remain at about the same level until lockup occurs in the foam at a strain near 50%. This means that approximately 50% of the energy absorbing capacity of the foam was utilized in the 30 ft. drop. Impact energy will increase in direct proportion to the drop height, so the calculations indicate that the CAMPACT should survive a 50 ft. longitudinal drop without foam lockup. At a drop height of 60 ft. some lockup of the foam will start to occur.

2. Lateral Impact

From the conservative analysis performed, it is not possible to give a definitive answer as to the survivability of the CAMPACT when subjected to a 30 ft drop onto an unyielding surface. A question arises as to the performance of the bolts connecting the door to the inner frame. The analysis indicates significant yielding of the bolts, yet a more realistic or detailed model might well reduce bolt strains. Thus, we believe that the design is marginal for lateral impact from a 30 ft. drop, but that a minor redesign, to relieve bolt shear, would make the CAMPACT acceptable for these conditions.

The percentage of crush in the foam for the 30 ft. drop was only 20%. Forces in the frame and door should remain at about the same level until lockup does occur at a crush of 50%. Since the impact energy is directly proportional to the drop height, calculations indicate a drop height of 75 ft. before lockup. This estimation indicates that, if the bolt shear loads are reduced, the CAMPACT has an excellant chance of surviving even higher drops, prehaps as high as 60-75 ft. A more detailed model, which represents all bolts and more realistic coupling between the foam and the truss members, can provide useful insight for CAMPACT redesign in the door region and for CAMPACT response to higher drop heights.

III. ESTIMATES OF M55 ROCKET FAILURE INSIDE THE CAMPACT

A. Longitudinal Impact

An estimate of rocket failure (failure of the agent canister) within the CAMPACT can only be postulated from the pallet analyses of Reference 1. In that document, an analysis of the rocket was made which simulated a longitudinal drop of the CAMPACT from a height of 40 ft. Results of the calculation showed that the rocket would survive and that the the strain level in the foam of the CAMPACT would reach 37.5%. This value of strain is somewhat higher than the 23.4% calculated for the CAMPACT in this report.

One explanation for this difference is that in the ADINA calculations for the CAMPACT, internal foam elements saw a triaxial state of stress; whereas, in Reference 1, a uniaxial representation for the foam was used. The triaxial state of stress effectively increased the stress level at which yielding of the foam occurred. As an upper bound, the effective compressive yield stress could be 41% higher than the uniaxial yield stress, for a Poisson's ratio of 0.3 as specified for the foam. Coupling between the rocket and the foam could also account for some of the difference observed.

It was also assumed in the analysis of Reference 1 that the loading from the top pallet (they are stacked end to end in the CAMPACT) would not crush the wooden longitudinal stringers and fiberglass launching tubes in the bottom pallet and transfer loads directly into the rocket. Calculations were made and included in an appendix of Reference 1 which shows that this is a valid assumption. Thus, we are confident that the rocket will survive a 30 ft. or 40 ft. longitudinal drop within the CAMPACT.

The effects of the CAMPACT on the survivability of the pallet for lateral impacts were not addressed.

IV. CONCLUSIONS AND RECOMMENDATIONS

A. Conclusions

From the analyses of the CAMPACT described in this report the following conclusions were drawn:

(1) The CAMPACT will survive a longitudinal drop of 30 ft. without failure;

(2) Based on the results computed for the 30 ft. drop, it is highly probable that the CAMPACT will survive a longitudinal drop from 40 ft. and likely that the CAMPACT will survive a longitudinal drop of 50 ft.; however, calculations for the 40 ft. and 50 ft. drops were not made;

(3) Within the CAMPACT, the M55 rockets will survive a longitudinal drop greater than 40 ft.;

(4) From the analyses performed, it is not possible to accurately predict survivability (or failure) of the CAMPACT when subject to a lateral drop of 30 ft; however, the analyses were conservative, which is confirmed by the fact that a prototype CAMPACT has survived side impact from a 30 ft. drop. We have not had access to detailed results from the CAMPACT drop tests. From such data one might be able to conclude that the CAMPACT has a high probability of surviving lateral impacts from 30 ft. drops.

B. Recommendations

The analyses performed in this study were based on our best efforts within the constraints of time, dollars and information available to us. Clearly, refinements to the analyses can be made and additional conditions can be examined to provide information on edge impact, corner impact, etc. The one aspect of the problem most in need of study is the coupled response of the CAMPACT and pallets. Coupled response was not addressed in this study, and we suggest that such calculations be made if failure of the M55 rocket within the CAMPACT is a critical issue to be resolved. This could be done for longitudinal and lateral impact by expanding the existing models. To study edge or corner impacts would require extensive changes to the existing models, but the information data base that we have accumulated would still be

applicable. Additional analyses for lateral impact with a more detailed model, as described previously, should be made. We further suggest that redesign of the door/inner frame connection be considered to reduce the high bolt shear loads observed in the calculations for lateral impact.

V. REFERENCES

1. Stewart, S. E. and Cox, P. A., "Nonlinear Dynamic Response Analysis of 115mm Chemical Rocket Packing Impact," Draft Final Report, SwRI Project 06-8461-001, April 1985.

2. Personal communications between SwRI staff and H&R Technical Associates personnel.

3. Telephone conversation between P. A. Cox, SwRI and Bob Burgoyne, General Atomic, February 25, 1985.

4. "ADINA, A Finite Element Program for Automatic Dynamic Incremental Nonlinear Analysis," Users Manual Report AE81-1, ADINA Engineers, Inc., September 1981.

5. The "Gifts" System, Graphics-oriented Interactive Finite Element Time-Sharing System Version 5.03 Users Reference Manual, April 17, 1981, University of Arizona.

6. Patel, M. R. and Finnie, I., "Structural Features and Mechanical Properties of Rigid Cellular Plastics," Journal of Materials, JMLSA, Vol. 5, No. 4, December 1970, 909-932.

7. ASTM Standards (Various for different materials).

8. Deutschman, A. D., Michel, W. J. and Wilson, C. E., Machine Design Theory and Practice, MacMillan Publishing Co., Inc., New York, 1975.

9. Woolam, W. E., "A Study of the Dynamics of Low Energy Cushioning Materials Using Scale Models," Society of Plastic Engineers, Inc., 3rd Annual Technical Conference, Technical Papers, Vol XIII, May 15-18, 1967, Detroit, Michigan, 475-479.

APPENDIX A

CAMPACT CRUSHING ANALYSIS FOR STATIC LOADING

CAMPACT COLLAPSE / CRUSHING LOAD

THE COLLAPSE LOAD / CRUSHING LOAD OF THE CAMPACT WILL BE BASED SOLELY ON THE COLLAPSE LOADS OF THE FRAME MEMBERS AND FOAM. FIRST CONSIDER LONGITUDINAL LOADING.

LONGITUDINAL LOADING

THE OUTER FRAMEWORK, SHOWN IN FIGURE 3 IN THE REPORT BODY, WILL BE LOADED FIRST FOR LONGITUDINAL LOADS, IT CONSISTS OF 4 MEMBERS, EACH ONE BEING A 3 IN. X 3 IN. X 0.12 in WALL S. STL. TUBE. THE TUBES ARE BRACED AT INTERVALS OF 76.43 INCHES. SECTION AND MATERIAL PROPERTIES OF THE TUBES ARE:

$$A = (3\,in)(3\,in) - (2.75\,in)(2.75\,in) = 1.4375\,in^2$$

$$I = \frac{1}{12}\left[(3)(3)^3 - 2.75(2.75)^3\right] = 1.984\,in^4$$

$$r = \sqrt{I/A} = 1.175\,in$$

$\sigma_y = 30{,}000$ psi $\qquad E = 29.5 \times 10^6$ psi

$\sigma_{ult} = 75{,}000$ psi

THE BUCKLING STRESS CAN BE COMPUTED FROM THE EULER FORMULA:

$$\sigma_e = \frac{P}{A} = \frac{C\pi^2 E}{(L/r)^2}$$

WHERE C = COEFFICIENT TO ACCOUNT FOR DIFFERENT END CONDITIONS = 1.0 FOR PINNED ENDS

L/r = SLENDERNESS RATIO

IF WE CONSERVATIVELY ASSUME THAT THE ENDS ARE PINNED, WE FIND

$$\sigma_E = \frac{(1.0)(\pi^2)(29.5\times10^6\ psi)}{\left(79.56/1.175\right)^2}$$

$$= 61,350\ psi$$

$$\sigma_y < \sigma_E < \sigma_U$$

THUS, THE YIELD STRESS/LOAD OF THE TUBES WILL BE REACHED. BECAUSE THE TUBE IS ATTACHED TO TWO MEMBRANE PANELS WHICH INTERSECT AT 90°, THE CRUSH LOAD COULD EASILY EXCEED THE YIELD LOAD; HOWEVER, FOR THIS ANALYSIS THE YIELD LOAD IS CONSERVATIVELY TAKEN AS THE CRUSH LOAD. IT IS

$$F_{TU} = \sigma_y A = (30,000\ psi)(1.4375\ in^2)$$
$$= 43,125\ lb$$

FOR ALL FOUR TUBES IN PARALLEL, THE TOTAL CRUSH

LOAD FOR THE OUTER FRAME IS

$$F_{IF} = 4 \times 43.25 = 172,500 \text{ lb}$$

ONCE THE OUTER FRAME HAS COLLAPSED, THE LOADING WILL BE TRANSFERED TO THE FORMAIN THEN TO THE INNER FRAME. FOR THE ASSUMPTION OF A RIGID INNER FRAME, THE CRUSH LOAD FOR THE FORM (BEFORE LOCK-UP) IS

$$F_{F_0} = \sigma_c A$$

WHERE

$$\sigma_c = 140 \text{ psi}$$

$$A = 88.75 \text{ in} \times 100.75 \text{ in}^{*} = 8942 \text{ in}^2$$

FOAM CRUSHING STRENGTH IS THEN:

$$F_{F_0} = (140 \text{ psi})(8942 \text{ in}^2) = 1.25 \times 10^6 \text{ lb}$$

OF THIS AMOUNT, THE INNER FRAME CARRIES

$$F_{IF} = 140 \times 96 \text{ in} \times 74 \text{ in} = 991,000 \text{ lb}$$

AFTER THE FORM "LOCKS-UP", HIGH LOADS MAY BE CARRIED BY THE INNER FRAME. IT IS COMPRISED

---

* INTERNAL DIMENSIONS OF THE OUTER FRAME FOR A SECTION NORMAL TO THE LONGITUDINAL AXIS

OF AXIAL AND DIAGONAL 3 in x 3 in x 0.25 in STAINLESS STEEL TUBES (SEE FIGS 4 AND 7 IN THE REPORT BODY). SECTIONAL AND MATERIAL PROPERTIES OF THE TUBES ARE:

$\sigma_y = 30{,}000$ psi $\quad E = 28.5 \times 10^6$ psi

$\sigma_U = 75{,}000$ psi

$A = 3\text{in} \times 3\text{in} - 2.5\text{in} \times 2.5\text{in} = 2.75\ \text{in}^2$

$I = \frac{1}{12}\left[(3\text{in})^4 - (2.5\text{in})^4\right] = 3.495\ \text{in}^4$

$r = \sqrt{I/A} = 1.127$ in

THE BUCKLING STRENGTH IS ESTIMATED BY THE EULER FORMULA

$$\sigma_B = \frac{C\pi^2 E}{(L/r)^2}$$

FOR PINNED ENDS, $C = 1.0$ AND THE MAXIMUM UNSUPPORTED LENGTH, L, IS 76.43 in. THE BUCKLING STRESS IS

$$\sigma_B = \frac{(1.0)(\pi^2)(28.5 \times 10^6)}{(76.43/1.127)^2} = 61{,}160 \text{ psi}$$

$$\sigma_y < \sigma_B < \sigma_U$$

THUS THE YIELD STRESS WILL BE CONSERVATIVELY USED FOR COMPUTING THE CRUSHING LOAD, IT IS

$$F_{TJ} = \sigma_{YA} = (30{,}000\ psi)(2.75\ in^2)$$
$$= 82{,}500\ lb$$

DISTRIBUTION OF LOADS IN THE INNER FRAME CAN BE CLOSELY APPROXIMATED FROM THE RESULTS OF THE STATIC ANALYSIS FOR 15401b LONGITUDINAL LOAD APPLIED AT ONE OF THE CORNERS, THE DISTRIBUTION, FOR LINEAR ELASTIC BEHAVIOR, IS APPROXIMATELY:

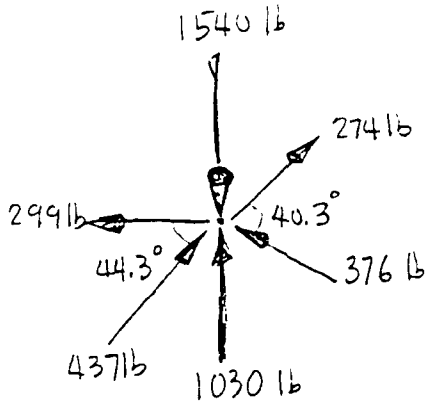

Figure A-1. LOADS IN THE INNER FRAME TRUSS MEMBERS

TO PRODUCE FIRST YIELD THE APPLIED LOAD IS

$$F = 1540 \times \frac{82500}{1030} = 123{,}350\ lb$$

SUMMING THE LOAD FOR THE FOUR CORNERS GIVES A TOTAL CRUSH LOAD FOR THE INNER FRAME OF

$$F_{IF} = 4 \times 123{,}350\ lb = 493{,}400\ lb$$

THIS IS HIGHER THAN THE OUTER FRAME BUT LESS THAN THAT APPLIED TO IT BY THE FORWARD THEREFORE THE

THE LONGITUDINAL CRUSHING LOAD FOR THE CAMPACT IN THE LONGITUDINAL DIRECTION IS, ASSUMING NO POST BUCKLING LOAD IN THE OUTER FRAME, THAT DUE TO THE INNER FRAME AND SURROUNDING FOAM OR

$$F_{LC} = 493{,}000\ lb + (1.25 \times 10^6 - 891{,}000)\ lb$$
$$= 493{,}000 + 359{,}000$$
$$= \underline{852{,}000\ lb}$$

THE CAMPACT SHOULD SUPPORT AT LEAST THIS MUCH LOAD, APPLIED UNIFORMLY THROUGH RIGID PLATENS, IN THE LONGITUDINAL DIRECTION. IT IS VERY LIKELY THAT IT WILL REACT A HIGHER LOAD BECAUSE OF STRAIN HARDENING IN THE INNER FRAME TRUSS MEMBERS AND SOME FINITE POST BUCKLING LOAD CARRIED BY THE OUTER FRAME.

VERTICAL LOADING

OF THE TWO DIRECTIONS, VERTICAL OR LATERAL, THE CAMPACT WILL HAVE A LOWER CRUSHING STRENGTH IN THE VERTICAL THAN IN THE LATERAL DIRECTION. THIS IS CAUSED PRIMARILY BY THE FACT THAT THERE IS LESS FOAM* ON THE SIDES AND ENDS OF THE INNER FRAME TO RESIST THE VERTICAL LOADS.

* A SMALLER CROSS-SECTIONAL AREA

THIS FACTOR IS OFFSET PARTIALLY BUT NOT FULLY BY A HIGHER CRUSHING STRENGTH OF THE INNER FRAME IN THE VERTICAL DIRECTION CAUSED BY HIGHER LOADS IN THE DIAGONAL MEMBERS.

FROM THE LONGITUDINAL ANALYSIS IT IS CLEAR THAT THE CRUSHING STRENGTH WILL BE GOVERNED BY THE CRUSHING STRENGTH OF THE INNER FRAME AND FOAM. AN ADINA ANALYSIS WAS PERFORMED TO ESTABLISH THE APPROXIMATE DISTRIBUTION OF LOADS IN THE INNER FRAME AND DOOR. RESULTS ARE SHOWN SCHEMATICALLY IN FIGURE A-2 ON P. 8. ASYMMETRY IN THE TRUSS LOADS WERE CAUSED BY THE FOAM ELEMENTS (NOT SHOWN) WHICH ARE ON THE LEFT-HAND SIDE, TOP AND BOTTOM OF THE MODEL.

A CHECK OF RESULTS SHOWS THAT THE DOOR REGION IS STRONGER & STIFFER THAN OTHER REGIONS OF THE CAMPACT. NEVER-THE-LESS, FOR THESE ESTIMATES THE CAMPACT CRUSH LOAD WILL BE BASED ON RESULTS FOR THE LOADS APPLIED AT "A" AND "B". THE CRUSH LOAD FOR THE INDIVIDUAL INTERNAL FRAME MEMBERS WILL BE THE SAME AS COMPUTED FOR LONGITUDINAL CRUSHING, BECAUSE THE YIELD LOAD GOVERNS FOR

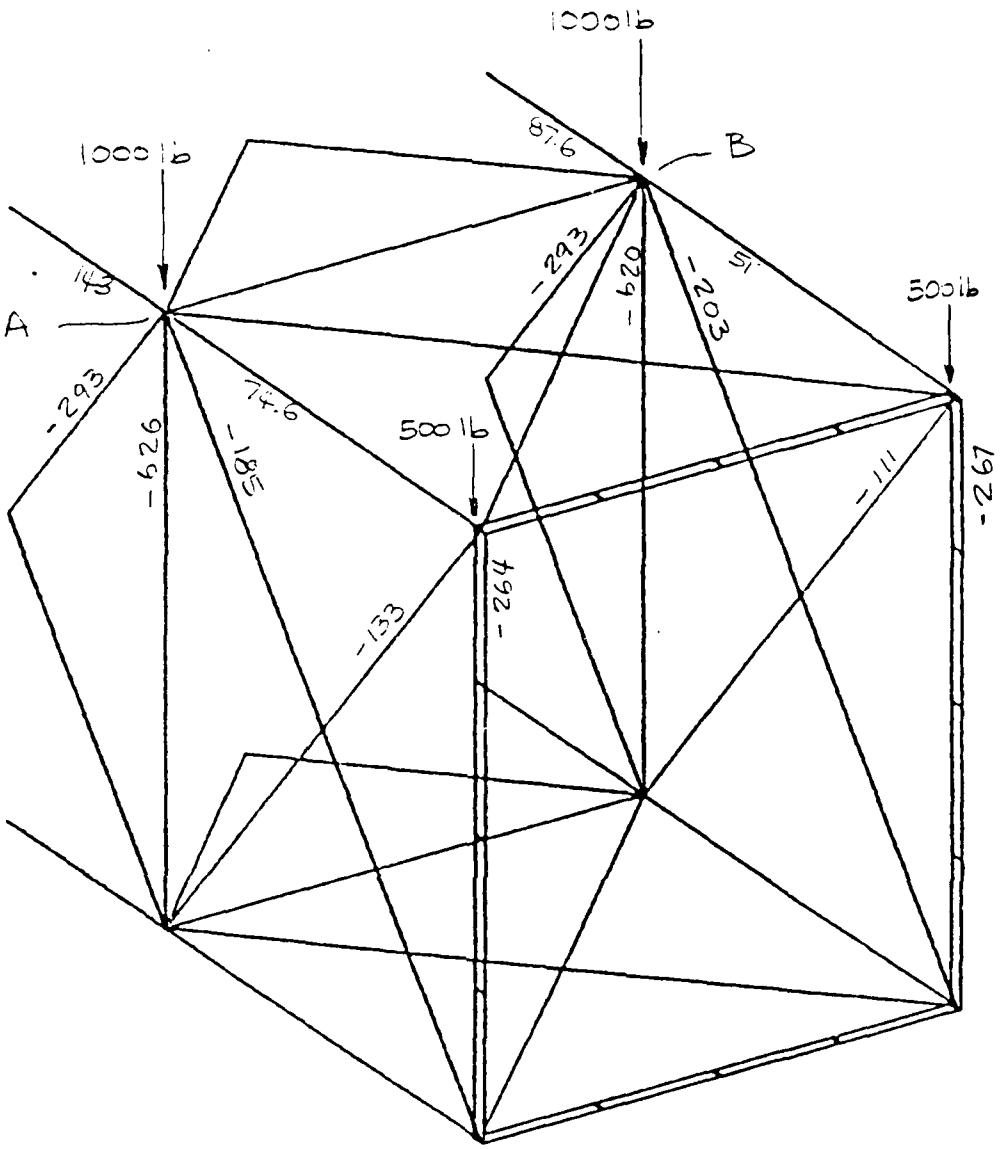

FIGURE A-2. STATIC LOADING OF THE INNER FRAME

THESE MEMBERS ALSO. IT IS (see pp. 4 & 5):

$$F_{TU} = 92,500 \text{ lb}$$

THE EXTERNAL LOAD, AT "A" and "B" OF

FIGURE A-2, TO CAUSE CRUSHING OF THE CANISTER IS THEREFORE

$$F = 1000 \times \frac{92500}{626} = 131{,}789 \text{ lb}$$

A LOAD OF THIS MAGNITUDE WILL BE RESISTED AT EIGHT POINTS ON THE INNER FRAME; THUS THE CRUSH LOAD OF THE INNER FRAME IS

$$F_{IF} = 8 \times 131{,}789 \text{ lb}$$
$$= 1.05 \times 10^6 \text{ lb}$$

TO THIS CAN BE ADDED THE CRUSH STRENGTH OF THE FOAM SURROUNDING THE INNER FRAME. IT IS

$$F_{FO} = \sigma_y A$$

$$\sigma_y = 140 \text{ psi}$$

$$A \approx 2 \times 7.31 \text{ in.} \times 233 + 31 \text{ in} \times 89 \text{ in} + 29'' \times 89 \text{ in}$$
$$\approx 3406 + 2759 + 2842 = 9007 \text{ in}^2$$

So

$$F_{FO} = 140(9007) = 1.26 \times 10^6 \text{ lb}$$

THE TOTAL CRUSH LOAD FOR THE CAMPAC IN THE VERTICAL DIRECTION IS THEN

$$F_{Vc} = F_{FD} + F_{IF} = 1.05 \times 10^{6} + 1.26 \times 10^{6}$$

$$= \underline{2.31 \times 10^{6}\ lb} \quad >> F_{Lc}$$

THE MIN. CRUSHING LOAD FOR THE CAMPAC IS THEREFORE THAT FOR THE LONGITUDINAL DIRECTION AND IS

$$F_c = \underline{852{,}000\ lb}$$

APPENDIX B

CRUSHING STRENGTH OF THE CAMPACT - IMPACT OF THE CAMPACT WITH A RIGID SURFACE

CRUSHING STRENGTH OF THE CAMPACT DURING IMPACT

A SIMPLE CALCULATION IS USED TO OBTAIN AN EQUIVALENT CONSTANT CRUSHING STRENGTH OF THE CAMPACT DURING IMPACT. THE KINETIC ENERGY AT IMPACT IS EQUATED TO THE DEFORMATION ENERGY ABSORBED BY THE CAMPACT DURING THE IMPACT EVENT OR

$$KE = F \cdot \Delta$$

WHERE

KE = KINETIC ENERGY AT IMPACT

$= \frac{1}{2} m V^2$

Δ = MAXIMUM CRUSH OF THE CAMPACT COMPUTED IN THE ADINA ANALYSES

FOR DROPS, KE IS EQUAL TO THE INITIAL POTENTIAL ENERGY OR

$$KE = PE = mgh$$

FOR DROP HEIGHT h AND WEIGHT mg.

LATERAL IMPACT

THE CAMPACT MASS REPRESENTED BY THE LATERAL MODEL WAS

$$mg = 22{,}593 \text{ lb} + (3150 \text{ lb of foam})$$
$$= 25{,}733 \text{ lb}$$

MAXIMUM CRUSH IN THE FOAM WAS CALCULATED IN THE ADINA ANALYSIS AS:

$$\Delta = 1.47 \text{ in.}$$

WHICH GIVES AN EQUIVALENT CRUSHING STRENGTH OF THE CAMPACT FOR LATERAL IMPACT OF

$$F = \frac{KE}{\Delta} = \frac{(25{,}733)(30 \text{ ft} \times 12 \text{ in/ft})}{1.47}$$
$$= \underline{6.30 \times 10^6 \text{ lb}}$$

THIS FORCE IS ALMOST TWICE THE CRUSHING STRENGTH OF THE FOAM WHICH IS:

$$F_{FO} = 100.36 \text{ in.} \times 229.44 \text{ in} \times 140 \text{ lb/in}^2$$
$$= 3.22 \times 10^6 \text{ lb}$$

MAXIMUM TOTAL CRUSH OF THE CAMPACT (BACK

FACE TO FRONT FACE) IS EQUAL TO THE CRUSH OF THE FOAM PLUS THE FRAME COMPRESSION, OR (SEE FIG. 3. IN THE REPORT BODY)

$$\Delta = 1.47 \text{ in.} + 2.34 \text{ in.} = 3.91 \text{ in.}$$

FOR THIS AMOUNT OF DEFORMATION THE CRUSH FORCE IS:

$$F = \frac{KE}{\Delta} = \frac{(25,733 \text{ lb.})(30 \text{ ft} \times 12 \text{ in/ft})}{3.91 \text{ in.}}$$

$$= 2.43 \times 10^6 \text{ lb}$$

THEREFORE, THE ACTUAL CRUSH FORCE SHOULD BE BOUNDED BY:

$$2.43 \times 10^6 \text{ lb} \leq F_{CRU} \leq 6.30 \times 10^6 \text{ lb}$$

END
DATE
FILM
4-88
DTIC